



Final Report

Solicitation #: RFP-38225-5/4/10-EMW

“Services to provide an improved understanding of water quality dynamics in the nearshore ocean waters of Long Bay, South Carolina, immediately adjacent to the Myrtle Beach ‘Grand Strand’”

Coordinated by:
Denise M. Sanger

Submitted May 11, 2012



South Carolina Sea Grant Consortium
287 Meeting Street
Charleston, SC 29401



Section I: Introduction

The nearshore region of Long Bay (Figure 1-1) has been the site of a growing number of hypoxic events (dissolved oxygen [DO] <2 mg/L) primarily during summer months. Although anecdotal evidence exists for earlier hypoxic events, researchers and resource managers documented low DO immediately adjacent to the shoreline in the summer of 2004. From July 15 to July 22, 2004, surveys from a number of piers in 7 m water depth indicated a stratified water column and bottom water DO concentrations < 2 mg/L (Sanger et al., 2011). Sustained hypoxia occurred again in 2009, from approximately August 17 to 28 and September 14 to 17, which showed generally similar patterns to what were observed during the July 2004 event. Since the 2004 event, South Carolina Sea Grant Consortium (SCSGC), South Carolina Department of Natural Resources (SCDNR), and South Carolina Department of Health and Environmental Control's Office of Ocean and Coastal Resource Management (SCDHEC-OCRM) have provided resources to begin characterizing oxygen dynamics in Long Bay to enhance understanding of the conditions that may lead to hypoxic events such as that of 2004 and 2009.

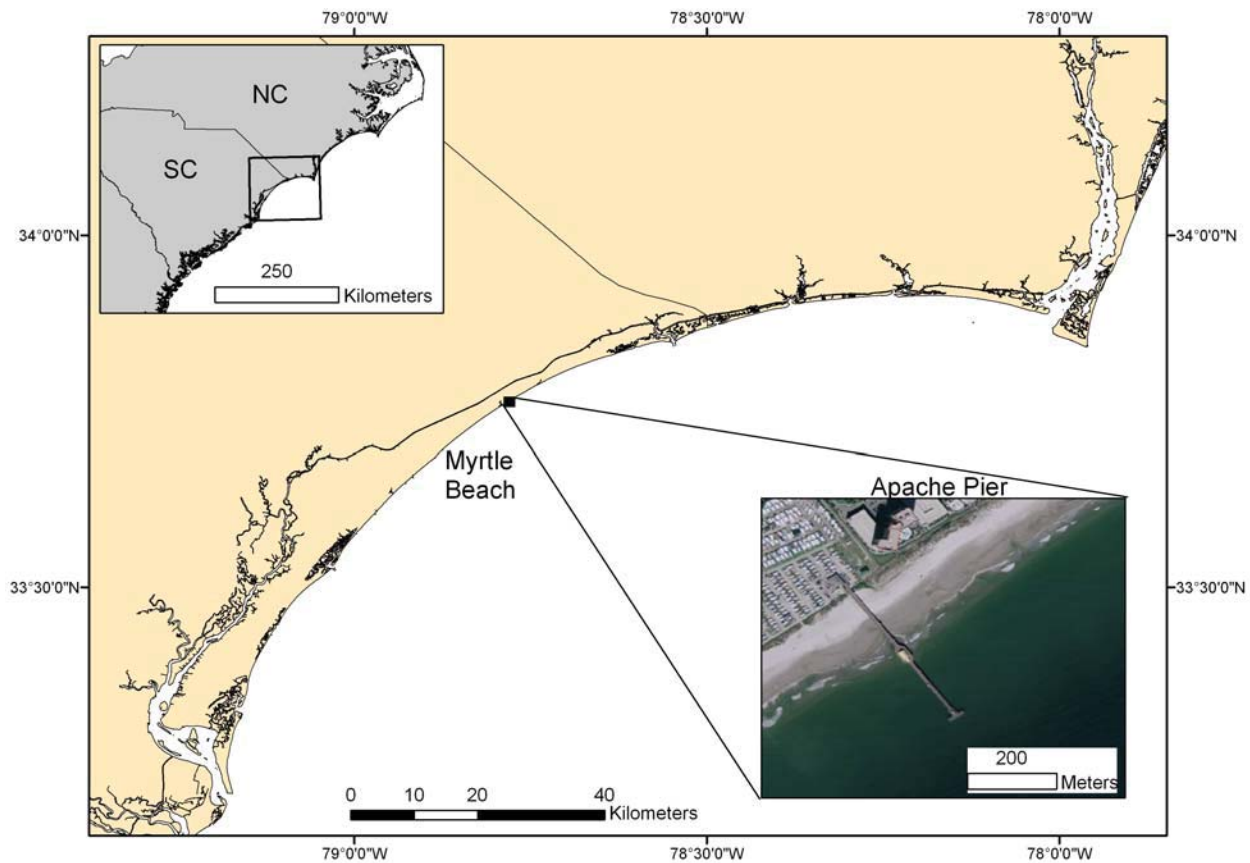


Figure 1-1. Map of Long Bay. Inserts indicate the position of Long Bay along the Carolina's coastline (upper left), and the site of Apache Pier in Myrtle Beach (lower right).

Long Bay represents a case where natural physically-driven oceanographic processes and anthropogenic loading combine in a synergistic manner not previously observed or recognized. Periods of low DO coincide with periods of upwelling-favorable conditions; however, not all upwelling events coincide with low DO. It is speculated that the duration of the upwelling conditions or the sequence of events plays an important role, although this has yet to be quantified. Periods of low DO also coincide with high concentrations of dissolved and particulate substrates in the immediate nearshore waters. While physical conditions appear to act to concentrate these substrates, key questions remain as to the importance of various sources for these substrates (i.e., groundwater, swashes, piped outfalls, rivers, etc), the conditions that enhance their delivery to the nearshore waters (e.g., local precipitation versus enhanced tidal exchange associated with spring tides), and the particular forms of substrate resources that are most important in fueling heterotrophic oxygen demand. Determining the threshold for development of hypoxia in Long Bay will require a mechanistic understanding of the relative roles that terrestrial loading, *in situ* biogeochemical O₂ uptake, and physical current conditions play in determining nearshore water quality and DO dynamics, as well as the conditions that influence them.

A multi-disciplinary team from SCSGC, Coastal Carolina University (CCU), and University of South Carolina (USC) participated in this effort. The project utilized a multi-disciplinary approach to gain additional insight into future hypoxic conditions by: (1) continuing nearshore water quality monitoring (salinity, temperature, DO) and expanding this monitoring to include ²²²Rn (a tracer of groundwater inputs) and chlorophyll, and CDOM; (2) examining the biological response (productivity) during times of enhanced nutrient input and low DO levels; and (3) analyzing prior and newly collected data to better understand the interconnection between offshore and onshore driving forces. The following sections each detail the research findings from this study.

Section II: Continuous Water Quality Monitoring at Apache Pier

Basic water quality measurements in surface and bottom waters – Susan Libes (CCU)

Pier-based monitoring of salinity, temperature, and dissolved oxygen was performed in the surface and bottom waters at the seaward end of Apache Pier in Myrtle Beach, SC using YSI 600 series data sondes. Ancillary data included meteorological measurements collected via a Vaisala Weather Transmitter WXT520 that measures wind speed, wind direction, air temperature, barometric pressure, humidity, and rain accumulation. Both data sets were relayed on 15 minute intervals via cell modem to a computer server maintained by YSI Econet, Inc. These data are provided to the public at:

<http://www.ysieconet.com/public/WebUI/Default.aspx?hidCustomerID=131>. Secchi depths were also measured during each maintenance visit. Additional sampling was undertaken to characterize hypoxia events that occurred during the summers of 2010 and 2011.

Periods of significant data loss and their causes are listed below:

<i>Dates</i>	<i>Type of data lost</i>	<i>Cause</i>
12/13/2010 to 1/13/2011	All meteorology data	Transmitter returned to OEM for repairs and calibration
1/7/2010 to 1/12/2011	All surface sonde data	Bad cable.

In 2010, new datasondes (YSI 600 OMS) were purchased to enable a switch from Clark cell to luminescent dissolved oxygen sensors and to add depth sensors. The goal was to improve the quality of the dissolved oxygen data, to reduce maintenance, and better establish the location of the sondes with respect to the sea surface. It also enabled the bottom sonde to be deployed on a zip line which eliminated concerns about sampling artifacts. The 600 OMS bottom sonde deployment began on March 1, 2011. The 600 OMS surface sonde deployment commenced on August 30, 2010 and used a novel counter weighting system. This system has stabilized the surface sonde at a depth approximately 1 m below the sea surface.

During the cold weather months, post-deployment calibration checks were performed weekly on-site. The sondes were cleaned and redeployed. If the sonde calibration was found to be out of QA/QC specifications, it was replaced with a freshly calibrated unit. The surface and bottom sondes' performance were also checked against a manually deployed sonde twice per visit, once before retrieval and then after redeployment of the cleaned continuous monitoring data sondes. These data were used to estimate *in situ* measurement uncertainties, which appear to be on the order of ± 0.4 mg/L for DO and ± 0.25 psu for salinity as shown in Figures 2-1 and 2-2. The manually deployed sonde was also used to measure the depth, DO, temperature and salinity just above the seafloor. This was done to: (1) verify the depth of the continuous monitoring bottom sonde with respect to the seafloor and (2) document when a bottom layer of extremely low DO was present. As shown in Figure 2-3, a low DO bottom layer has been frequently observed suggesting that hypoxic conditions are more common in this region than where the continuous reporting bottom water sonde is located, i.e., we are under-estimating the occurrence of hypoxia by not sampling closer to the seafloor. Bottom depths at the deployment site ranged from 6.0 to

7.5 m depending on the tide. We have also verified that the bottom sonde is positioned 1.5 m above the seafloor.

During the warm weather months, we performed calibration and performance checks on Mondays and Fridays. The sondes were also cleaned three times a week, on Mondays, Wednesdays and Fridays. Cleaning three times a week was required to prevent biofouling from impairing the sensor function.

During the project period, the Apache Pier Campground provided financial support to cover half of the annual subscription costs for the YSI Econet service. CCU continued to maintain a real-time display of all the continuous data via a plasma screen mounted in the Apache Pier Campground's bait shop. The feed for the display is available at: <http://bccmws.coastal.edu/apachepierkiosk/offshore2.html>. At the Campground's request, we also participated in several public outreach events for their customers and the general public.

All QC'd data from the Apache Pier datasondes and the meteorology sensor have been posted to <https://longbay.basecampHQ.com/>. YSI Econet provides the data in LST, so GMT was added to the QC'd data files. These files cover the period from 06/22/06 through 11/09/11. Data QC was performed using AQUARIUS Informatics V. 2.7.219, which enabled production of QC reports and data. In cases where a sonde failed a post deployment calibration check, all of the data since the last calibration check were removed from the QC'd data file. Spurious data of known origin were also removed, such as air spikes associated with retrieval of the sondes.

The DO time series for the warm seasons of 2010 and 2011 are shown in Figure 2-4. Hypoxic conditions were observed more frequently in 2010 than in 2011. These occurred episodically during May through October in 2010 and during June through August of 2011. The duration of each of these episodes is shown in Figure 2-5. Hypoxic conditions were extant for a cumulative total of 2 and 0.4 days in 2010 and 2011, respectively. DO concentrations below 4 mg/L were extant for a cumulative total of 15 and 6.3 days in 2010 and 2011, respectively. As shown in Figure 2-6, the monthly rain accumulation during these months was much lower in 2011 than in 2010 with the exception of May, October, and November. August and September 2011 water temperatures were also lower than observed in 2010 (Figure 2-7). The lower rainfall in 2011 probably contributed to somewhat higher average salinities in June and August as compared with 2010 (Figure 2-8).

Comparisons of the 2010 and 2011 DO records to prior years are provided in Figures 2-9 and 2-10, which show the monthly mean surface and bottom % saturation of DO. The % saturation eliminates the influence of temperature on DO solubility and illustrates the degree of DO deficiency relative to a gaseous equilibrium state. Figure 2-9 shows the standard deviation of the monthly means, and Figure 2-10, the range of values for each month. Figure 2-10 indicates that a period of very low % DO was observed during Dec 2010. This occurred from 12/18/2010 to 1/8/2011 and was confirmed with manual measurements. The bottom % DO reached a minimum of 48 % during this period and coincided with highly turbid bottom water. The low DO occurred during a period of very low wind speeds and was preceded by, and then briefly interrupted by, periods of upwelling favorable winds blowing around 20 mph.

Examples of low DO events in 2010 and 2011 during the months of May through August are presented in Figures 2-11 through 2-15. A general pattern is sometimes observed with these events beginning on a flooding tide and ending on an ebbing tide. They co-occurred with low water temperatures and low wind speeds, typically during spring tides. In most cases, muted effects were concurrently observed in the surface waters. In some cases, significant increases in salinity co-occur. The step function nature of the temperature shifts suggests that a low temperature, low DO and saline water mass is being driven onto the sondes with the flooding tides. Thus the low DO must be developing close to shore where it can be readily carried onshore and detected by the sondes. Where Rn measurements were available, high values coincided with low DO.

In some cases, we confirmed that the low DO was widespread by measuring detailed vertical profiles at fishing piers as far south as Surfside and as far north as Cherry Grove. Examples are shown in Figures 2-16 and 2-17 for the low DO event that occurred in early August 2011. Turbidity, TSS/VSS, chlorophyll and TN/TP data were also collected. High chlorophyll concentrations were observed, reaching a maximum of 56 $\mu\text{g/L}$, with the usual inverse correlation to DO and positive correlations with TSS, VSS and turbidity. VSS was 25 to 30 %. Microscopic screening of water samples provided no evidence of a bloom.

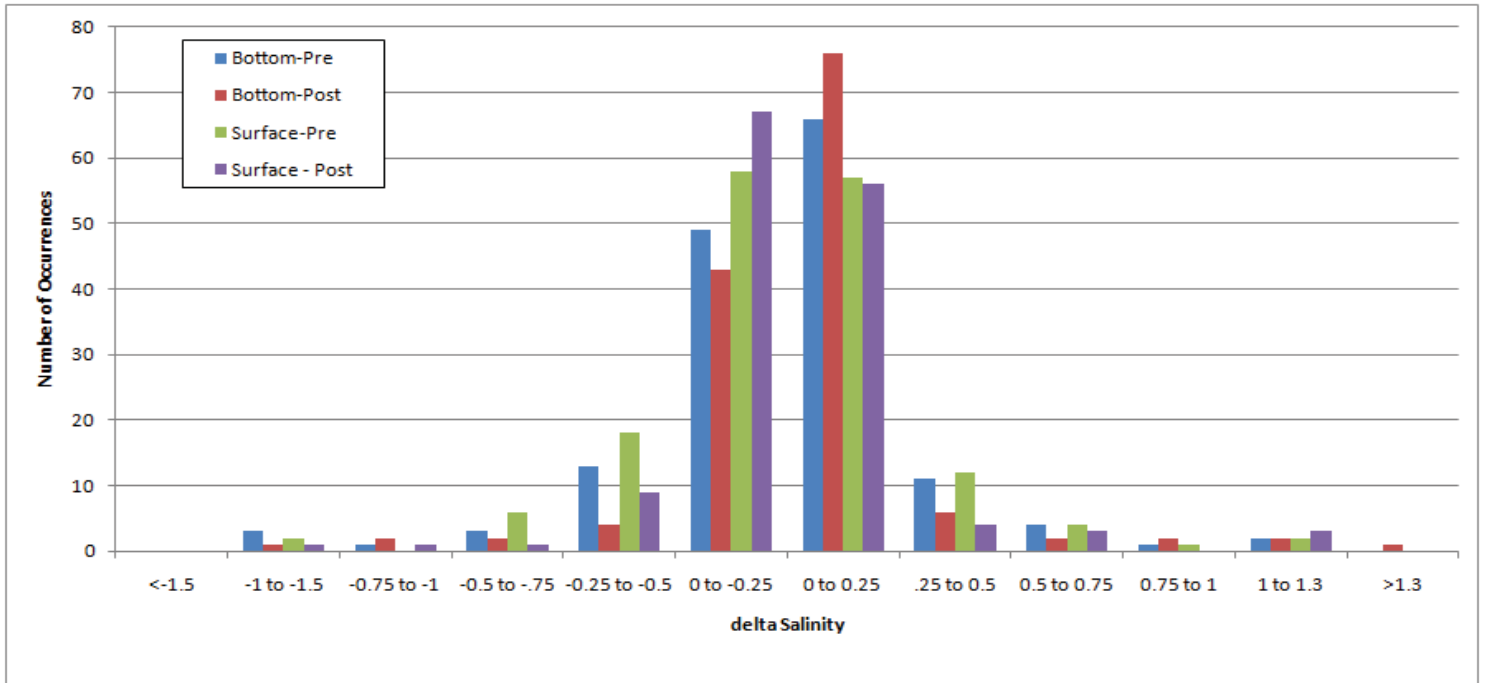


Figure 2-1. Frequency distribution of differences in salinity measurements by a YSI sonde continuously deployed at Apache Pier and a performance check conducted using an independently calibrated and deployed sonde in the surface and bottom waters. A positive value reflects higher concentrations in the manually deployed sonde. N = 153, 141, 160 and 145 for bottom water performance checks done before calibration checks, bottom water performance checks done after calibration checks, surface water performance checks done before calibration checks, and surface water performance checks done after calibration checks, respectively. Data were collected from 8/7/09 to 3/1/2011 and 3/1/2011 to 5/16/2011 with 600R series sondes. Only data that passed post deployment calibration checks are plotted in the histogram. Calibration checks are performed against laboratory control check standards.

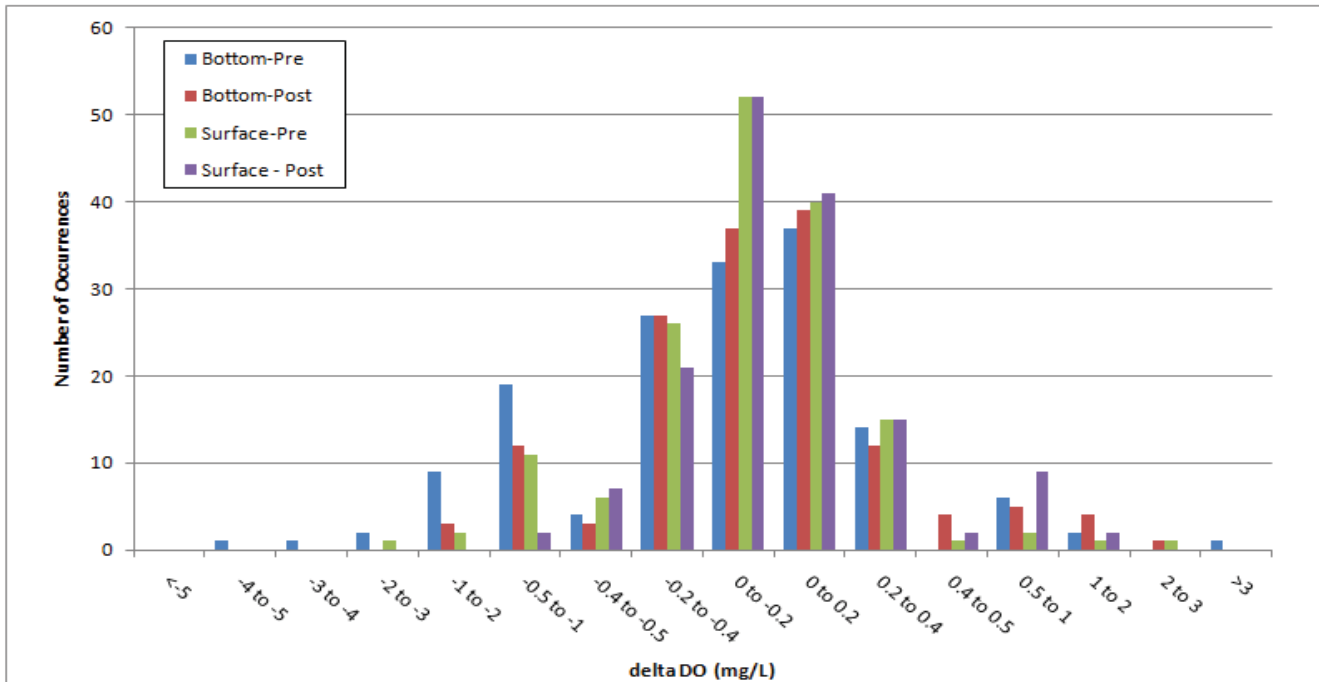


Figure 2-2. Frequency distribution of differences in DO measurements by a YSI sonde continuously deployed at Apache Pier and a performance check conducted using an independently calibrated and deployed sonde in the surface and bottom waters. A positive value reflects higher concentrations in the manually deployed sonde. N = 156, 147, 158, 151 for bottom water performance checks done before calibration checks, bottom water performance checks done after calibration checks, surface water performance checks done before calibration checks, and surface water performance checks done after calibration checks, respectively. Data were collected from 8/7/09 to 3/1/2011 and 3/1/2011 to 5/16/2011 with 600R series sondes. Only data that passed post deployment calibration checks are plotted in the histogram. Calibration checks are performed against laboratory control check standards.

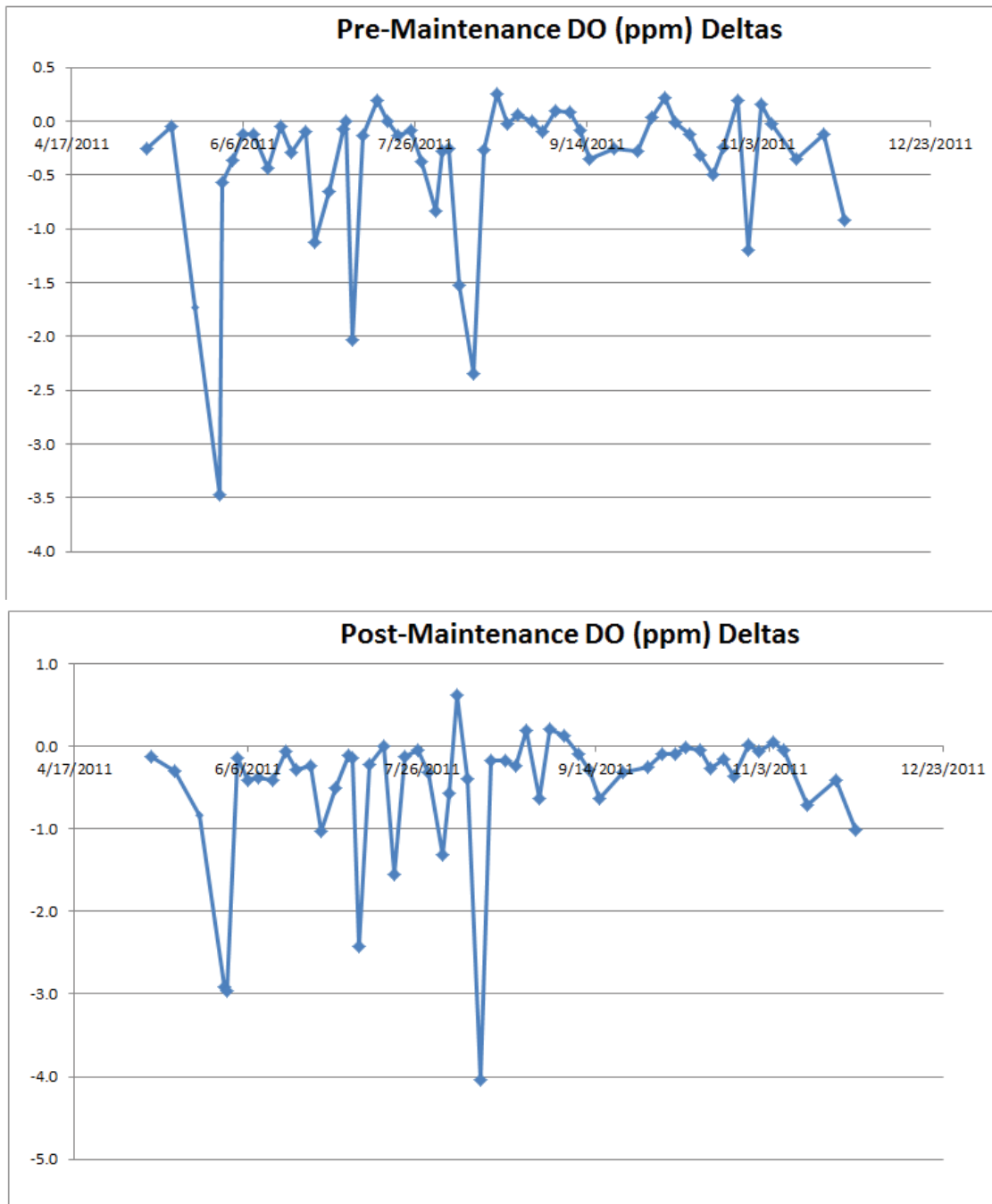


Figure 2-3. Comparison of DO concentrations measured at the seafloor as compared to DO concentrations measured 1.5 m above the seafloor. Negative values mean the benthic boundary layer has a lower DO concentration than the overlying water column. These comparisons were made on days where sonde maintenance (calibration checks and cleaning) was performed so data were available to do comparison before and after these activities.

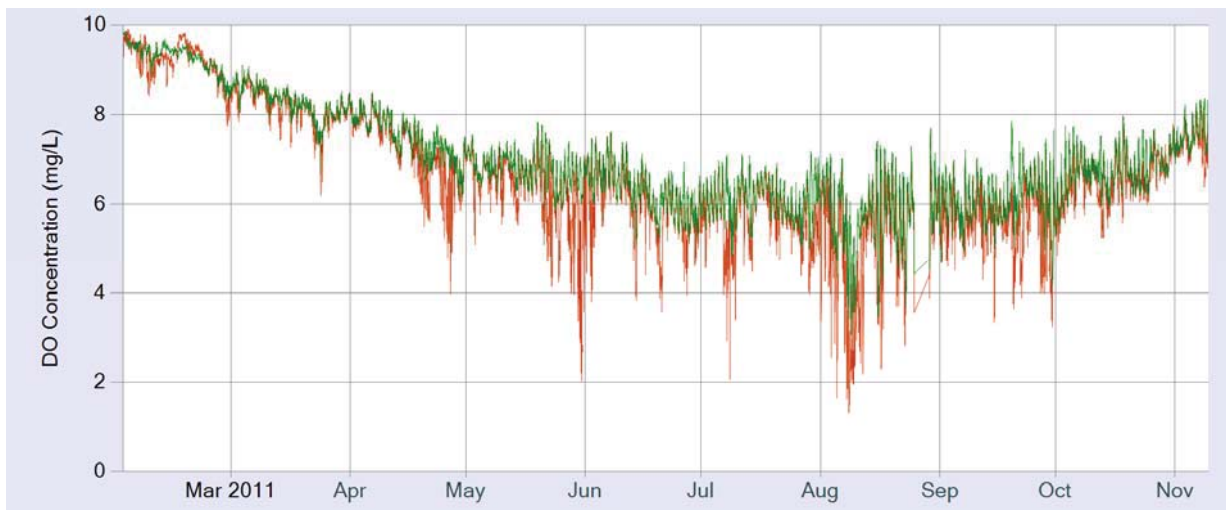
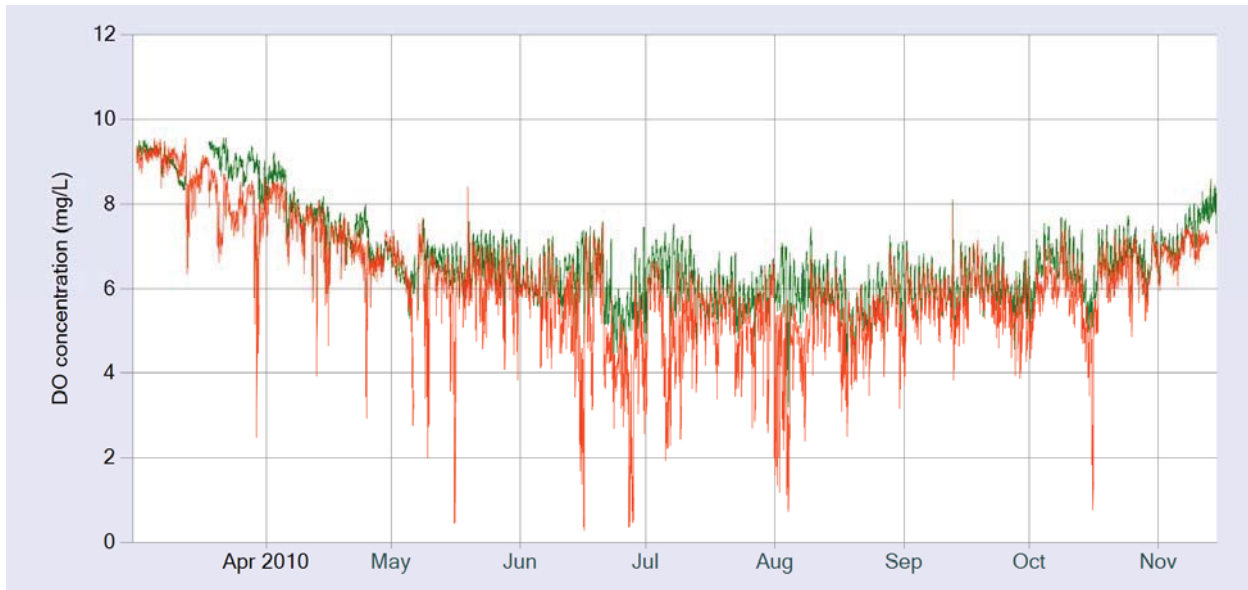


Figure 2-4. Time series of DO concentration in the surface (green) and bottom (red) waters during warm seasons (June through Sept) of 2010 (top panel) and 2011 (bottom panel).

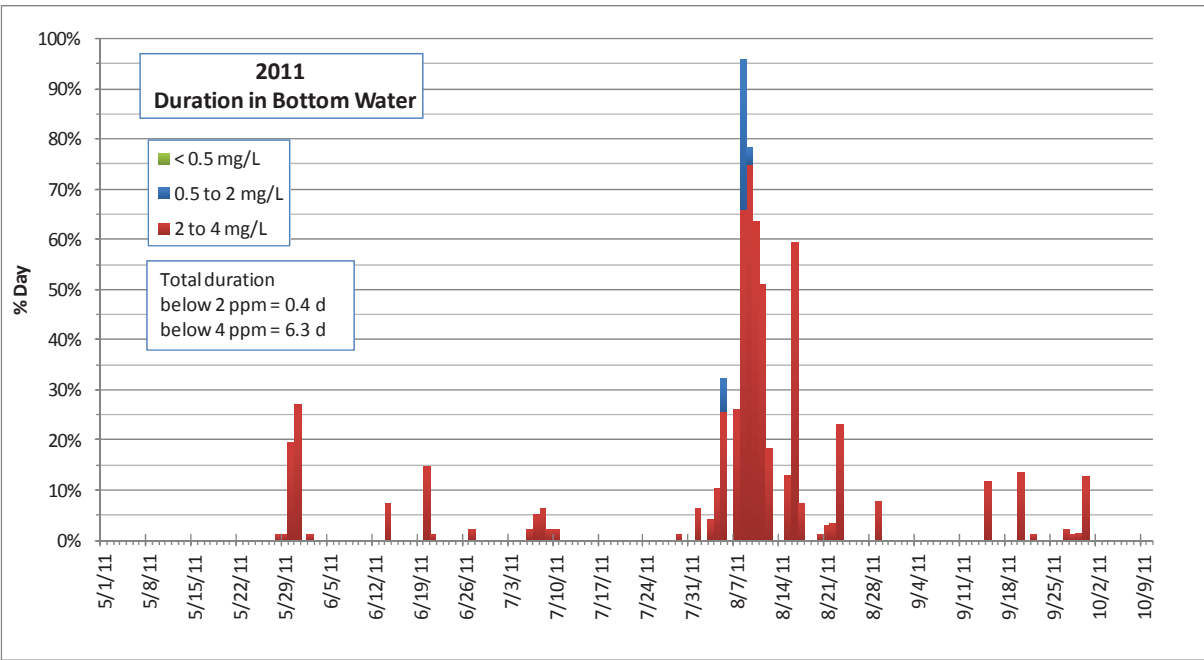
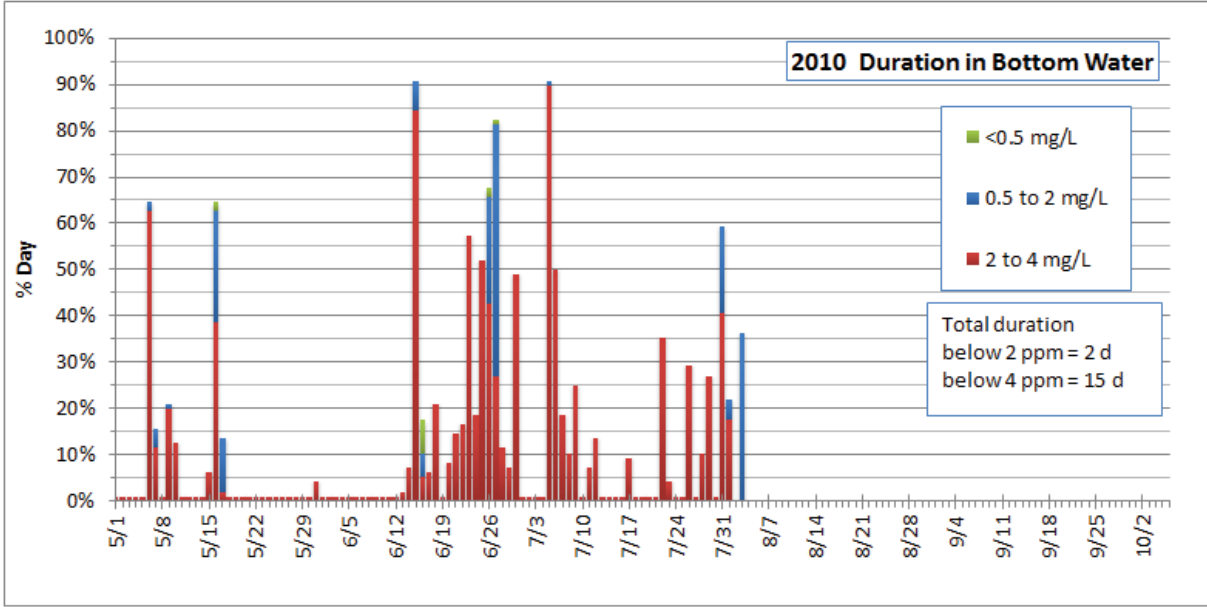


Figure 2-5. Duration of low DO conditions in the bottom water at Apache Pier during hypoxia season (May through October) of 2010 (top panel) and 2011 (bottom panel).

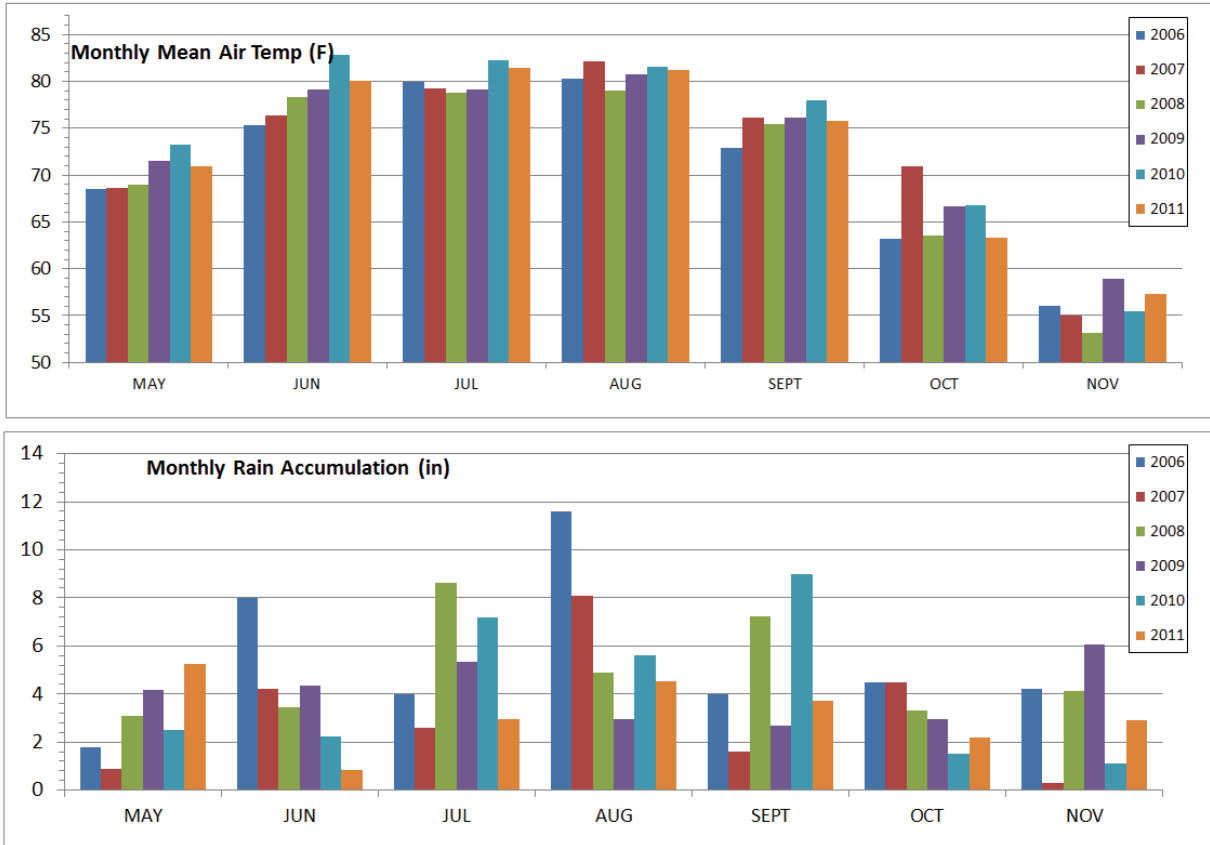


Figure 2-6. Meteorological conditions at the North Myrtle Beach airport (NCDC station: KCRE). Top panel is the monthly mean air temperature (F) and the lower panel, monthly rain accumulation (in).

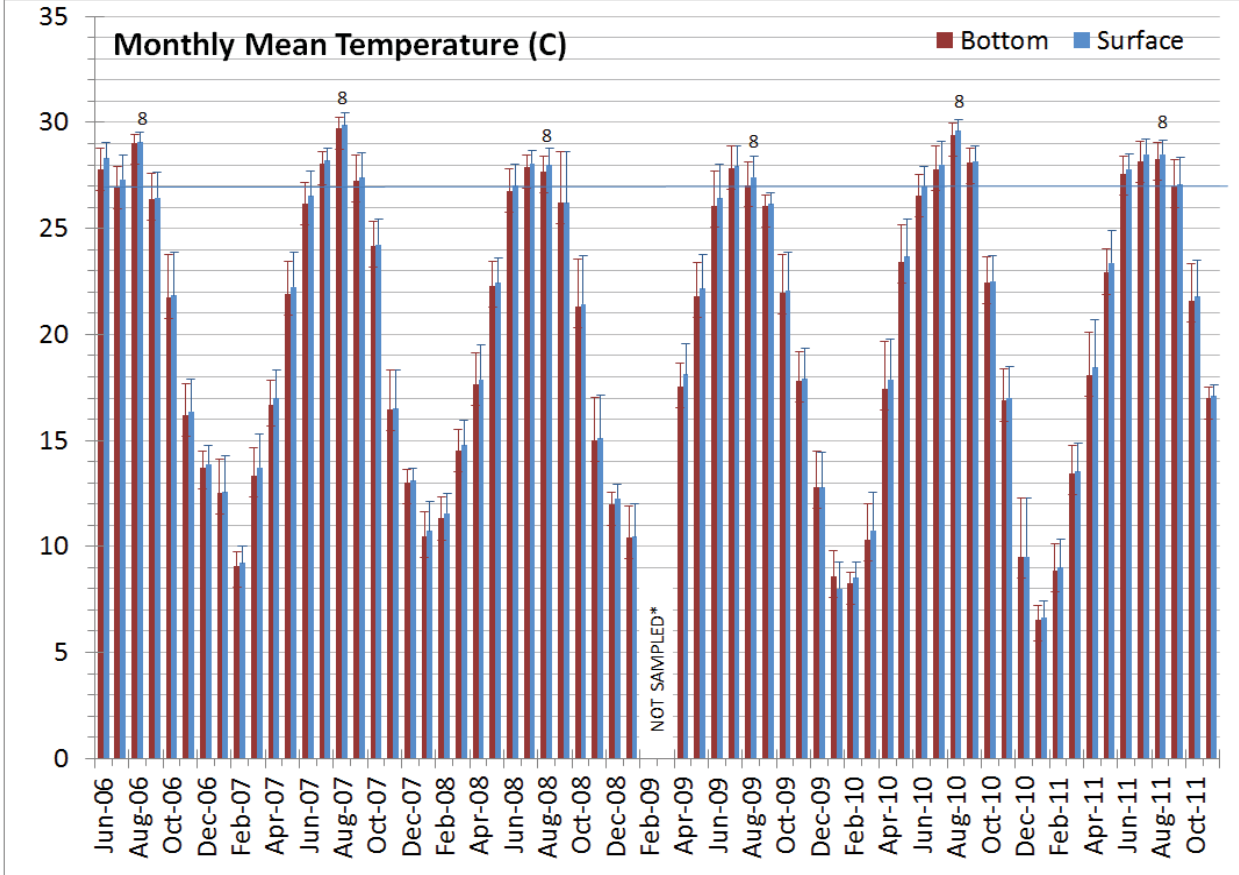


Figure 2-7. Average monthly temperatures in the bottom and surface waters of Apache Pier. Months of August are marked with “8”. The blue line is provided to facilitate comparison of summer temperatures on an interannual timescale.

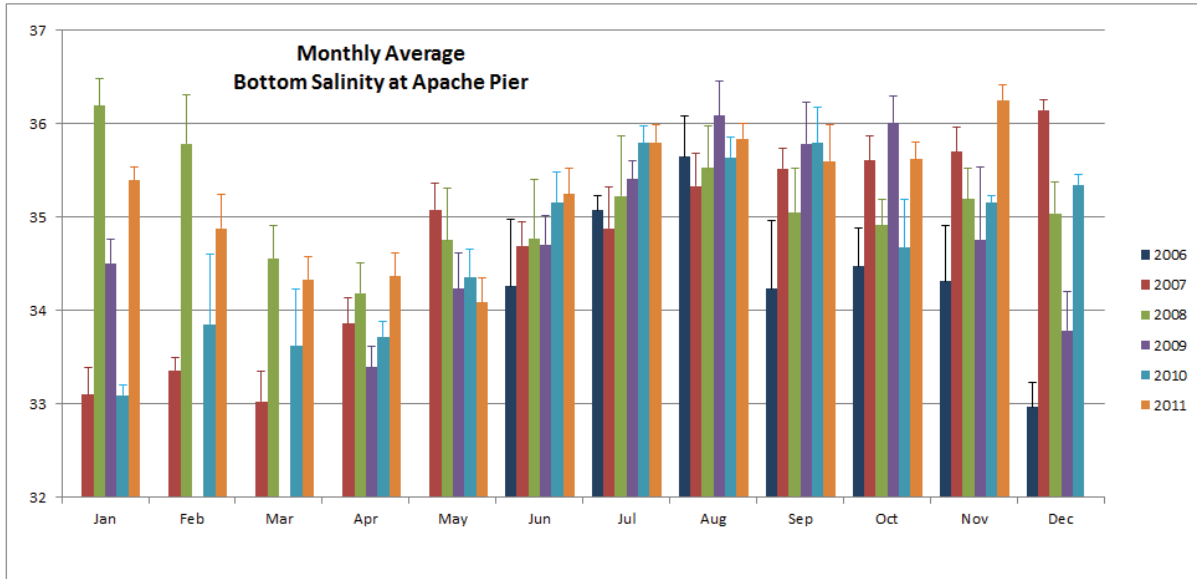


Figure 2-8. Average monthly salinity in the bottom waters off Apache Pier for 2006 through 2011.

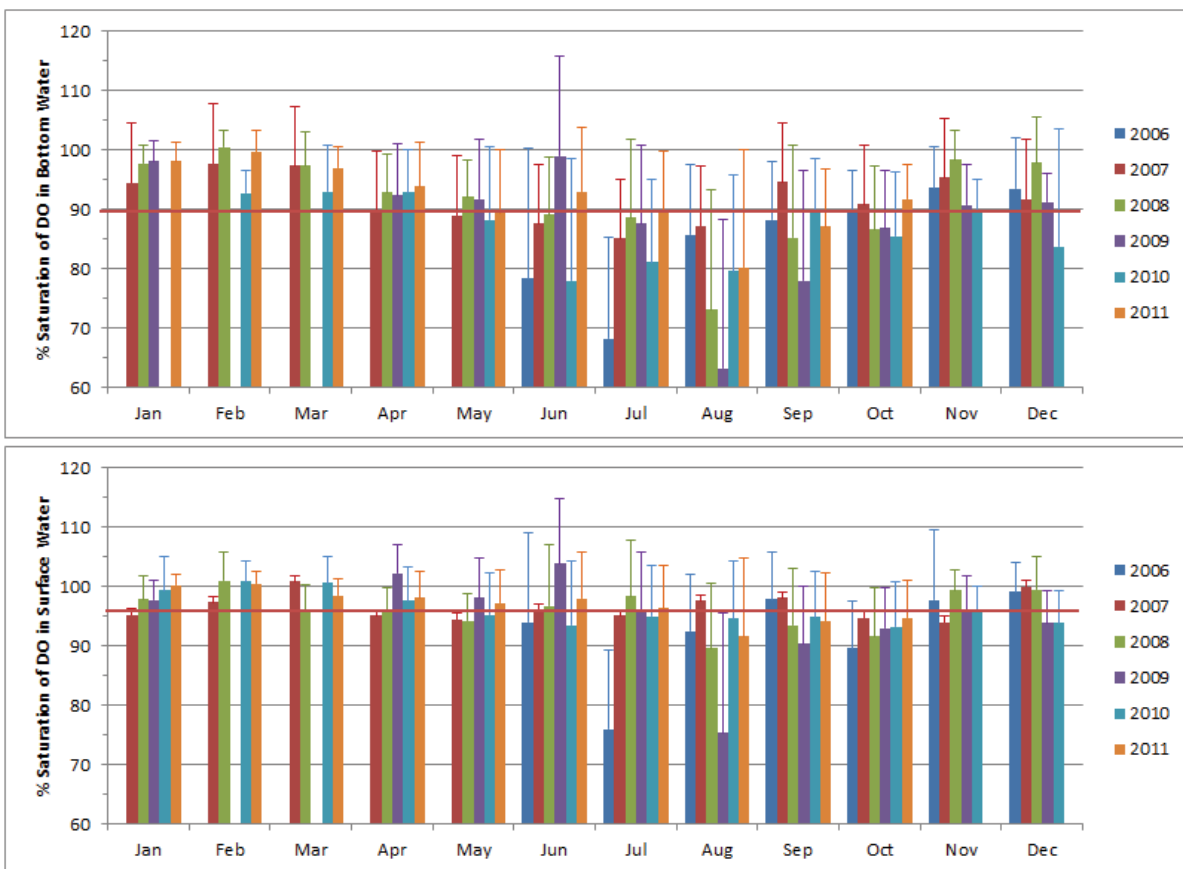


Figure 2-9. Average monthly percent saturation of dissolved oxygen in the bottom waters (top panel) and surface waters (bottom panel) off Apache Pier for 2006 through 2011. The red line marks the overall mean value. The error bars represent 1 standard deviation (SD) of the mean monthly value.

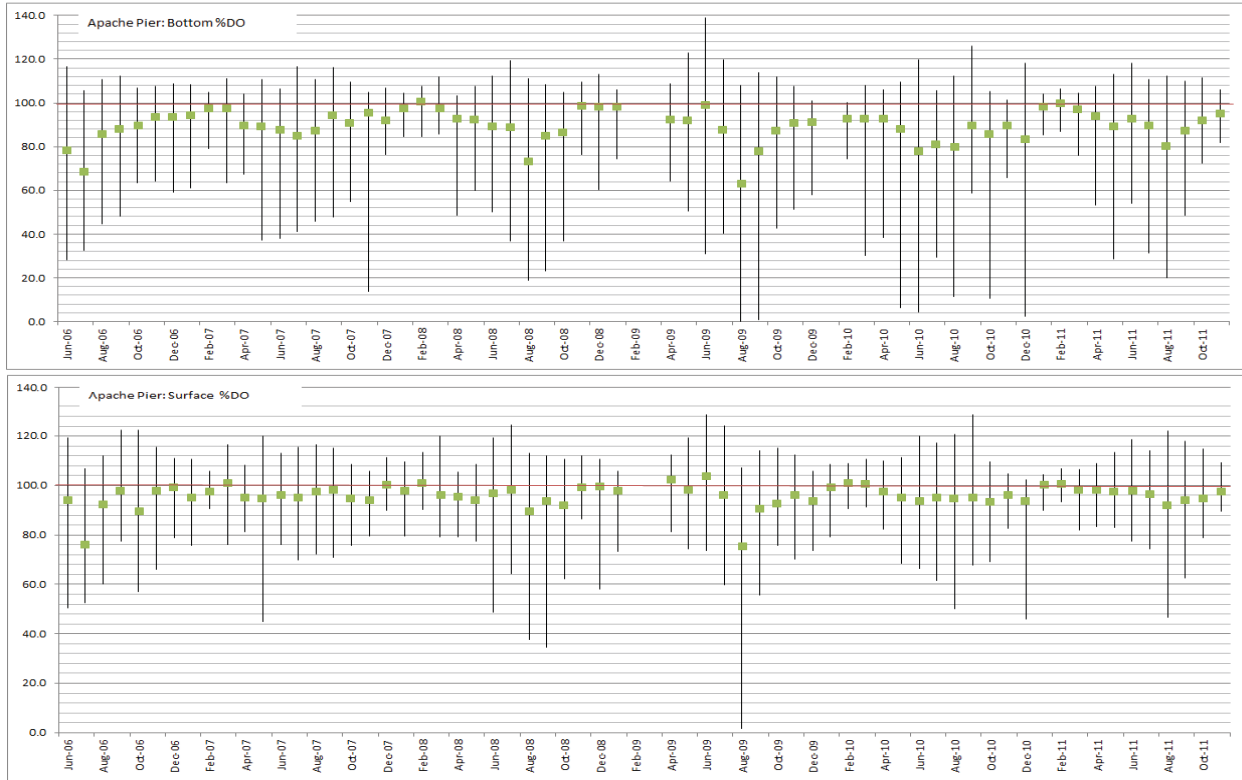


Figure 2-10. Average monthly % saturation of dissolved oxygen in the bottom waters (top panel) and surface waters (bottom panel) off Apache Pier for 2006 through 2011. The red line marks 100% saturation. The black lines represent the monthly maximum and minimum values.



Figure 2-11. Step function nature of low temperature/low DO event during June 2010. Effects are most pronounced from 6/25 to 6/26 where salinity increases also occur. 0.54” of rain fell on 6/19 to 6/20.

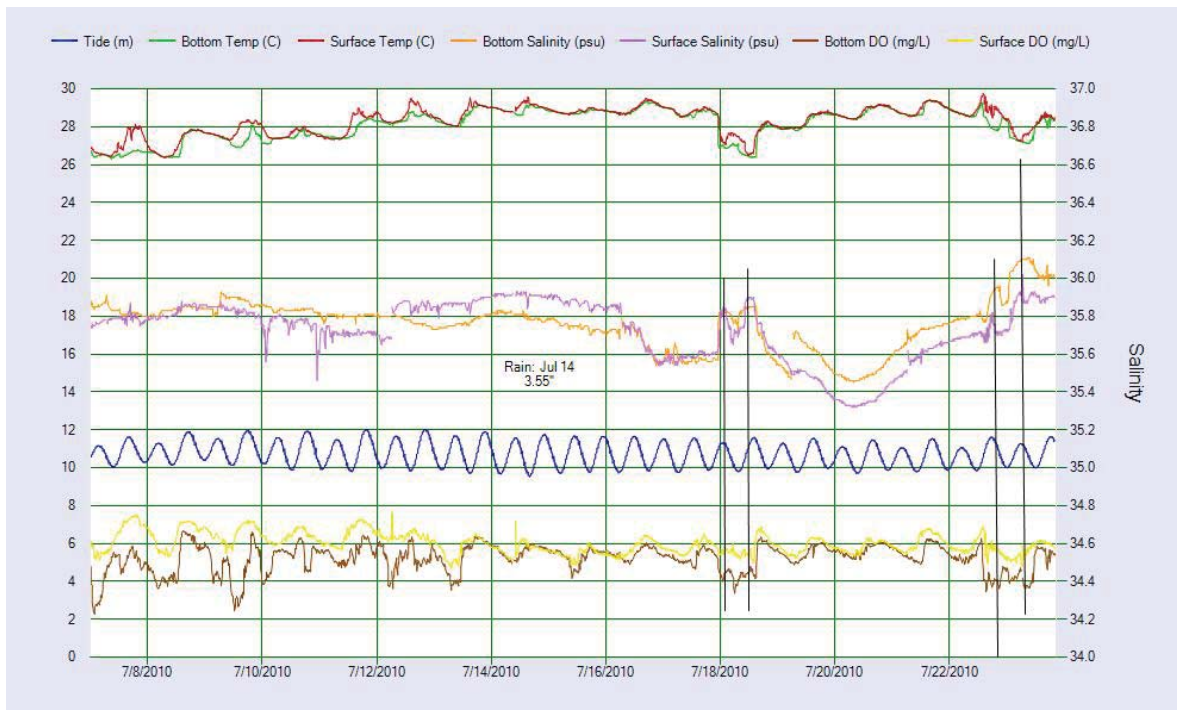


Figure 2-12. Brief low temperature/low DO events during July 2010 that coincided with salinity increases. 3.55” of rain fell on 7/14.

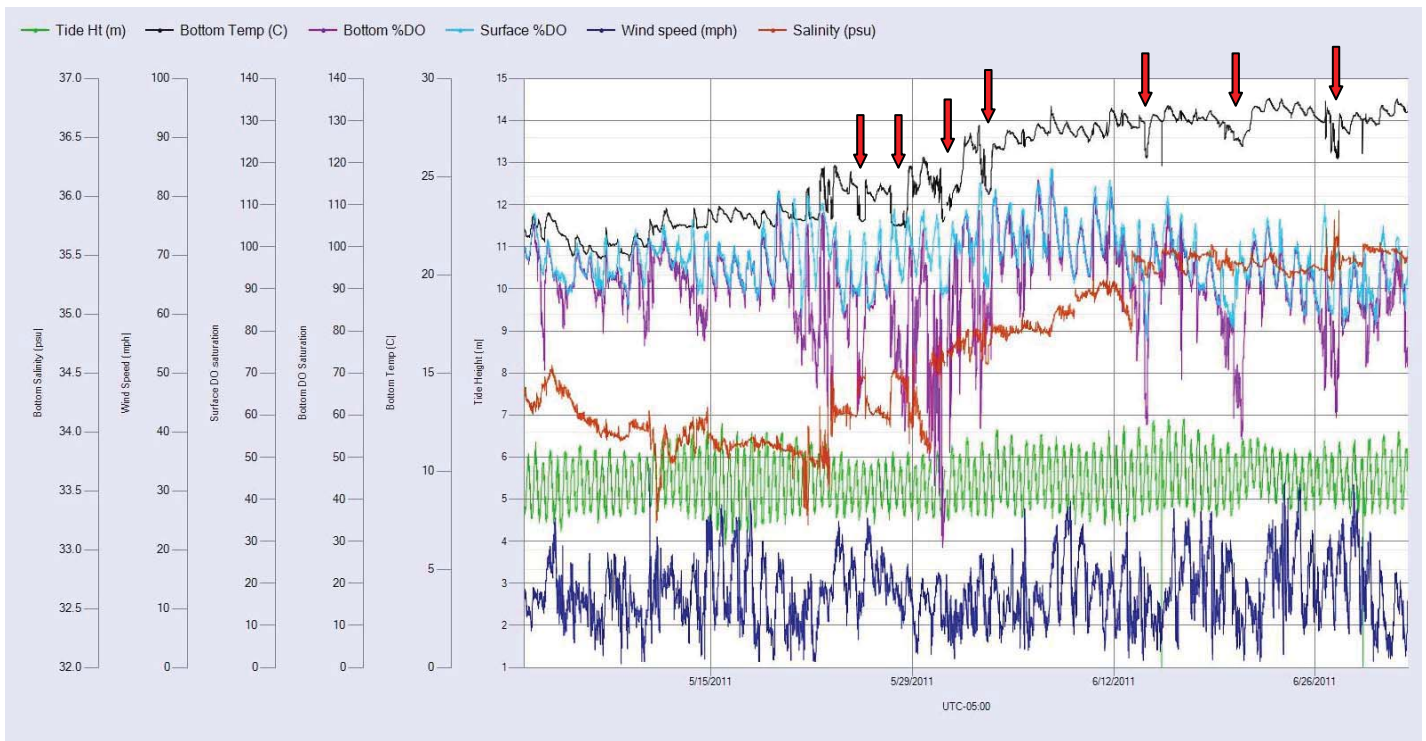


Figure 2-13. Apache Pier water quality and meteorology observations in May 2011. Red arrows mark periods of low temperature and concurrent low DO as represented by % saturation of DO. Note that wind speeds were below 10 mph during each of these events.

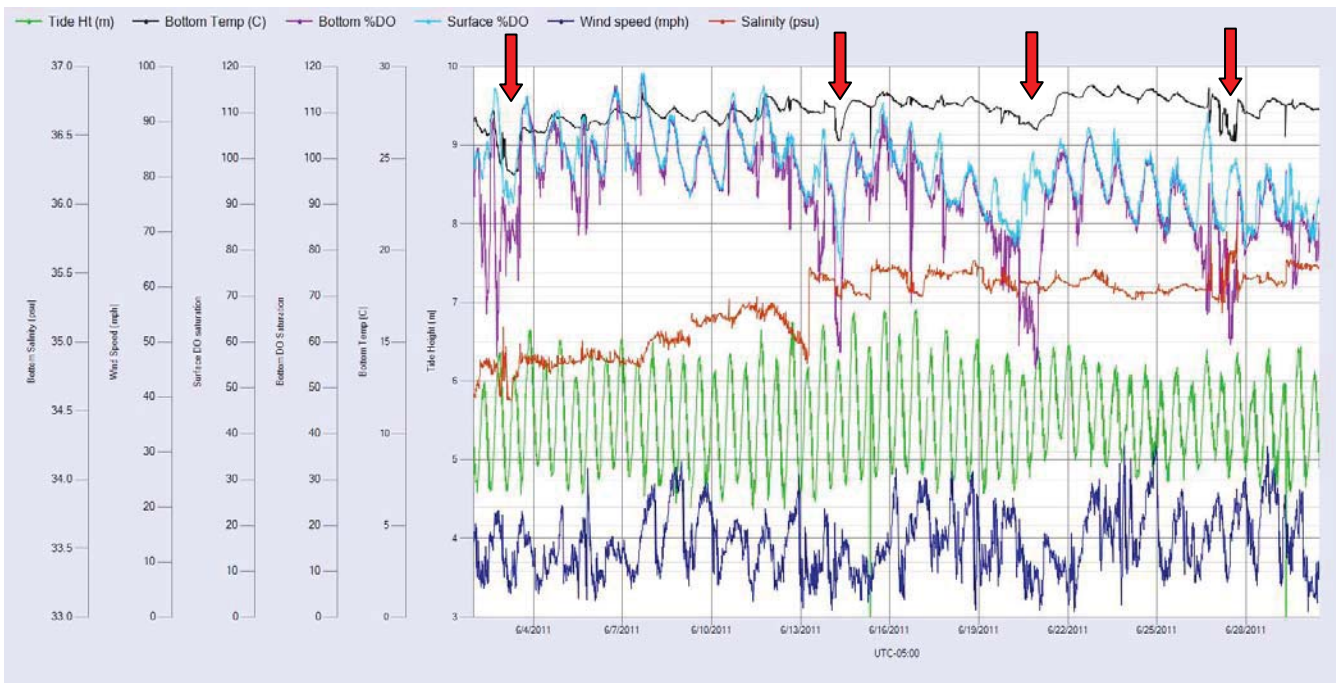


Figure 2-14. Apache Pier water quality and meteorology observations in June 2011. Red arrows mark periods of low temperature and concurrent low DO as represented by % saturation of DO. Note that wind speeds were below 10 mph during each of these events.

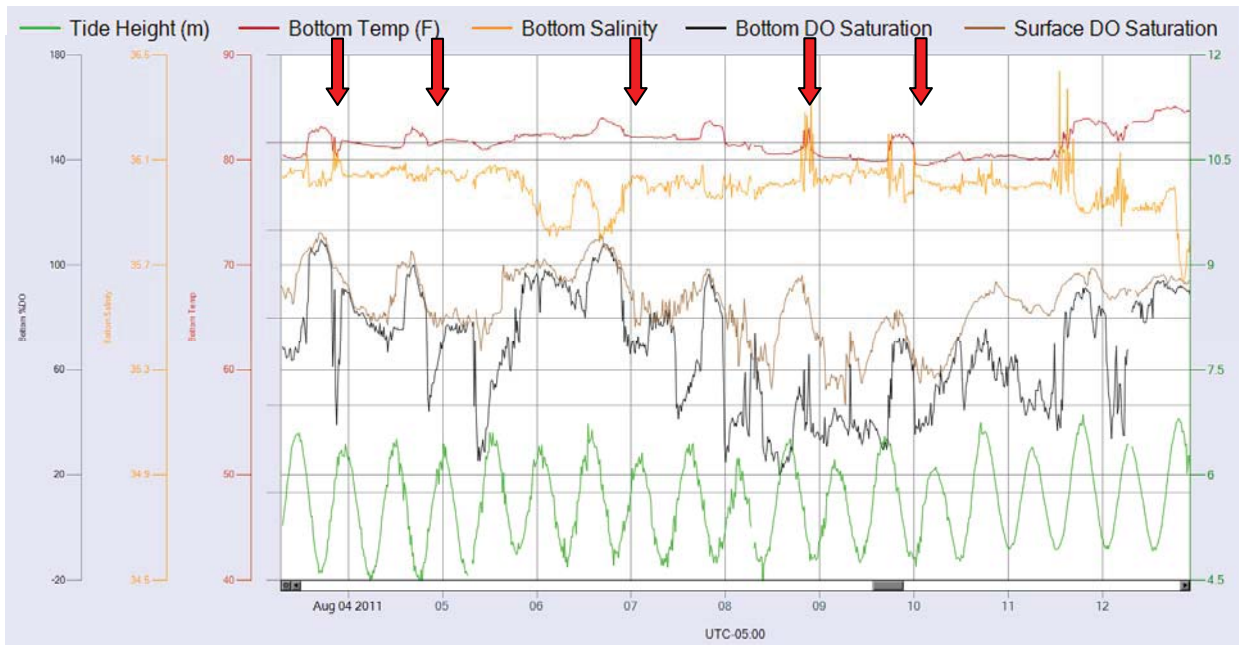


Figure 2-15. Apache Pier water quality and meteorology observations in August 2011. Red arrows indicate periods of low temperature and concurrent low % saturation DO.

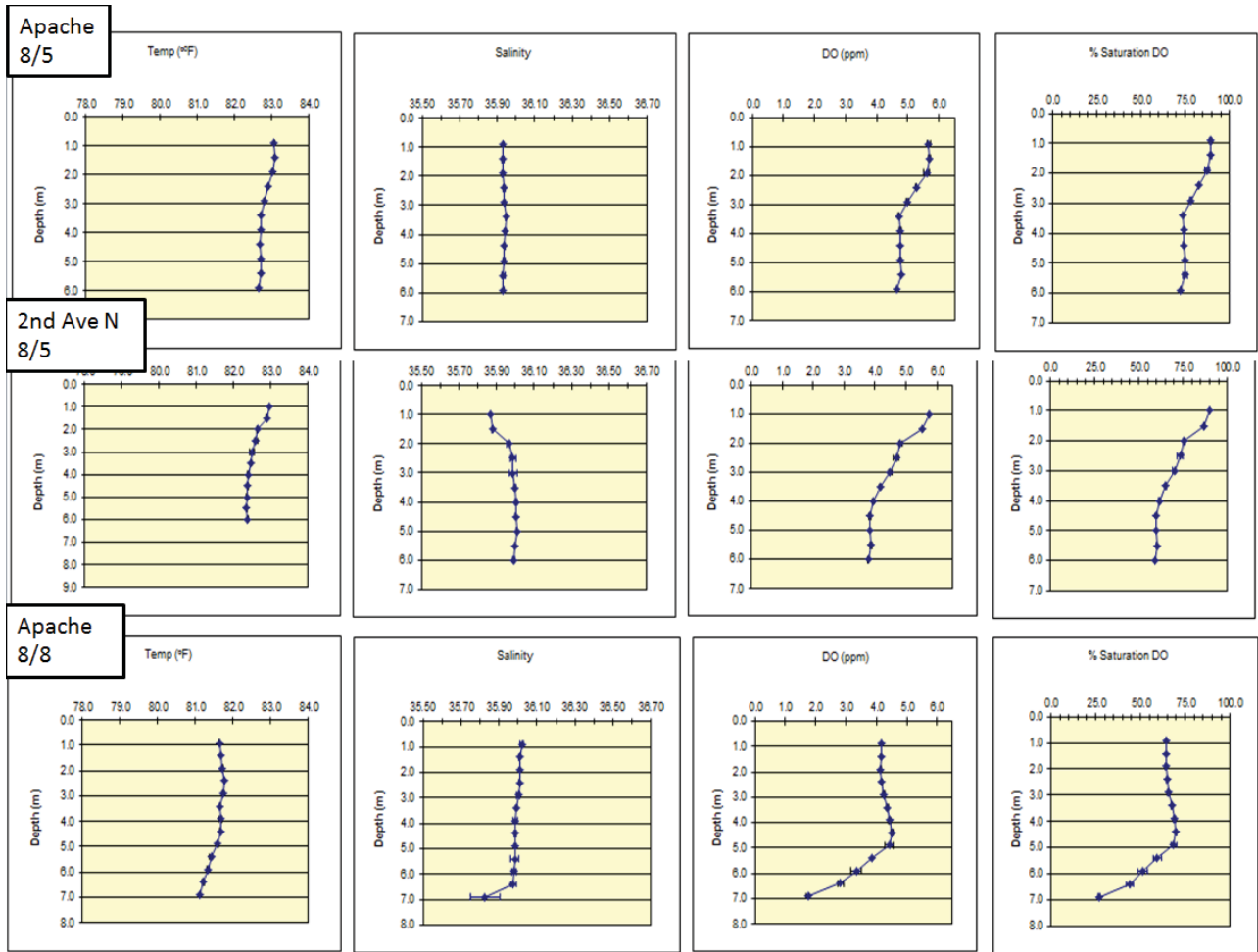


Figure 2-16. Vertical profiles measured on 8/5/11 and 8/8/11 during the low DO event which occurred in early August 2011.

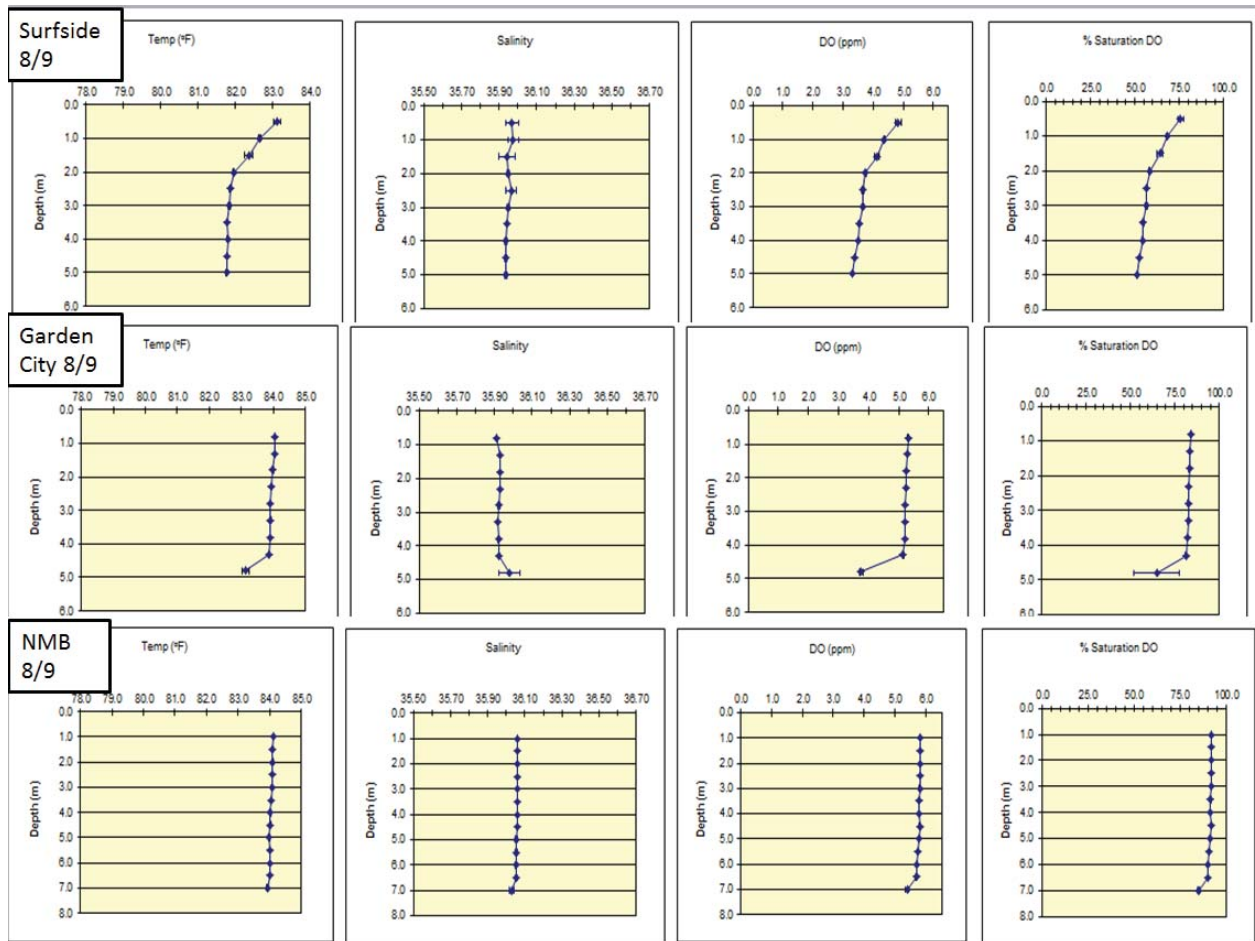


Figure 2-17. Vertical profiles measured on 8/9/11 during the low DO event which occurred in early August 2011.

Radon measurements in bottom waters – Rick Peterson and Rich Viso (CCU)

Based on individual grab sampling efforts during the 2009 hypoxia periods (see McCoy et al. 2011), high radon activities in the bottom waters correlated with low oxygen, low temperature water masses. Since radon is considered a highly effective biogeochemical tracer of groundwater discharge, these observations led the authors to speculate that a groundwater source was contributing to the occurrence of hypoxia in the nearshore zone of Long Bay. Alternatively, the prevalence of high radon with low oxygen conditions could also be indicative of less dispersive mixing with offshore waters during hypoxia periods. An important note here is that groundwater discharge can be composed of both fresh, terrestrial water from continental drainage, or re-circulated seawater flushing through shallow sediments (Burnett et al. 2006). Either mechanism is capable of transporting nutrients and organic matter buried in the sediments back into the water column, where it can support primary and/or secondary producers. If the groundwater discharge transports labile organic carbon, it has the possibility of supporting a net heterotrophic system, where oxygen will ultimately be drawn down.

In an effort to create a more robust data set of radon activities correlating with oxygen dynamics, radon was measured continuously in the bottom water at Apache Pier through the course of this project. We used a commercially-available radon monitor (RAD7; DurrIDGE Co.) connected to an air-water equilibrium chamber (WAT-H₂O; DurrIDGE Co.). Water delivered from a submersible pump suspended ~1.5 m above the bottom at the end of Apache Pier flowed through the air-water equilibrium chamber, where the radon was degassed for subsequent analysis on the RAD7 (Burnett et al. 2001). The RAD7 would integrate radon counts over 30 minute intervals to maximize our temporal resolution while maintaining adequate measurement resolution. It is worth noting that this project represents the first attempt anyone has made to deploy this equipment for an extended period of time in such an exposed (uncontrolled) environment.

We began the measurements on September 20, 2010 and continued the analysis through October 25, 2010 when a pump failure decommissioned the RAD7. Results were representative of non-hypoxia radon behaviors, with low concentrations generally present with no apparent variation due to tidal fluctuations (Figure 2-18). Even though equipment failures caused us to miss a substantial hypoxia episode during this time, this fall 2010 deployment offered the opportunity to experiment with the best equipment setup to maximize our efforts.

Peterson was out of the country for November and most of December 2010, so these early efforts were not continued in his absence. Preceding the onset of hypoxia season in 2011, we re-deployed the radon equipment at Apache Pier on March 1. With the exception of the occasional submersible pump failure, the equipment ran continuously at Apache Pier until a catastrophic failure occurred on July 13, 2011, destroying the RAD7.

Radon data records from spring and summer 2011 confirms the strong relationship originally suspected by McCoy et al. (2011) between radon and dissolved oxygen concentrations. Beginning in March 2011 (Figure 2-19), we observe occasional excursions from ambient radon concentrations (~1400 dpm/m³) that directly coincide with decreases in dissolved oxygen concentrations. Not only are the temporal variations between the two parameters coupled, but the magnitude of excursion from ambient concentrations between them are also inherently linked

(i.e., higher radon spikes coinciding with lower oxygen levels). We observe these patterns during April 2011 (Figure 2-20), May 2011 (Figure 2-21; during which a hypoxic episode occurred when radon concentrations reached over 7000 dpm/m³), June 2011 (Figure 2-22), and July 2011 (Figure 2-23).

During July, pump problems manifested over much of the month, and were the underlying issue with such a deployment. Most submersible pumps are not designed for continuous use, nor are they intended for use in a saline environment. In addition, July 2011 was a particularly intense month for biofouling, and all these issues combined to severely degrade our water flow to the equipment. Proper radon measurements rely on a continuous and fast flow of water to the air-water equilibrium chamber, and the data suffered during this time from unreliable, low flow.

The inherent link revealed by this data set between radon and oxygen concentrations is beyond circumstantial at this point. This link raises the question as to which parameter represents the cause, and which represents the effect? Certainly micro and macro nutrients (including organic carbon) as well as radon transported by groundwater discharge could cause an oxygen dynamic response, but we can envision no scenario by which oxygen dynamics could lead to a groundwater discharge effect. Therefore, we conclude that increased radon concentrations are related to the cause, and lower oxygen concentrations are the effect.

This data set, therefore, further supports the original assertions of McCoy et al. (2011) that a groundwater source seems inherently and undeniably linked to oxygen dynamics in the nearshore zone of Long Bay. Our conclusions from this work are similar to those of McCoy et al. (2011), but based on a much more rigorous and long-term data set: increased radon activities and the associated drawdown of oxygen in the nearshore waters of Long Bay are due to either (1) enhanced discharge of groundwater, or (2) reduced dispersive mixing with offshore waters. Either possibility seems reasonable. Increased groundwater discharge can occur following rain events, or be a function of various oceanographic driving forces causing additional recirculation of seawater through the shallow sediments (e.g., higher tidal range, winds forcing more water on the beach, etc.). Reduced dispersive mixing could occur via horizontal/vertical stratification due to oceanographic scenarios.

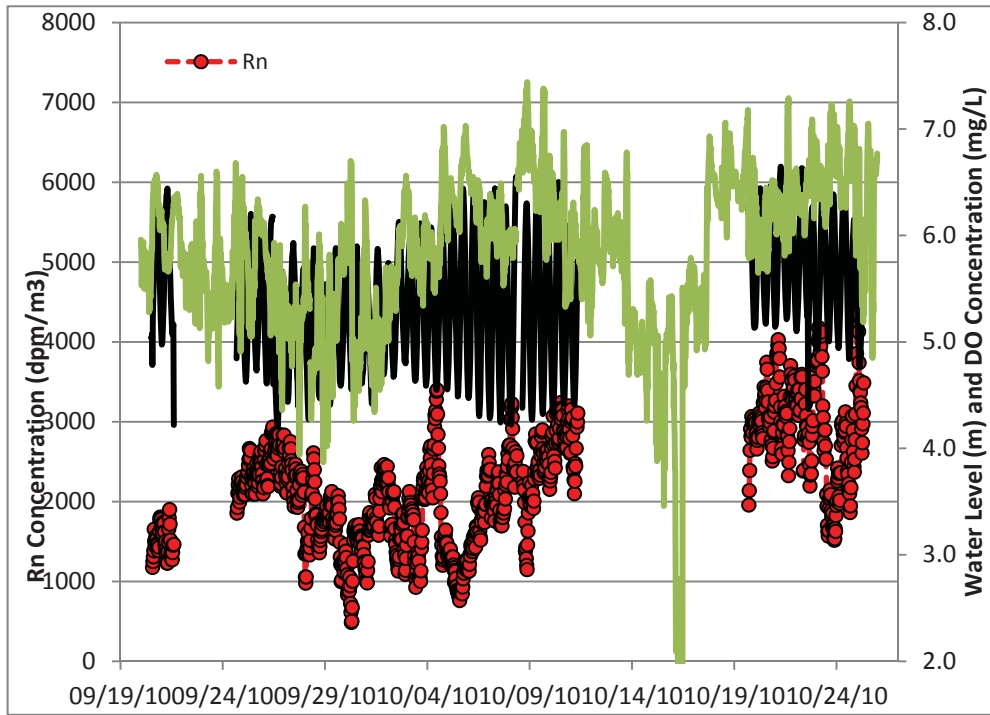


Figure 2-18. Record of radon activity (red circles), dissolved oxygen (green line), and tidal amplitude (black line) from September and October 2010 at Apache Pier.

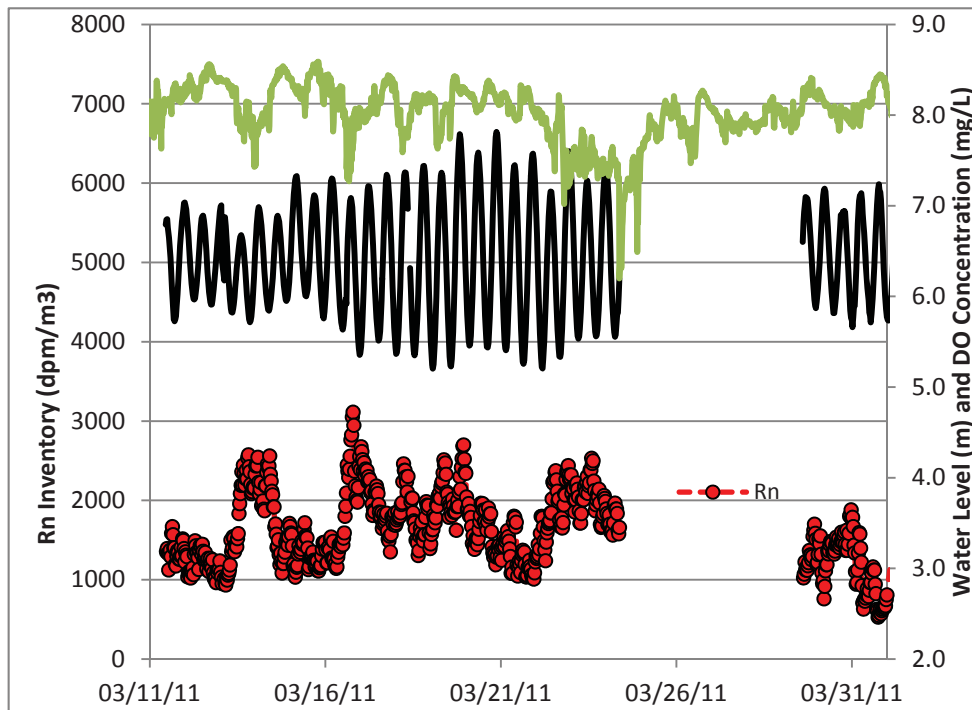


Figure 2-19. Record of radon activity (red circles), dissolved oxygen (green line), and tidal amplitude (black line) from March 2011 at Apache Pier.

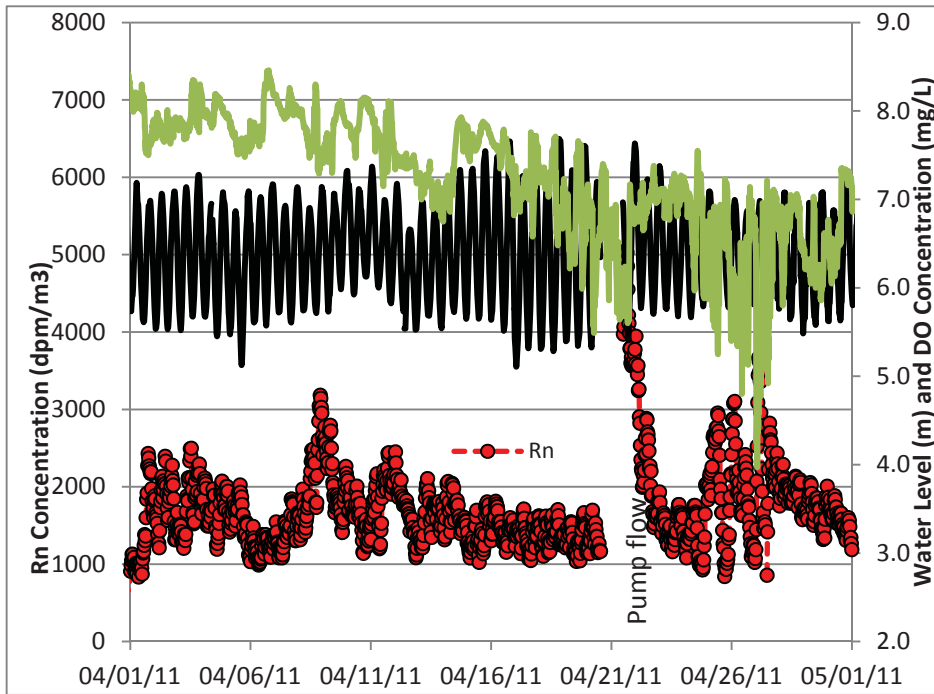


Figure 2-20. Record of radon activity (red circles), dissolved oxygen (green line), and tidal amplitude (black line) from April 2011 at Apache Pier.

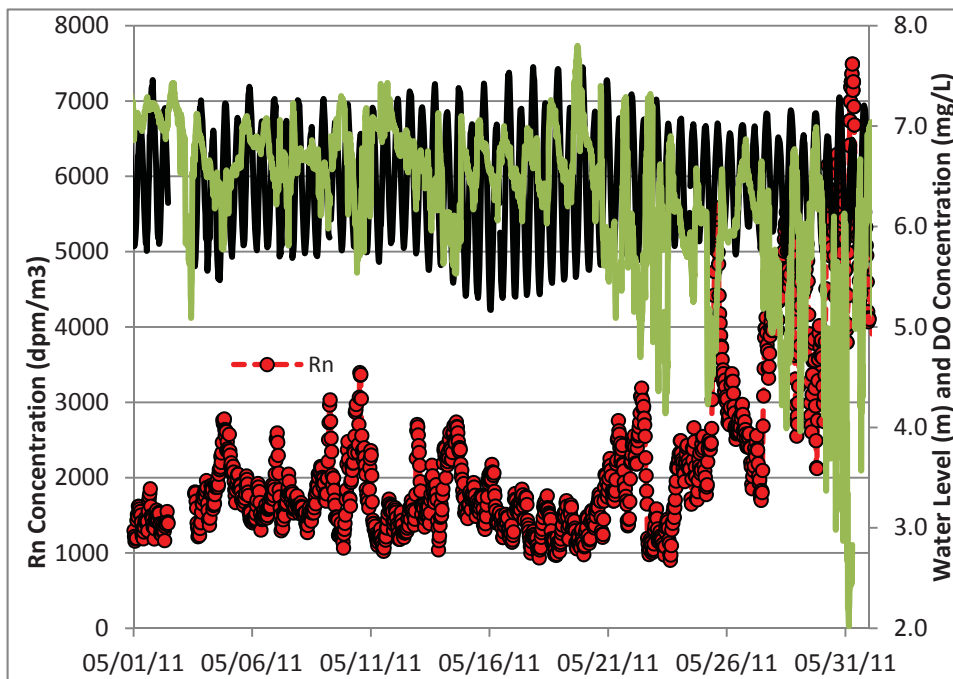


Figure 2-21. Record of radon activity (red circles), dissolved oxygen (green line), and tidal amplitude (black line) from May 2011 at Apache Pier.

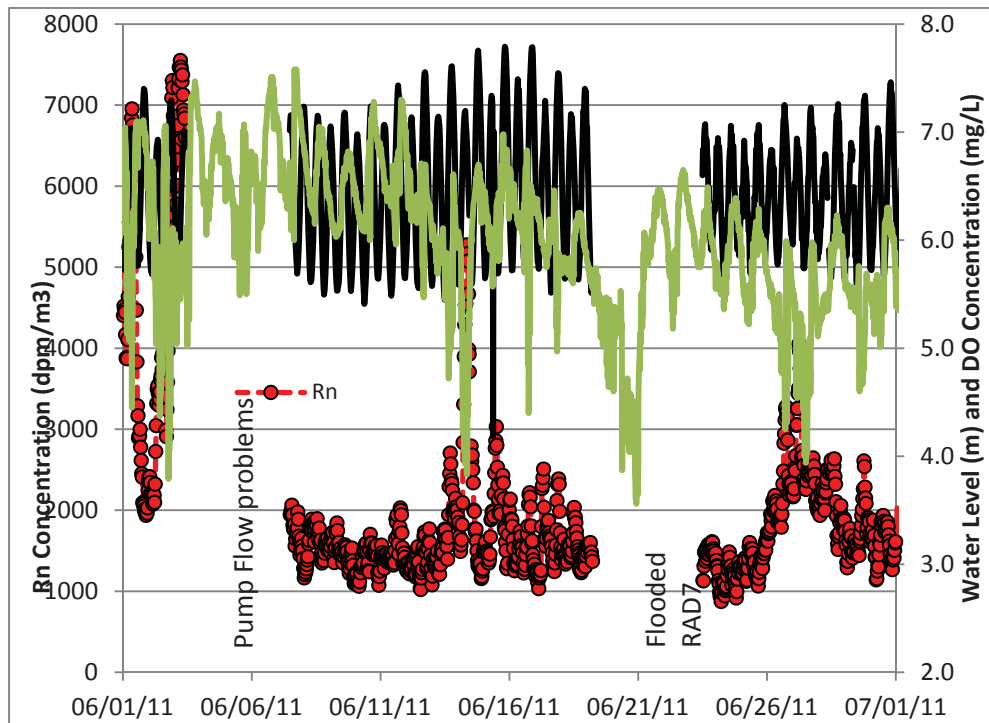


Figure 2-22. Record of radon activity (red circles), dissolved oxygen (green line), and tidal amplitude (black line) from June 2011 at Apache Pier.

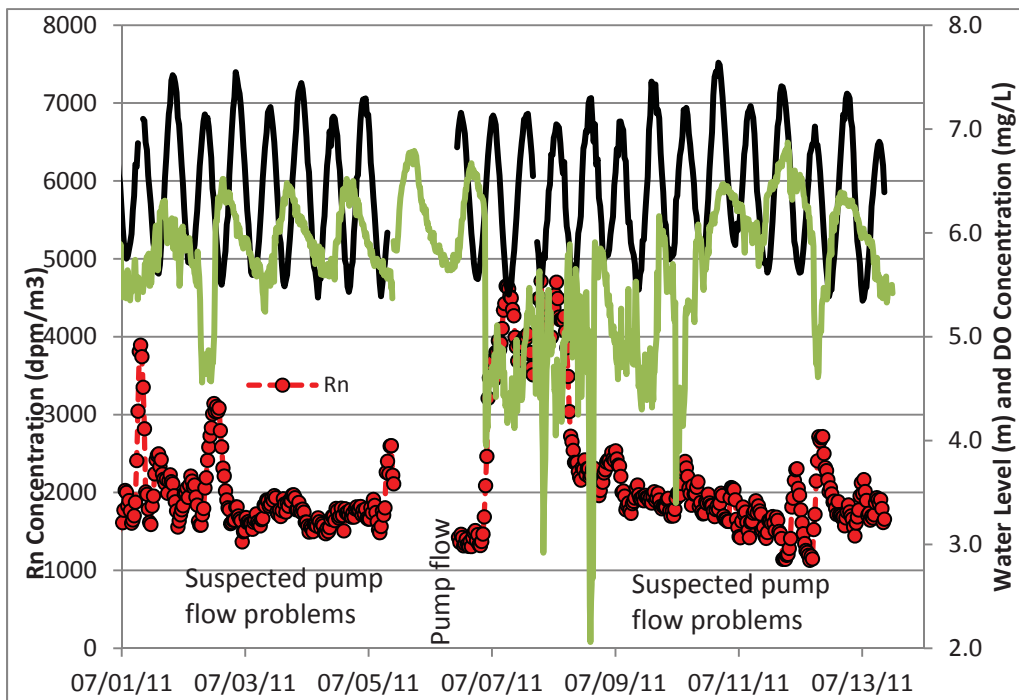


Figure 2-23. Record of radon activity (red circles), dissolved oxygen (green line), and tidal amplitude (black line) from July 2011 at Apache Pier.

Chlorophyll, CDOM and turbidity in bottom waters – Eric Koepfler (CCU)

The sampling of a multi-seasonal time series of chlorophyll *a* (*in vivo* fluorescence) and CDOM at Apache Pier was not successful due to a series of unforeseen events including manufacturer delays in recalibration, equipment failures and computer crashes which resulted in the loss of data. Therefore, only a short 12 day record was obtained and analyzed. In addition, a synergistic class research, not required in the contract, will be presented.

During the time period of the study, the spring semester 2011 Marine Plankton class at Coastal Carolina University (under Dr. Koepfler's supervision) conducted bioassay and field studies based out of Apache Pier. Bioassay experiments were conducted on two occasions including 3/1/11 and 4/1/11 (Figure 2-24). For the bioassays, nutrient additions of ammonium, phosphate, and organic carbon (glucose) and combinations thereof were added at concentrations based upon field observed values for extreme hypoxia and anoxia conditions observed in the summer of 2009. These 1 L samples were incubated for 5 days in climate controlled incubators under 12h / 12h light dark cycles, at *in situ* temperatures and under light conditions of 200 $\mu\text{E cm}^2/\text{s}$. Samples were taken from replicate (n=3) polystyrene containers at 1, 3 and 5 days for chlorophyll *a* and bacterial direct count using acridine orange. Patterns of bacterial abundance on day 5 (Figure 2-24, a-b) were similar on both bioassay dates, although replicate variability was more dramatic in the first bioassay resulting in no significant difference by a single factor ANOVA. The second bioassay showed highly significant results (ANOVA $p= 9.84\text{E}^{-12}$) with 6 overlapping subgroups determined by Tukey multiple range test ($\alpha=0.05$). These results suggested that bacterial growth was limited primarily by carbon, secondarily by phosphorus, and lastly nitrogen. Phytoplankton growth responses (Figure 2-24, c-d) based upon chlorophyll *a* were unequivocal (ANOVA $p= 3.16\text{E}^{-3}$ and $p= 8.53\text{E}^{-4}$ respectively) in each bioassay with 2 overlapping subgroups resulting from each. These results indicated strong phosphorus stimulation followed by nitrogen and organic carbon in the first bioassay and a slightly different ranking of equal phosphorus and organic carbon and secondarily nitrogen stimulation in the second bioassay. The phosphorus and organic matter stimulation of the phytoplankton was not expected but does provide a mechanism for both trophic categories of plankton to be stimulated with the proper type of nutrient loading.

The field study performed by the class looked at temporal changes in bacterial abundance and phytoplankton biomass (chlorophyll). Figure 2-25 shows results for bacterial abundance and chlorophyll *a* from surface and bottom waters. Two factor ANOVA indicated highly significant date and depth variation but both bacterial abundance and chlorophyll *a* had significant interaction terms meaning that the temporal patterns of these factors varied by depth. Both bacteria and chlorophyll showed low values in January and February, a spike in bottom water values in March followed by a decline and an increase again associated with the final sampling at the end of April. Surface water values of bacteria and chlorophyll *a* were more tightly correlated ($R^2 = 0.56$) over this time period than were associations in the bottom waters ($R^2 = 0.17$). Chlorophyll *a* was always higher in bottom waters with values in March and April increasing to 2-3 times higher than observed for surface. Bacterial abundance showed no significant trend for surface to bottom water differences and depth was marginally significant in the ANOVA analysis ($p = 0.035$). The significant increase in bacterial abundance and chlorophyll *a* in both surface and bottom waters between 4/11 and 4/20 coincided with a break in ambient O^2 decline

rates relative to the Apache pier record from 3/1 through 4/10 which was roughly -0.02 mg/d. The O² decline rate between 4/11 through 4/20 was 0.24 mg/d, roughly 10 times higher.

Size fractionated chlorophyll *a* was also collected during this field study (Figure 2-26, a-b) and demonstrated very strong temporal change and treatment effects. Between the beginning date and ending date of this study the % chlorophyll <10µm increased from 28% to 42-45% for bottom and surface water respectively.

A secondary peaking in chlorophyll on 3/21 for surface and 3/7 for bottom waters had differing size characteristics being represented by 50 % of chlorophyll <10 µm in surface waters, but much larger sized plankton for bottom waters (13 % was <10 µm). The oxygen record regarding these secondary chlorophyll peaks was more responsive (declined by roughly 0.5 mg over several days) to the surface chlorophyll having the smaller cell sized characteristics. The chlorophyll peaks observed in March may help explain the occurrence of March-time O² declines that have been seen in other years at Apache pier. Again, similar to finding from the SCSGC funded hypoxia study a tendency for O² declines with chlorophyll increases was observed.

Analysis of the fluorometer data as previously mentioned was minimal, however a good record was obtained during one of the most significant low DO drops observed in 2011 (Figure 2-27). This record from 5/24 through 6/3 includes a period prior to the O² decline where chlorophyll varied directly with oxygen (from 0 to case 90) followed by a period leading beyond the DO minimum value of ca. 2.05 observed on 5/31. Correlation of the fluorometer *in vivo* chlorophyll records and the pier sonde oxygen records for these time periods versus each other and ancillary variables are indicated in Figure 1-28. To incorporate Radon into this assessment the dataset had to be trimmed to encompass the time series of roughly case number 0-170 from Figure 1-13 above. Correlation analysis using the Pearson method revealed transitions in relationships between many biological variables. Chlorophyll was positively correlated to DO during the before event period (p=0.038) but was strongly negatively correlated after (p=8.78E-8). Both CDOM and Radon were negatively correlated to chlorophyll during the before event period (p=4.81E-6 and 1.61E-4), but were uncorrelated or positively correlated after the event (Radon p=2.14E-5). The contrast regarding the Apache pier sonde record for DO revealed Radon as correlated during both periods but becoming much more highly correlated during the after event (p=1.68E-5 versus 1.11E-13). This record and events were bracketed by a meteorological condition of sustained upwelling favorable winds (160-220°) and sustained velocity (5-25 km/h) for approximately 7-8 days prior to the event. Bottom sonde temperature records also indicated the arrival of a tidally fluctuating colder water mass appearing on the 26th and persisting for 3-4 days. The interpretation of this correlation analysis is that the increases frontal retention of shallow shelf waters associated with the front concentrated chlorophyll and particulate organics which also contained heterotrophic microbial communities that possessed a oxygen demand that led to this DO decline. The inverse relationship between chlorophyll and DO during this period simply reflected a concentration mechanism that collected particulates but diminished offshore advection.

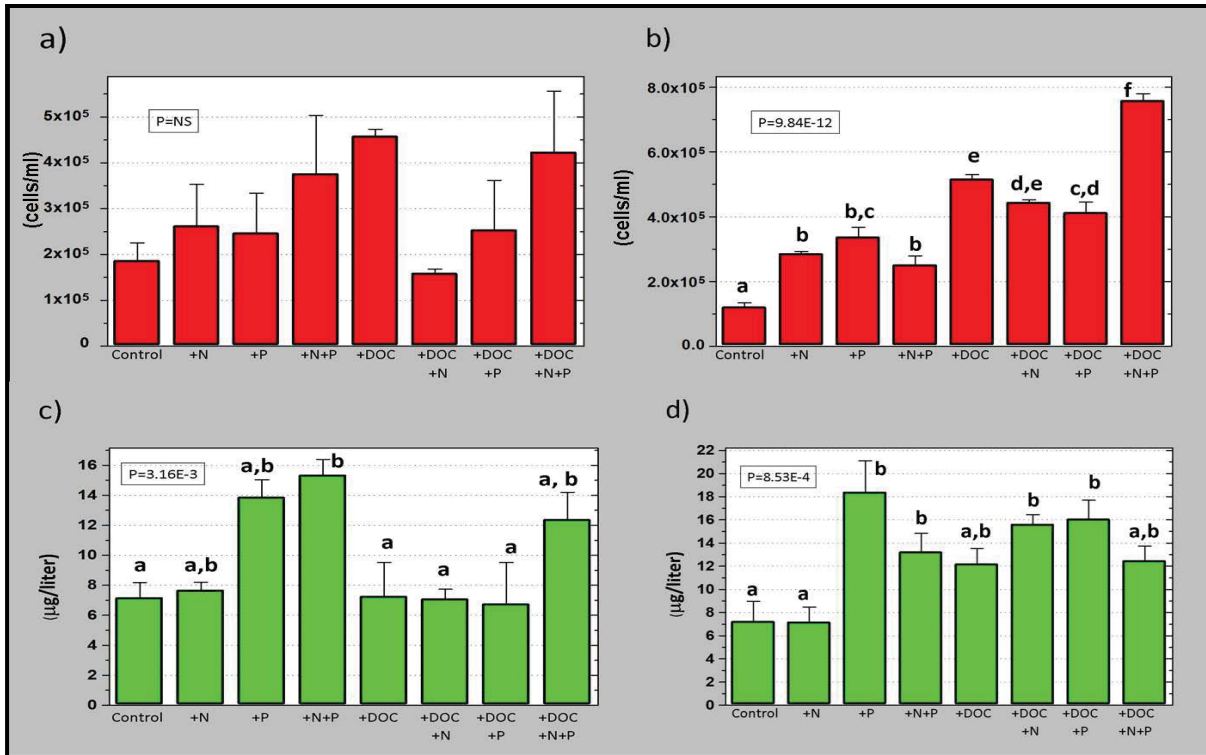


Figure 2-24. Nutrient and organic carbon bioassay results from experiments performed on 3/11 (a and c) and 4/11 (b and d). Treatment measurements of bacterial abundance are shown in red (a and b), while chlorophyll a results are shown in green (c and d) for day 5 of the bioassay.

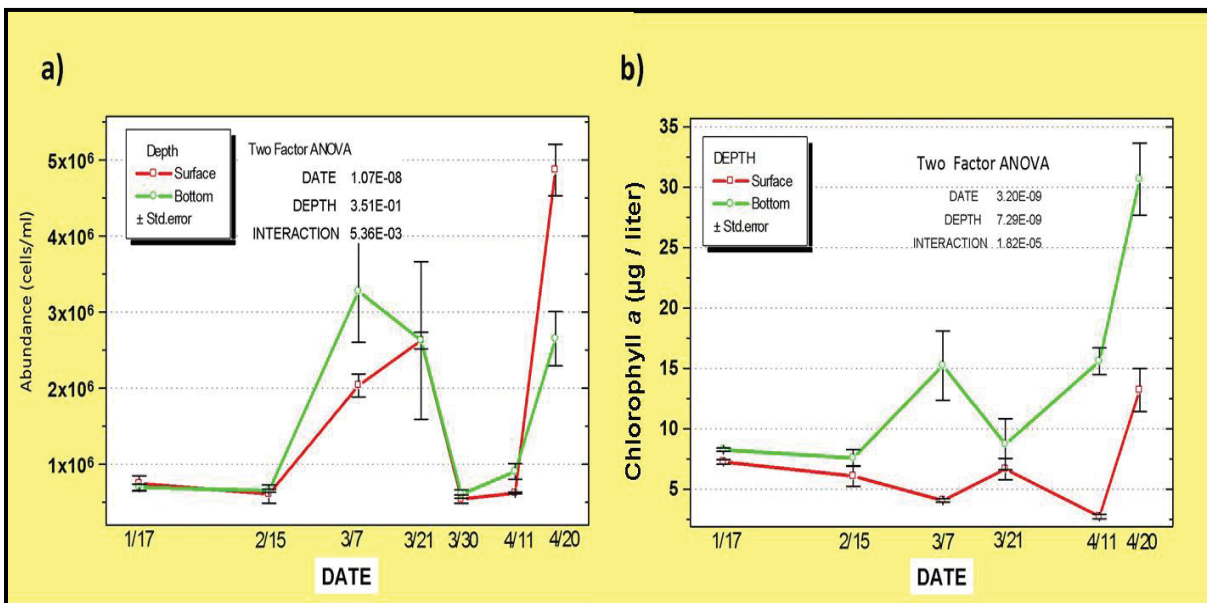


Figure 2-25. Field results from sampling at Apache pier for surface and bottom water bacteria (a) and chlorophyll a (b). Surface waters are shown in red while bottom waters are shown in green.

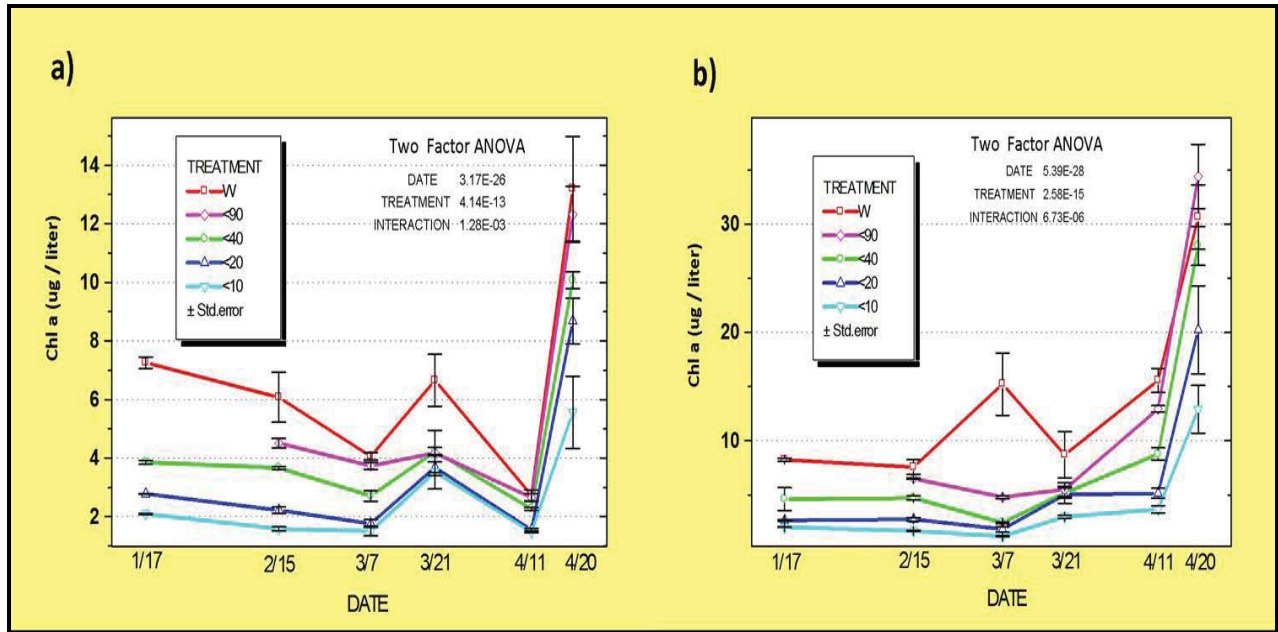


Figure 2-26. Field results from sampling at Apache pier for size fractionated chlorophyll *a* in surface (a) and bottom waters (b).

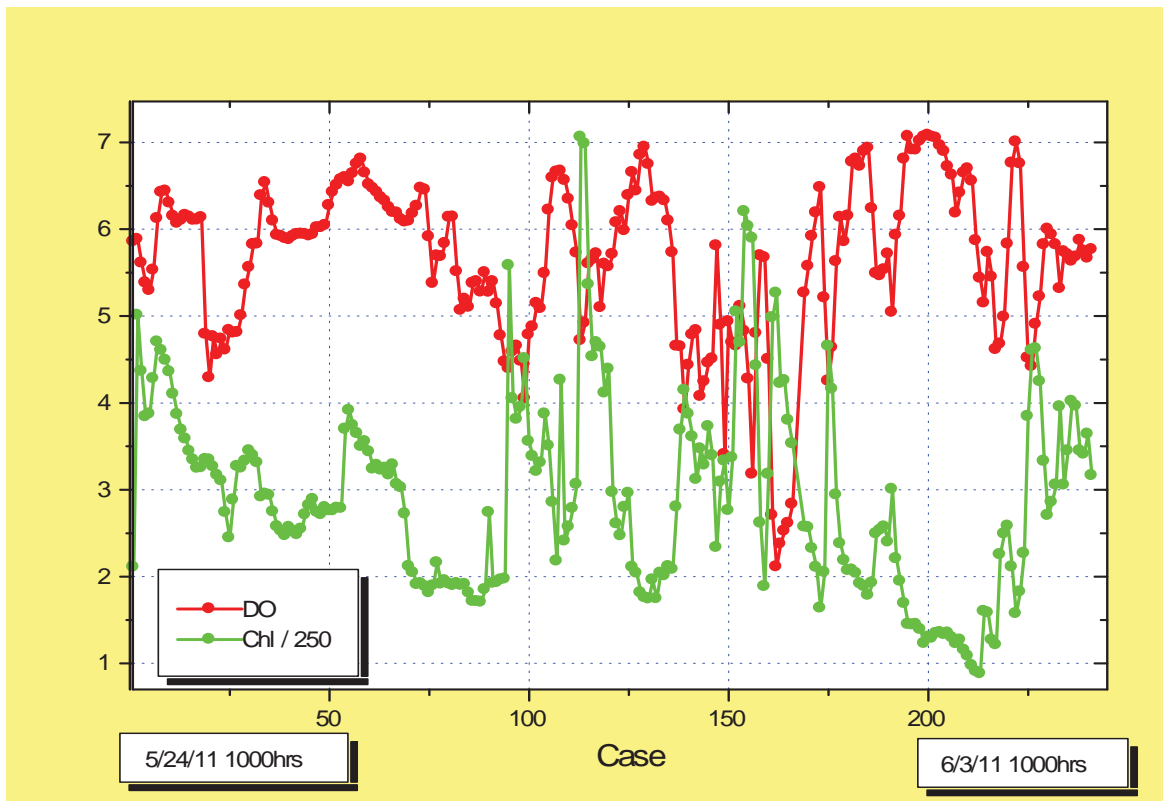


Figure 2-27. Time series of Ecotriplet chlorophyll fluorescence (RFU) and dissolved oxygen concentration records from the bottom-water pier sonde. Data have been reduced by determining hourly averages for both variables with the record indicating values from 5/24/2011 through 6/3/2011. The extreme low DO event occurred on 5/31/2011 within the early morning period.

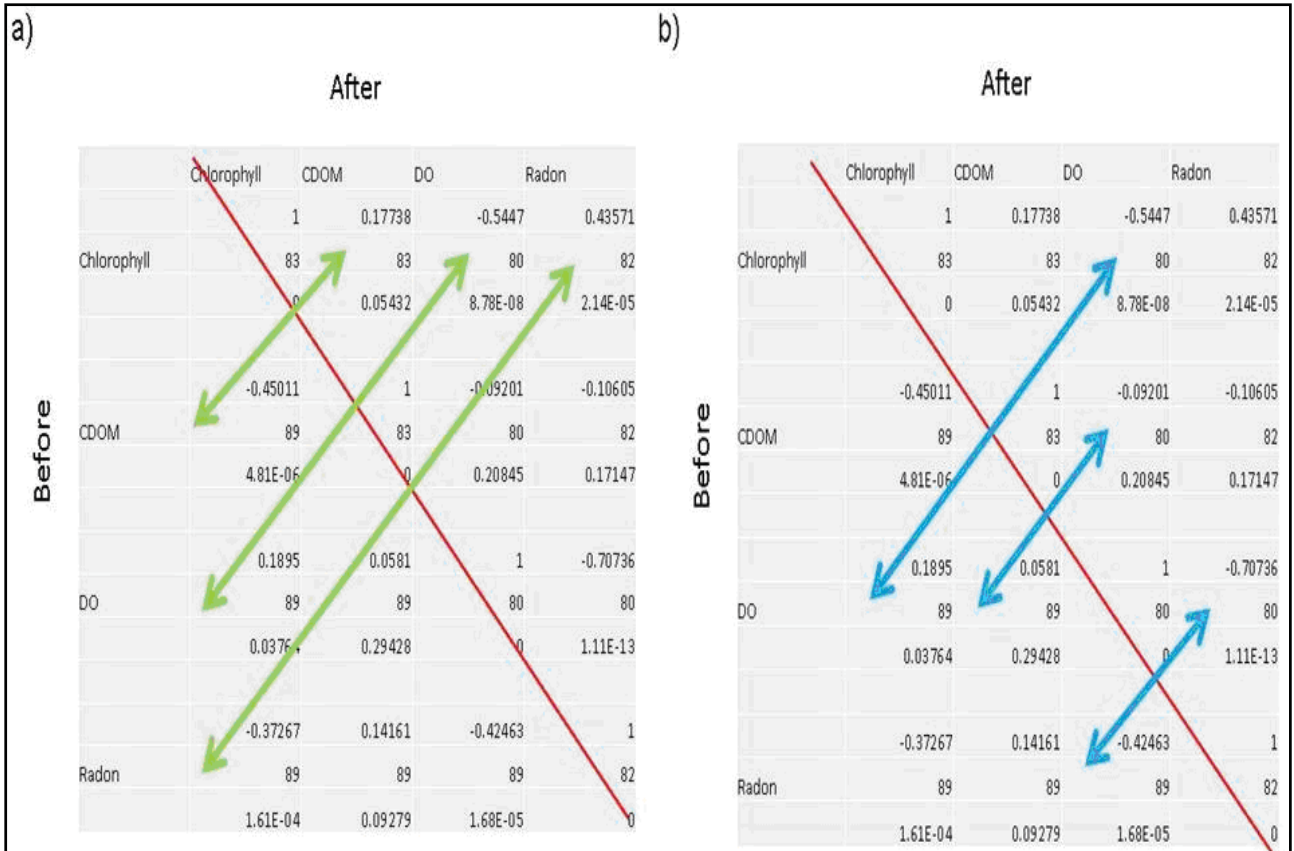


Figure 2-28. Pearson Correlation analysis results of case numbers 0-170 from hourly condensed data from Ecotriplet chlorophyll fluorescence (RFU) and dissolved oxygen records from the bottom-water pier sonde. Panel a) shows correlation results of chlorophyll *in vivo* fluorescence, while panel b) shows DO from the bottom water sonde. Red diagonal line separates the before event period from the during event period. Three term vertical cells indicate correlation coefficient, n, and p values for discrete correlations. Arrows assist in orienting the reader to similar variable pair correlation before and during the event period.

Section III: Biogeochemical Processes of Oxygen Depletion – Erik Smith (USC)

Biogeochemical process studies conducted for this project focused on quantifying water column nutrient and organic matter chemistry and understanding the role of particulate versus dissolved resources in fueling bacterial metabolism and associated oxygen demand. Bacteria are responsible for the bulk of the total respiratory consumption of oxygen in planktonic communities. Consequently, understanding the nutrient and organic matter conditions that affect bacterial activity and metabolic rates are critical to understanding the oxygen balances and the potential for hypoxia formation in Long Bay. Bacterial metabolism can be ascribed to that of the particle-associated bacteria and that of the free-living bacteria. Although the activity of the free-living bacteria typically dominates total bacterial metabolism, in particle-rich environments the activity of the particle-associated assemblage can become substantial. Our previous work in Long Bay demonstrated significant relationships between total water column oxygen demand and concentrations of particulate organic matter and nutrients. This suggests that particulate resources may be more important than dissolved resources in fueling bacterial heterotrophy in these waters. Dissolved organic carbon concentrations observed previously in these waters were substantial, however, and if only a small portion of this pool is turning over to support heterotrophic respiration, this would not be apparent in relationships with the bulk pool. Thus the need for additional research to explore the relative roles of particulate and dissolved substrates fueling oxygen consumption leading to low dissolved oxygen conditions in Long Bay.

The primary goal of the present study was to test the hypothesis that water column heterotrophic processes responsible for oxygen consumption, and therefore hypoxia formation, in nearshore waters of Long Bay are driven by particulate organic matter availability, rather than dissolved organic matter availability. Since water column respiration rates cannot operationally be partitioned into rates directly supported by particulate matter and rates directly supported by dissolved matter, we used measures of bacterial production, which can be subject to size-fractionation to distinguish the activity of free-living bacteria utilizing dissolved resources and particle-attached bacteria (determined by difference between total and size-fractionated rates). Further, since time-series measures of dissolved oxygen have shown these waters to generally be under-saturated with respect to physical equilibrium (as described above), combined measurements of gross primary production and total water column respiration were included in the sampling effort to test the hypothesis that DO saturation deficits in these waters are a reflection of net heterotrophy. Persistent net heterotrophy implies, by definition, that consumption of organic matter cannot be sustained by local production, and thus oxygen consumption rates fueling hypoxic conditions in these waters must be the result of organic matter produced elsewhere and imported to nearshore waters.

All water chemistry and biogeochemical process measurements were conducted at the seaward end of Apache Pier, coincident with the location of sensors deployed. Water samples were conducted on a monthly to bi-monthly basis from 17 January, 2011 to 8 December, 2012, from both surface (0.5 m below sea surface) and bottom (0.5 m above sediment surface) waters with a horizontally mounted ‘Van Dorn’ type water sampler. To facilitate comparisons among sampling events, all samples collections were made on a mid-ebb tide between the hours of 7:00 am and 8:30 am (EST). Upon collection, water samples were returned to the laboratory (< 1.5 h

transit time) for analysis, as described below. Vertical profiles of water column physical properties (temperature, salinity, dissolved oxygen, pH and turbidity) were conducted at the time of water sampling using a YSI 6600 V2 datasonde that was manually lowered through the water column and averaging results at approximately 0.25 to 0.5 m depth intervals. The datasonde was calibrated according to manufacturer's specifications prior to each sampling event. Estimates of the water column light attenuation were also conducted on each sampling event via secchi disk depth measurements.

Surface and bottom water samples were analyzed for total nitrogen, total phosphorus, orthophosphate, nitrate + nitrite, and ammonium using a Technicon nutrient auto analyzer. Total suspended solids (TSS) concentrations were determined by standard gravimetric methods, with the organic fraction of TSS determined by loss on ignition at 450 °C (volatile suspended solids, or VSS). Dissolved organic carbon (DOC) concentrations were determined on filtered (GF/F) water samples and quantified by high-temperature combustion using a Shimadzu TOC-VCPN. Particulate organic carbon and nitrogen concentrations were determined on samples retained on GF/F filters and analyzed on a Costech CHN elemental analyzer after vapor-phase acidification to remove inorganic carbon. Chlorophyll *a* concentrations (as an estimate of phytoplankton biomass) and pheophytin (the degradation product of chlorophyll) were quantified on acetone-extracted samples using a Turner Trilogy fluorometer.

Estimates of bacterioplankton production rates in both the whole water (total community) and < 2 µm filtered ("free-living") fractions were determined for both surface and bottom water samples. Bacterial production was determined from incorporation rates of ³H-labelled leucine in water samples incubated with 35 nM (final concentration) of ³H-labelled leucine (~ 5 TBq mmol⁻¹) at *in situ* temperatures for 1 h. ³H activity was determined on PerkinElmer Tri-Carb 3100 liquid scintillation counter and converted to carbon production rates using a conversion factor of 257.6 mole carbon per mole leucine. The difference between bacterial rates in the unfiltered and < 2 µm filtered fractions is, by definition, due to the particle-associated community.

Although not an original component of the OCRM funding, surface and bottom water samples collected as part of this project were also used for estimates of phytoplankton gross primary production rates and total plankton community respiration rates. Gross primary production rates were determined from incorporation rates of NaH¹⁴CO₃ (1 µCi mL⁻¹ final activity) in water samples incubated at *in situ* temperatures for 30 minutes at a range of natural light intensities (0 to ~ 1800 µmole photons m⁻² s⁻¹). ¹⁴C activity were determined on whole samples after acidification to remove unincorporated ¹⁴C on a PerkinElmer Tri-Carb 3100 liquid scintillation counter and converted to chl-specific primary production rates by standard methods. Vertically integrated daily rates of gross primary production were estimated from individual relationships between chl-specific production and light, vertical light attenuation, and total photosynthetically active radiation measurements made at the Oyster Landing meteorological station at the Baruch Marine Field Laboratory. Rates of water column respiration were measured as *in vitro* changes in dissolved oxygen in dark bottle incubations conducted at *in situ* water temperatures for 4-6 hours, with oxygen concentration measured by automated Winkler titrations. Vertically integrated daily rates of respiration for surface and bottom water column layers were estimated by interpolating volumetric rates over depths of surface and bottom layers estimated based on

vertical profiles of water column temperature and salinity and scaled to 24 hours assuming respiration rates in each layer were constant over the course of a day.

Over the course of annual sampling, the range in concentrations of nutrients, chlorophyll and organic matter (Table 3-1) were generally similar to values observed in nearshore waters of Long Bay during previous studies, conducted from 2006 to 2009. Highest nutrient, organic matter and chlorophyll concentrations, which were observed during periods of upwelling-favorable winds and low bottom water dissolved oxygen conditions (5/27, 7/9, and 8/11, see Section II), were generally similar to values observed during the sustained hypoxic events of August, 2009. The sampling event of 10/10 occurred during upwelling-favorable wind conditions and was associated with greatly elevated nutrient and organic matter concentrations, but bottom water dissolved oxygen concentrations were only slightly depressed at this time. High wave action observed during this sampling event, which likely caused enhanced vertical mixing of the water column at Apache Pier, may have been responsible for the lack of low dissolved oxygen concentrations at this time. Similar to previous years, particulate matter concentrations (TSS, VSS, Chl, Pheo) and TN and TP concentrations tended to be higher in bottom water samples, while concentrations of dissolved constituents tended to show relatively less temporal variability or differences between surface and bottom waters.

Overall, dissolved organic matter (DOC) concentrations varied from 1.33 – 1.91 mg C L⁻¹ while particulate organic matter (POC) concentrations varied from 0.61 – 32.2 mg C L⁻¹ (Figure 3-1). POC concentrations were more variable than DOC concentrations in surface water (CV of POC = 47.6%, CV of DOC = 9.5%) and especially in bottom waters (CV of POC = 164.2%, CV of DOC = 10.0%). While DOC concentrations showed little variation between surface and bottom waters, POC concentrations were often much greater in bottom waters than in surface waters, and the largest differences were observed during above mentioned periods of upwelling-favorable wind conditions. The proportion of total organic carbon represented by POC ranged from 31% to 70% (mean = 44%) in surface waters and from 34% to 95% (mean = 59%) in bottom waters. The C:N ratio of particulate organic matter ranged from 5.5 to 10.3 and showed no significant differences between surface and bottom water samples.

Rates of bacterial production in the free-living fraction remained relatively low and constant throughout the year in both surface and bottom water samples. In contrast, total bacterial production rates increased with seasonally increasing temperatures and were substantially greater than rates of the free-living fraction during summer and fall (Figure 3-2). Highest rates of total bacterial production occurred during sampling dates associated with upwelling favorable winds and high concentrations of particulate material, especially in the bottom waters (Table 3-1), which with the exception of the 10/10 sampling event also coincided with low bottom water oxygen concentrations. Increased bacterial production in the whole water fraction relative to the < 2 μm filtered fraction must, by definition, be the result of increased activity of the particle-associated bacterial community. Over the annual cycle, production associated with the particle-associated bacterial community accounted for 76% ±17% of the total bacterial community production measured in both bottom and surface waters (this average excludes two sampling events when filtered rates exceeded whole-water rates, but both events occurred when bacterial production rates were close to the annual minimum and whole and filtered rates were within the statistical measurement error of each other).

Water temperatures in both surface and bottom layers at Apache Pier exhibited a typical annual cycle, with annual temperature minima during January – February and annual temperature maxima during July – August (see Section II). This annual cycle in temperature could, on its own, explain 58 % of the temporal variability in natural log transformed (to meet assumptions of normality) total community bacterial rates ($\text{LN}[\text{BP}] = 0.14 * \text{Temp} - 3.39$; $r^2 = 0.58$, $p < 0.0001$). However, due to variability in particulate matter concentrations, and the strong influence of particle-attached bacteria on total community rates, temporal variability in total bacterial production was best predicted by a regression model that included both temperature and POC concentrations (Figure 3-3).

Rates of total water column respiration were strongly correlated with rates of bacterial production (Figure 3-4), indicating the importance of heterotrophic bacterial activity in driving oxygen consumption rates in nearshore waters of Long Bay. As with bacterial production, variability in water column respiration was a function of both water temperature and particulate organic matter concentrations and peaks in water column respiration corresponded to occurrences of upwelling favorable winds and low bottom water dissolved oxygen conditions.

To estimate the depth of light penetration into the water column at Apache Pier, secchi disk (SD) depth measurements were converted to attenuation coefficients (k_d) using a relationship between SD and k_d developed for waters of North Inlet, which is on the southern end of Long Bay and experiences a similar range of light attenuation and turbidity values as was observed at Apache Pier. Based on this relationship ($-k_d = 1.45 * \text{SD}^{-0.83}$; $r^2 = 0.85$), k_d ranged from -0.73 m^{-1} to -3.31 m^{-1} over the course of the study. This corresponds to a euphotic depth (depth of 1% surface light penetration) ranging between 1.4m to 6.3m, with a mean ($\pm 1 \text{ Std. Dev.}$) of $2.6\text{m} \pm 1.2\text{m}$. Thus, except on two occasions, light did not penetrate below the pycnocline to the lower water column layer, and 1% surface irradiance never reached the sediment surface at this location (Figure 3-5). Temporal variability in k_d was significantly predicted by measures of turbidity ($\text{LN}[K_d] = 0.47 * \text{LN}[\text{NTU}] - 0.46$; $r^2 = 0.79$, $n = 18$, $p < 0.001$), which were themselves highly related to variations in measured TSS values ($\text{LN}[\text{NTU}] = 1.43 * \text{LN}[\text{TSS}] - 2.05$; $r^2 = 0.80$, $n = 18$, $p < 0.001$). Adding measures of chlorophyll to the regression model did not improve the predictive relationship with turbidity.

Rates of phytoplankton gross primary production were estimated from relationships between light and chlorophyll-specific production modeled as a hyperbolic tangent function (Figure 3-6). The model fits yielded estimates of a^b , the initial slope of the relationship, and P_{max}^b , the maximum, light-saturated photosynthetic capacity (Figure 3-7). Over the course of the study, a^b ranged from $0.003 - 0.012 \text{ mg C (mg Chl)}^{-1} \text{ h}^{-1} (\mu\text{mol photons m}^{-2} \text{ s}^{-1})^{-1}$ and showed relatively little temporal variability, although values for a^b were generally higher in surface waters than in bottom water samples, particularly in the colder months. By contrast, values of P_{max}^b , which ranged from $0.27 - 3.02 \text{ mg C (mg Chl)}^{-1} \text{ h}^{-1}$, exhibited a more obvious annual cycle, with peak rates during the warmer months, and little difference between surface and bottom water samples. The pronounced decrease during early August was associated with exceptionally clear waters (lowest k_d values and the deepest euphotic depth [Figure 3-5]). Because light rarely penetrated below the upper surface layer, vertically integrated rates of primary production (discussed below) were based on a^b and P_{max}^b values measured in surface water samples; for the two

occasions that light penetration extended into the lower water column layer, values of a^b and P_{\max}^b measured in surface and bottom layers on these dates were not significantly different.

Vertical profiles of water column properties often revealed the presence of a distinct bottom turbidity layer. Generally, this layer tended to be confined to just above the seafloor, although the absolute of turbidity and its vertical distribution varied substantially among sampling dates (Figure 3-8). Since estimates of microbial metabolism and associated oxygen consumption rates were shown to be a function of both temperature and particulate substrate availability, and turbidity was a strong predictor of water column particulate matter concentrations, vertical profiles of turbidity were combined with a regression model predicting respiration rates from temperature and turbidity values (Figure 3-9) to estimate vertically integrated rates of respiration through the water column (discussed below). While this added another source of error to the calculation of integrated respiration rates, it avoided a substantial over-estimation that resulted from a simple linear extrapolation of respiration rates measured in surface and bottom water grab samples (taken at 0.5 m below sea surface and 0.5 m above sediment surface, respectively).

Daily rates of vertically integrated phytoplankton gross primary production and total community respiration in the water column at Apache Pier indicate this location to be substantially net heterotrophic throughout the year; total respiration far exceeded primary production on all sampling dates (Figure 3-10). Daily rates of gross primary production ranged from 38.6 to 362.5 $\text{mg C m}^{-2} \text{d}^{-1}$, while total water column respiration rates (converted to C units based on an RQ [CO_2 produced to O_2 consumed] of 0.8) ranged from -80.2 to -1240.8 $\text{mg C m}^{-2} \text{d}^{-1}$. As a result, net ecosystem production rates were always negative and ranged from -41.6 to -905.5 $\text{mg C m}^{-2} \text{d}^{-1}$ and variations in respiration strongly predicted the temporal pattern in net ecosystem production rates, while its relationship to gross primary production was not significant ($p = 0.17$).

Conclusions

As has been observed in previous sampling conducted in the nearshore waters off the Grand Strand, temporal variability in particulate organic matter concentrations were substantially greater than that of dissolved organic matter concentrations. Sampling dates coincident with distinct upwelling-favorable winds and low bottom water dissolved oxygen conditions (5/27, 7/9, and 8/11) were associated with elevated concentrations of particulate organic matter, total nitrogen and phosphorus, and chlorophyll. In contrast to most ocean environments, where DOC is by far the largest pool of organic carbon, POC represented a substantial proportion of the total organic carbon pool, averaging 45% of TOC in surface waters and 59% of TOC in bottom waters, and temporal variability in POC concentrations was far greater than that of DOC.

A comparison of rates of bacterial production between the total community (whole water sample) and the free-living fraction ($< 2 \mu\text{m}$ filtered fraction) strongly supports the hypothesis that heterotrophic bacterial metabolism, and thus oxygen consumption rates, in nearshore waters of Long Bay are strongly dependent on particulate organic matter concentrations. On average, production associated with the particle-associated bacterial community accounted for $76\% \pm 17\%$ of the total bacterial community production; this greatly contrasts with observations made in North Inlet (a salt marsh dominated estuary at the southern end of Long Bay) using the exact

same methodology, where the production associated with the particle-associated bacterial community accounted for $38\% \pm 16\%$ of the total bacterial community production.

Light attenuation is substantial at Apache Pier, such that there is generally insufficient light for primary production to occur below the pycnocline and there is never sufficient light for benthic primary production to occur. The robustness of this conclusion is supported by additional, higher frequency, measurements of light attenuation (as Secchi disk depth) at Apache Pier made during YSI datasonde deployment/retrieval (S. Libes, unpublished data).

Despite occasionally high concentrations of phytoplankton (as determined from chlorophyll measurements), gross primary production at Apache Pier was rather limited and far from sufficient to support measured rates of water column respiration. As such, this location is substantially net heterotrophic throughout the year. These results confirm that high rates of oxygen consumption measured at this location cannot be supported by local organic matter production and must, by definition, be dependent on organic matter produced elsewhere and imported to and/or entrained in the nearshore region. This is consistent with previous hypothesized mechanisms for the formation of hypoxia in the nearshore waters off the Grand Strand. That is, regional-scale oceanographic processes generated by upwelling-favorable wind conditions tend to constrain water masses to the nearshore and thus prevent the wider dispersion of local-scale terrestrial inputs; the resulting enhanced material concentrations stimulate heterotrophic oxygen demand, which can lead to low dissolved oxygen conditions in the immediate nearshore waters.

Measurements of water column turbidity made with *in situ* optical sensors proved to be exceptionally valuable. Turbidity data strongly correlated with water column light attenuation values and total suspended sediment concentrations at Apache Pier and, when combined with measures of water temperature, predicted water column oxygen consumption rates with a high degree of confidence. As turbidity sensors are amenable to continuous *in situ* deployment, future monitoring efforts aimed at quantifying the occurrence and cause of hypoxia in Long Bay would greatly benefit from the inclusion of continuous turbidity monitoring.

Table 3-1: Mean (n=3) concentrations of water chemistry parameters measured in surface and bottom waters at the end of Apache Pier. TSS = total suspended solids; VSS = volatile (organic) suspended solids; Chl = total chlorophyll; Pheo = pheophytin (the degradation product of chlorophyll); TN = total nitrogen (unfiltered); TP = total phosphorus (unfiltered); PO₄ = orthophosphate; NH₄ = ammonium; NO₂₊₃ = nitrate plus nitrite. “n.d.” = no data (TN & TP data for these dates were lost due to analytical instrumentation malfunctions).

Date	Depth	TSS (mg/L)	VSS (mg/L)	Chl (µg/L)	Pheo (µg/L)	TN (µg/L)	TP (µg/L)	PO ₄ (µg/L)	NH ₄ (µg/L)	NO ₂₊₃ (µg/L)
1/17/11	Surface	11.0	2.4	5.1	2.1	259.2	14.64	6.25	40.2	2.19
1/17/11	Bottom	14.6	3.2	7.1	2.7	269.5	22.97	4.57	32.9	1.12
2/15/11	Surface	26.6	7.2	4.4	2.1	338.4	34.69	7.08	25.2	0.80
2/15/11	Bottom	47.2	10.6	8.0	4.9	458.9	71.07	7.06	15.1	0.38
3/17/11	Surface	16.0	4.5	4.1	1.8	246.2	18.76	9.19	25.7	2.51
3/17/11	Bottom	32.5	7.6	4.6	3.6	338.0	43.91	7.83	31.2	3.21
4/15/11	Surface	19.6	4.5	4.9	1.9	337.6	30.73	3.28	15.6	0.57
4/15/11	Bottom	23.6	5.1	4.7	2.3	368.4	22.08	3.61	11.6	0.57
5/16/11	Surface	49.6	9.6	11.6	7.1	392.4	62.91	9.97	30.6	2.61
5/16/11	Bottom	39.2	8.7	7.6	6.4	269.4	39.60	11.11	34.0	2.39
5/27/11	Surface	18.0	5.0	14.3	2.9	282.1	20.01	7.25	15.4	2.17
5/27/11	Bottom	519.1	83.3	39.3	27.2	1365.9	34.63	14.77	36.7	3.10
6/13/11	Surface	16.0	4.3	6.9	2.9	272.3	20.68	3.95	40.3	2.02
6/13/11	Bottom	26.9	5.6	8.2	4.1	358.5	36.94	5.65	22.0	1.85
6/27/11	Surface	17.2	4.2	8.3	3.0	294.2	7.90	7.15	33.0	1.54
6/27/11	Bottom	108.7	21.3	28.0	18.8	792.9	110.87	7.30	19.7	1.99
7/9/11	Surface	50.2	11.8	18.9	9.8	n.d.	n.d.	6.26	21.1	1.28
7/9/11	Bottom	145.3	28.3	25.4	18.1	n.d.	n.d.	6.38	38.3	0.25
7/12/11	Surface	11.0	4.0	4.7	1.3	n.d.	n.d.	3.10	45.1	0.82
7/12/11	Bottom	18.4	5.0	6.2	2.2	200.5	15.32	5.75	27.7	1.66
7/27/11	Surface	27.0	6.3	15.8	5.4	n.d.	n.d.	6.99	23.5	0.24
7/27/11	Bottom	47.5	8.9	19.2	8.6	n.d.	n.d.	9.70	34.2	2.11
8/11/11	Surface	11.7	4.4	4.4	1.1	331.4	14.62	6.45	28.2	23.91
8/11/11	Bottom	24.7	7.2	21.1	5.3	380.7	50.15	6.57	37.0	2.08
8/25/11	Surface	16.9	3.2	7.4	2.5	301.4	30.27	3.16	24.9	1.27
8/25/11	Bottom	19.3	3.4	7.3	2.9	334.8	37.37	3.08	20.3	1.76
9/8/11	Surface	22.9	6.5	14.6	4.9	371.6	38.06	3.45	13.1	0.99
9/8/11	Bottom	33.3	8.3	13.9	5.1	409.2	49.85	1.96	21.3	1.39
9/25/11	Surface	17.6	5.5	9.2	2.5	345.9	24.87	4.75	42.3	1.32
9/25/11	Bottom	25.4	7.0	8.5	2.8	361.4	30.02	7.89	37.9	2.77
10/10/11	Surface	34.9	8.8	17.8	7.4	428.8	49.33	4.66	39.0	1.55
10/10/11	Bottom	629.7	90.9	40.8	44.6	300.2	13.34	5.24	22.3	2.38
11/7/11	Surface	25.1	6.9	23.1	6.2	520.0	28.61	4.10	53.8	4.24
11/7/11	Bottom	52.1	10.0	26.2	10.1	835.8	59.41	6.47	45.9	4.46
12/8/11	Surface	25.9	6.7	18.6	5.8	511.1	28.70	4.20	46.4	6.77
12/8/11	Bottom	36.9	8.3	19.1	6.4	576.4	45.63	5.33	47.8	9.26

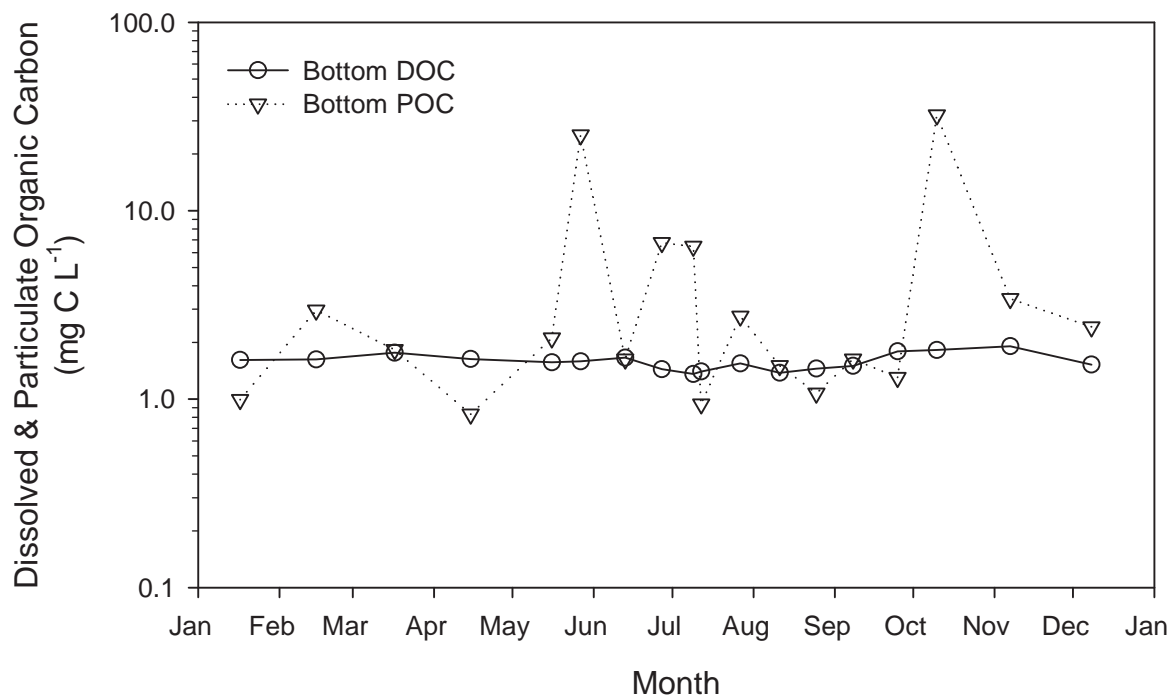
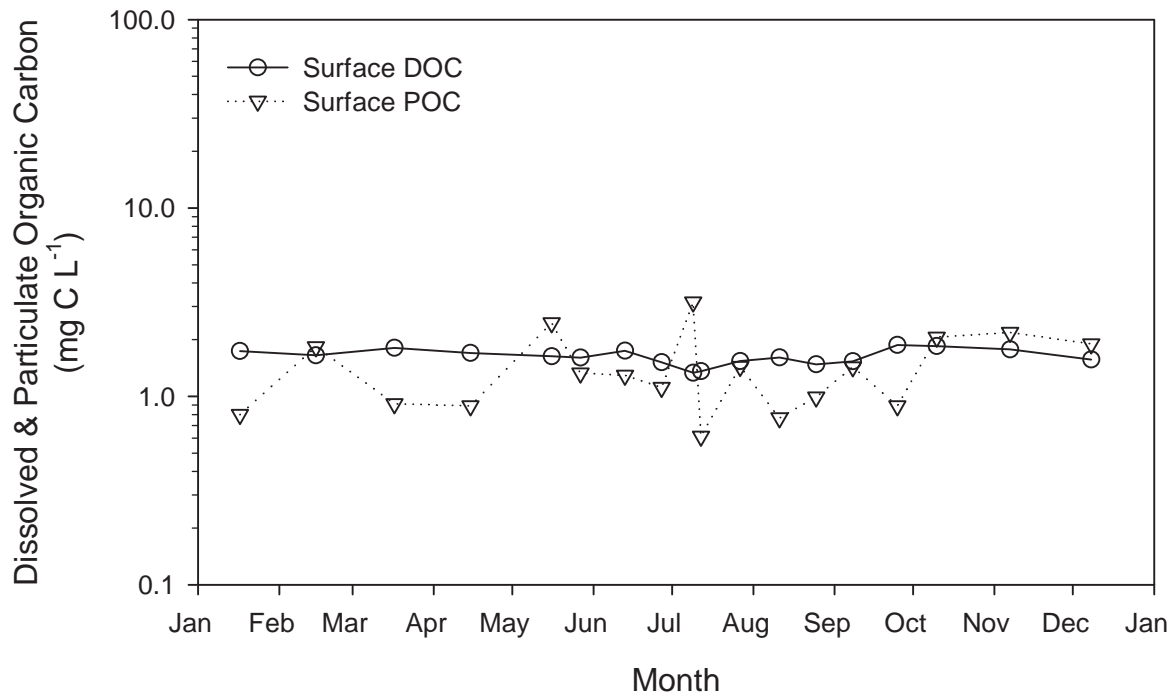


Figure 3-1. Mean ($n=3$) concentrations of particulate and dissolved organic carbon in surface water (upper panel) and bottom water (lower panel) grab samples.

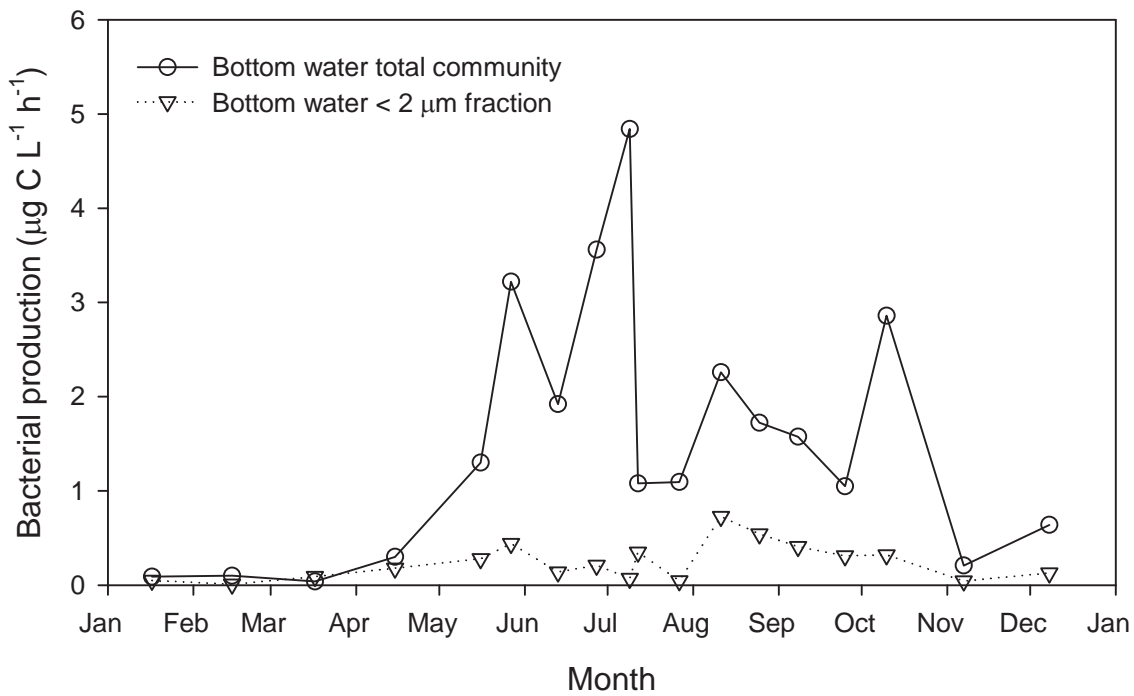
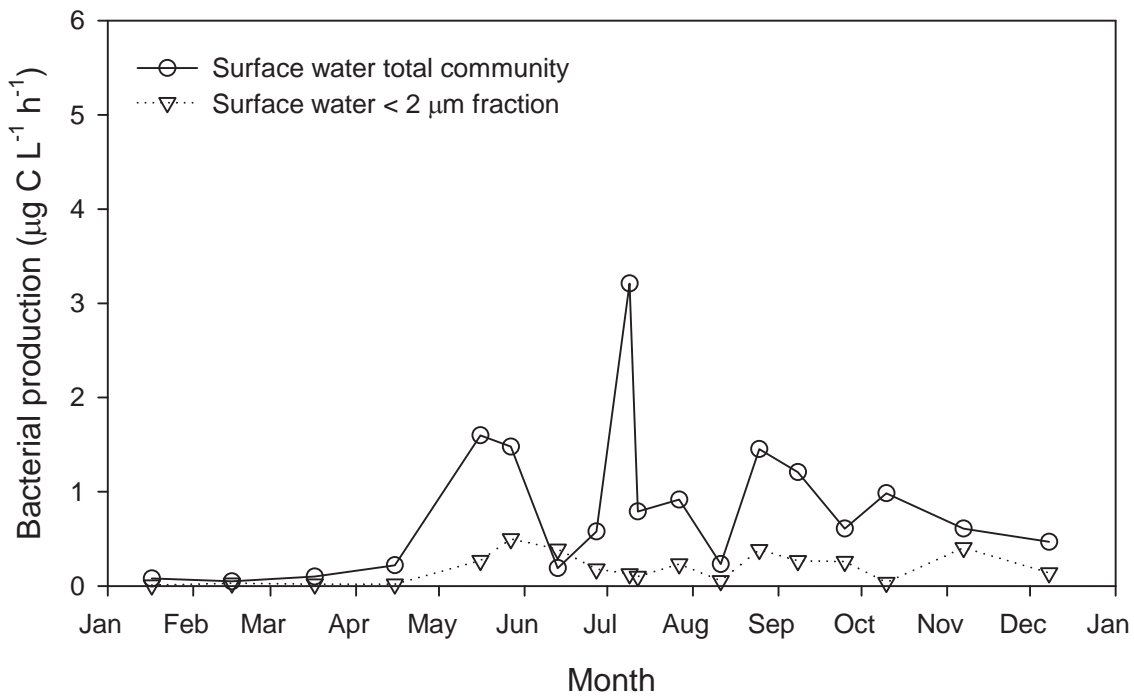


Figure 3-2. Surface water (upper panel) and bottom water (lower panel) rates of bacterial production for the total bacterial community (whole water rates) and the free-living bacterial community (< 2 μm filtered fraction).

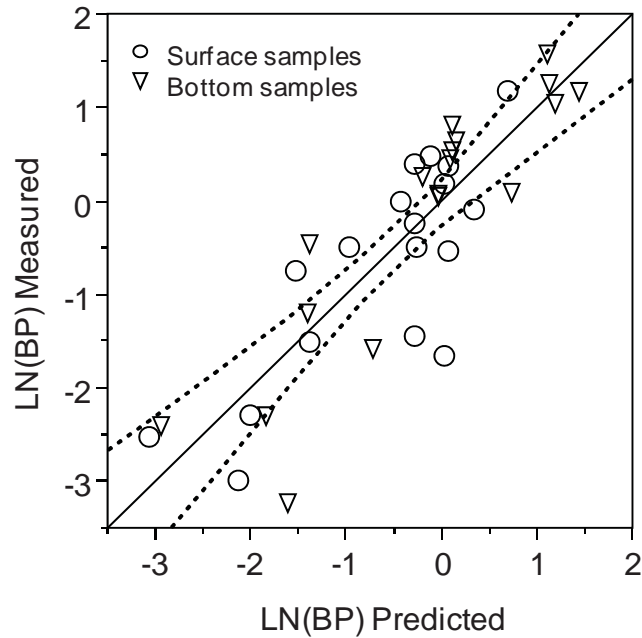


Figure 3-3. Relationship between predicted and observed values of natural log transformed bacterial production rates in surface and bottom water samples based on the regression model: $\text{LN}(\text{BP}) = 0.131 \cdot \text{Temp} + 0.589 \cdot \text{LN}(\text{POC}) - 3.66$; $r^2 = 0.74$, $n = 36$; $p < 0.001$ for all terms. Solid line equals model fit, dotted lines represent 95% confidence limits.

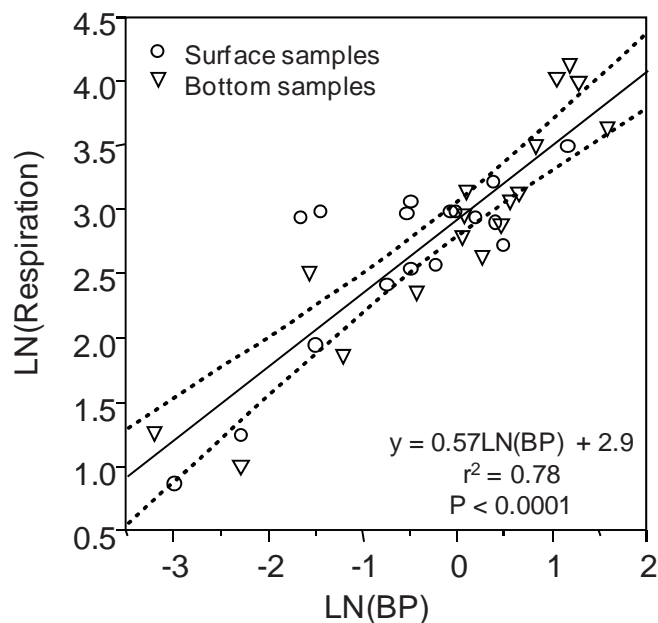


Figure 3-4. Relationship between the natural log of total bacterial production and the natural log of plankton community respiration for surface and bottom water samples combined. Solid line equals model fit, dotted lines represent 95% confidence limits.

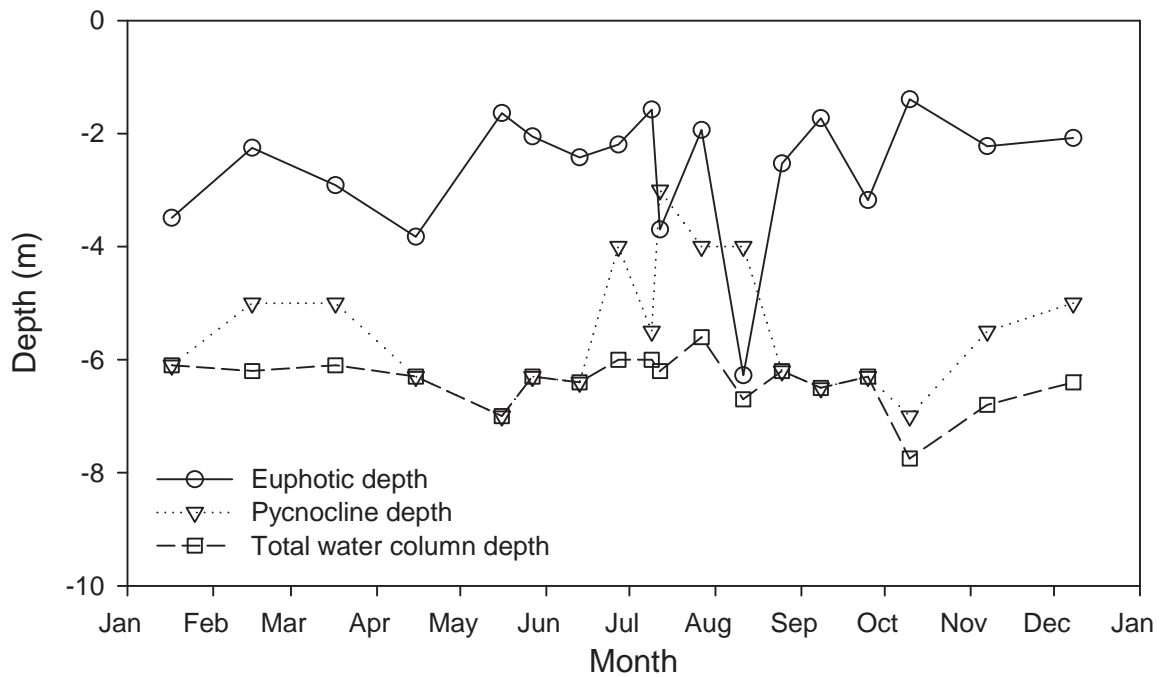


Figure 3-5. Observed depths for euphotic zone (determined as depth of 1% surface light penetration), pycnocline, and total water column. On dates of no apparent water column stratification, pycnocline depth equals total water depth.

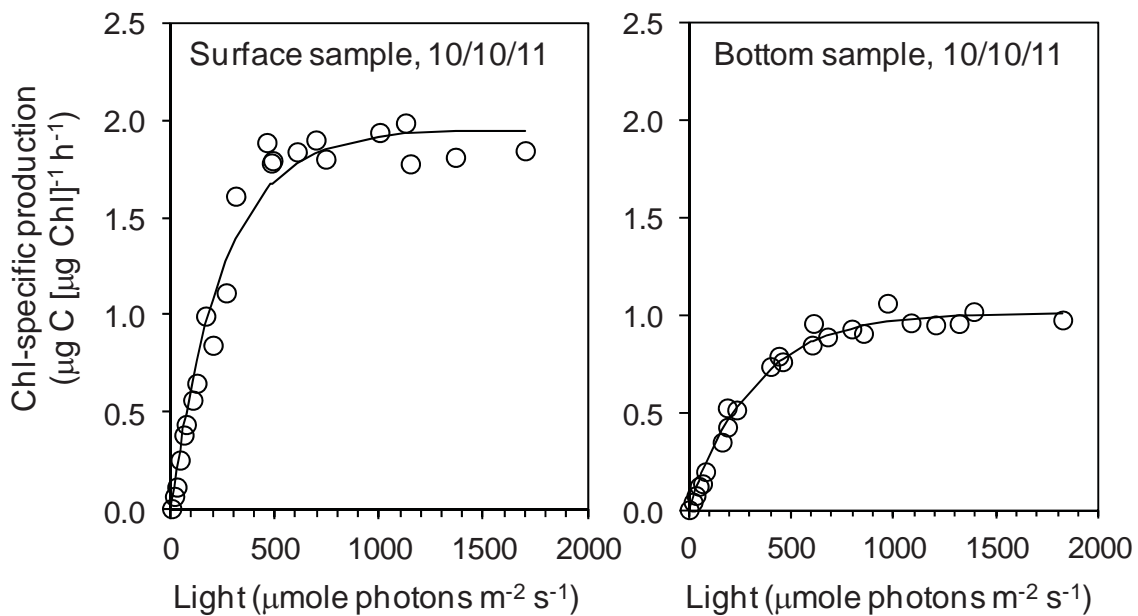


Figure 3-6. Example production versus light curves from 10 October 2011 sampling for both surface and bottom water samples. Raw data depicted by open circles, solid line equals the model fit.

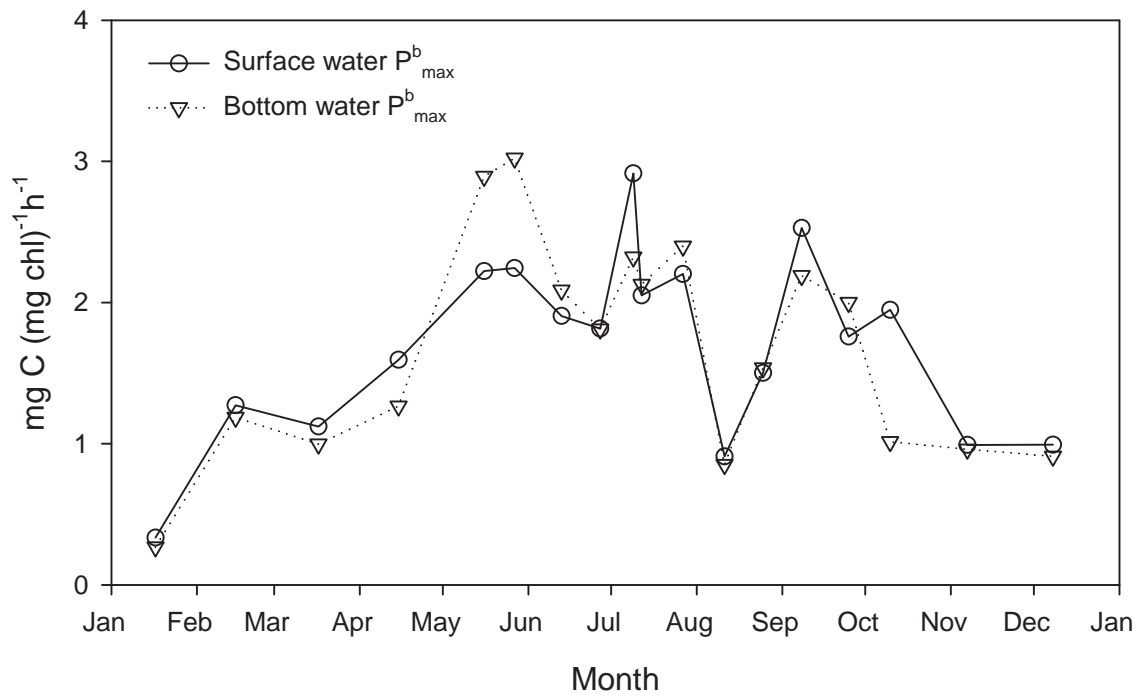
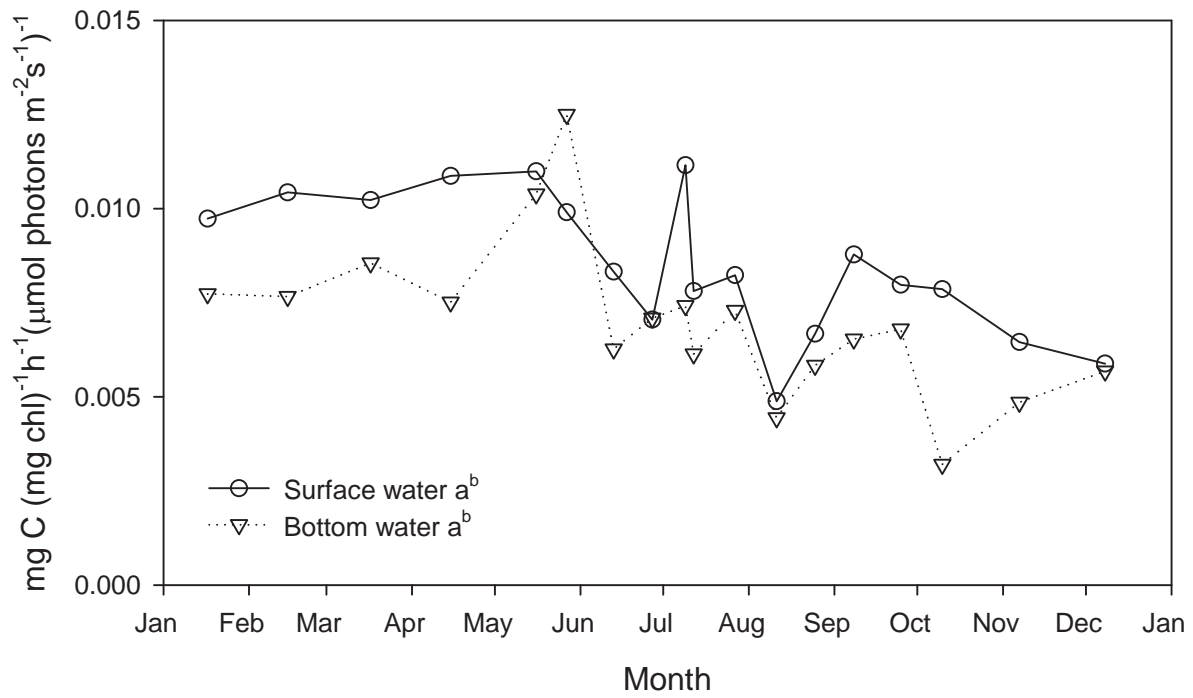


Figure 3-7. Rates of a^b , the initial slope (top panel) and P^b_{max} , the maximum photosynthetic capacity, (bottom panel) determined from production versus irradiance curves for surface and bottom water samples.

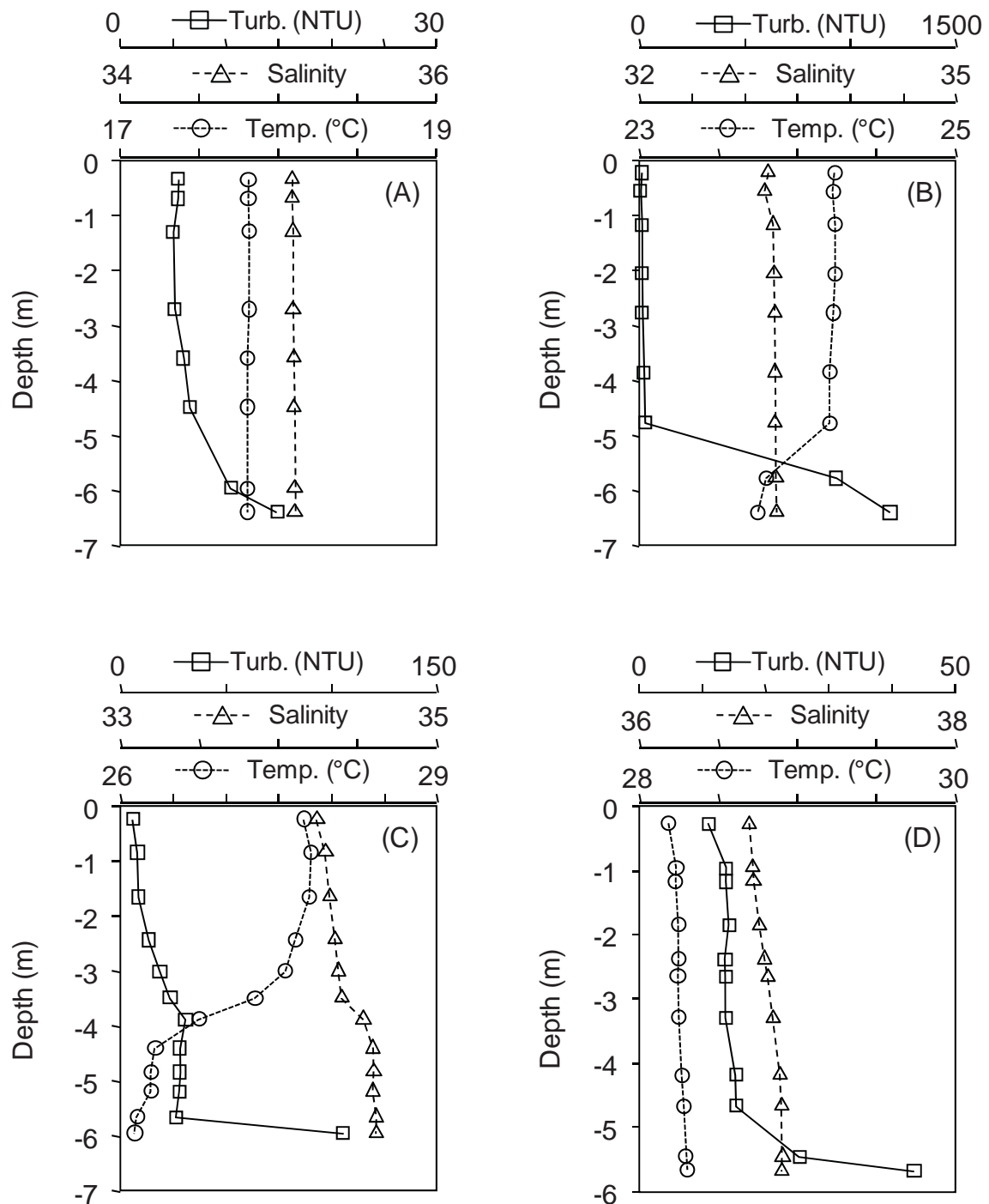


Figure 3-8. Example vertical profiles of temperature, salinity, and turbidity at Apache Pier measured on 15 April (A), 27 May (B), 27 June (C), and 27 July (D).

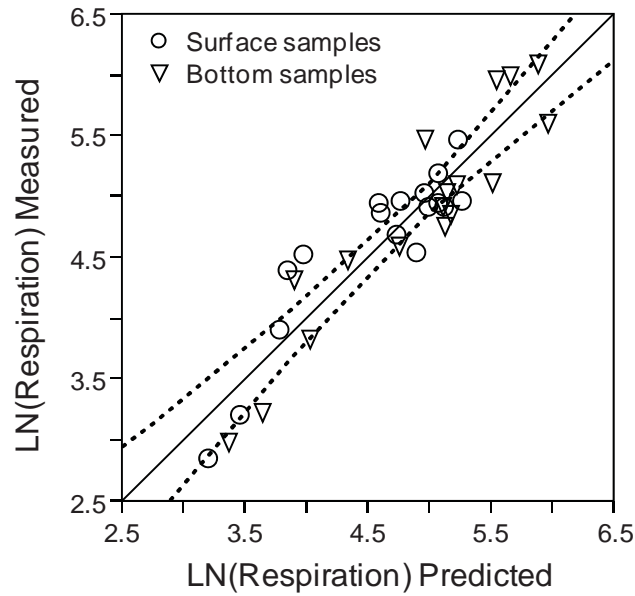


Figure 3-9. Plot of predicted versus measured respiration rates (natural log transformed) based on the regression model: $\text{LN}(R) = 0.1087 \cdot \text{Temp} + 0.2585 \cdot \text{LN}(\text{NTU}) + 1.4831$; $r^2 = 0.85$, $n = 34$, $p < 0.001$. Solid line equals model fit, dotted lines represent 95% confidence limits.

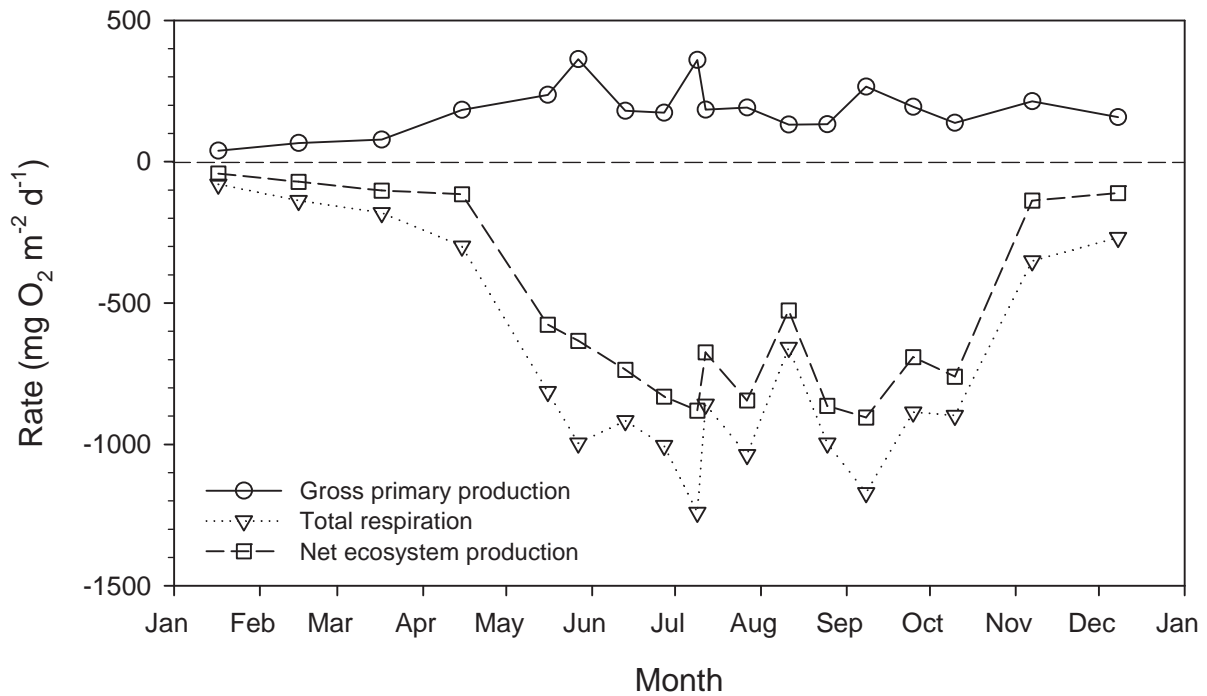


Figure 3-10. Daily rates of gross primary production, total community respiration, and net ecosystem production integrated over the depth of the water column.

Section IV: Spectral Analysis of Continuous Data – George Vougaris (USC)

Datasondes have been deployed from fishing piers since 2006 (Apache Pier, Springmaid Pier) providing a 15-minute record of DO, salinity and temperature in the surface and bottom waters; development of a numerical model to describe wind-driven circulation patterns in Long Bay; surveys of nearshore water quality conditions (nutrients, organic matter, and phytoplankton biomass) and vertical structure water column physical properties (temperature, salinity and DO); measurements of pelagic respiration rates in nearshore waters; some limited bioassay work designed to examine substrate regulation of bacterial metabolic demand; and characterization of groundwater to Long Bay.

These data have been supplemented by data on oceanographic currents at Springmaid from a station operated as part of a Southeast Coastal Ocean Observation Research Association (SECOORA) funded project. These data in conjunction with meteorological data from the same location from NOAA/NOS provided the basis for the integration of physical oceanography, meteorological and water quality data to reveal relationships and associations captured by the time-series.

The objective of the work presented here was to analyze and synthesize all existing time-series of data collected in Long Bay since 2006. This analysis was aimed at providing information into the “state of knowledge” as this is revealed through the time-series of:

- (i) Wind speed and direction
- (ii) Oceanographic current analysis
- (iii) Sea surface elevations
- (iv) Temperature, salinity and DO time-series

Although a number of exploratory analyses were carried out, one major issue encountered was the limitation in temporal and / or spatial resolution. Data with high temporal resolution were collected mainly as part of instrument installation on stationary locations. A large number of the data collected – especially as the result of a rapid response assessment – were examined but it was soon revealed that these data are of limited temporal and spatial resolution to provide conclusive evidence. However, they have been interesting in building the case for the mechanism operating in this environment that potentially leads to the generation of hypoxic conditions during the summer and these are all summarized in Sanger et al (Accepted, see Section V). In this report only results with resolution sufficient to providing some solid conclusions are presented.

The methodology employed included:

- (1) Generating the climatology of the system as this is revealed by the analysis of Pier collected data over a period of 5.5 years (2006 to 2011);
- (2) Focusing on the characteristics during the summer periods, when hypoxic events do occur; and
- (3) Examining the variability of the signal during the summer period based on its temporal variability and identifying the signals present in this variability that can be related to other environmental conditions.

Meteorological conditions were used from the Springmaid Pier station. Although data exist from the Apache Pier, the Springmaid Pier NOAA NOS station 8661070 was selected for the analysis presented in here, mainly because of (i) the rigorous QA/QC performed by NOAA; and (ii) larger continuity in the record when compared to that from Apache Pier. Furthermore, intercomparison of concurrently collected data from the two stations revealed that the data were almost identical, something not unexpected given the close proximity of the two location. The meteorological data used were hourly wind velocities and directions, air temperature, water temperature and atmospheric pressure. The mean monthly values and corresponding variability of the meteorological data can be seen in Figure 4-1.

The water quality data collected at the Apache Pier provide the longest record of this type of data in the region and are the most suitable for the time-series analysis performed in this work. Monthly means of the collected data, together with the standard deviation and min and maximum values occurring in each month for the whole period of data collection available are shown in Figure 4-2.

The seasonal variability is visible in the water temperature record with lower temperature values found during the month of February and maximum values ($\sim 30^{\circ}\text{C}$) during the summer period (Figure 4-2a). Salinity on the other hand, although variable, does not exhibit a clear pattern (Figure 4-2b). During the years of 2009 and 2010 higher monthly salinity values were found in the summer and lower during March, a period coinciding with the largest discharge of the local rivers in the area. The variability in salinity during the earlier years appeared to be related to major river discharges. Overall it can be concluded that lower salinities were found in the months of February-March which correspond with the maximum river discharges in the region. Overall, dissolved oxygen monthly values showed a trend of lower values near the bed compared to the surface (Figure 4-2c and d). This difference is clearly exaggerated during the summer months, which coincides with the periods of higher salinity and higher sea water temperature.

The same data are shown aggregated in Figure 4-3 as monthly climatologies. Similar patterns were observed with mean DO values being lower near the sea bed and the difference being larger during the summer months. Also, it worth noticing that the variability in DO values was larger in the near bed sensor while the variability in temperature and salinity was much more similar between surface and near bed.

All meteorological and water quality time-series for all years starting in 2006 were combined in to a common database and all time stamps were converted to a common one based on UTC time. Wind vectors were decomposed into alongshore (u) and cross-shore (v) components and all time-series were subjected to low pass filtering analysis with a cut-off frequency of 33 hrs with the main objective being to identify the following patterns:

- Existence of tidal signature in water quality measurements;
- Existence of a non-tidal, diurnal signal (day/night, due to solar radiation);
- Decomposition of signal into tidal, non-tidal diurnal and subtidal (i.e., low-passed); and
- Correlation of the subtidal signal with the meteorological conditions prevailing at the times of hypoxic events.

These analyses were carried out for the months of June, July, August, and September as these are the months that hypoxic conditions have been encountered in the study area.

Simple correlation analysis is used to define the forcing/response mechanism between DO and physical and meteorological data for each of the temporal scales identified above (i.e., tidal, day/night and subtidal).

Figure 4-4 shows the low passed signal of sea surface variation (left) for the summer months while the corresponding tidal signal in sea surface variation is shown on the right. The low passed signal shows general variability of the sea surface as this was driven by larger scale oceanographic and meteorological conditions.

A similar analysis was carried out on the sea surface elevation from Springmaid Pier (see Figure 4-5) where the sea surface elevation has been separated to subtidal water level variation due to wind forcing (Figure 4-5, left panel) and tidal variability (Figure 4-5, right panel). It is worth noticing that most depressions in subtidal sea surface level correspond to periods of upwelling (positive alongshore wind) conditions (for example, see periods in mid-June, end of June, and beginning of July in 2010).

The subtidal component of the dissolved oxygen signal (Figure 4-6, left panel) varies at temporal scales similar to those of the subtidal wind signal. This pattern of low frequency variability is coherent for both measurement levels in the water column, with the exception of periods when the lower sensor shows more reduction in DO levels than the upper sensor. These differences between subtidal variability in DO level are better exhibited using the difference of the values between the top and bottom sensor (Figure 4-6, left panel, see black line). This difference was always < 0 indicating lower DO levels in the lower part of the water column and shows periods with duration from 1 day to 4-5 days where the difference was very large. The high frequency component of DO levels (see Figure 4-6, right panel) on the other hand was similar for both sensors without a distinct vertical gradient being identified indicating a particular mechanism operating at these short time-scales. The difference of the high frequency signal of the difference of the two sensors at the two levels does not show a distinct pattern as it oscillates between negative and positive values at the same frequency as the individual sensor signal, indicating a coherent change in the high frequency DO signal at the two elevations with a time-delay that produces these positive and negative values.

A similar pattern was found in the high frequency water temperature signal (Figure 4-7, right panel) suggesting a coherence between fast varying temperature and DO levels which can be related to diurnal changes in water temperature due to solar heating and corresponding respiration rates in response to light intensity (day-night cycle). The low frequency temperature signal (Figure 4-7, left panel) shows the gradual increase in overall water temperature at these times which constitute part of the seasonal cycle. However, the difference of low frequency water temperature near the sea surface to that recorded near the sea bed (Figure 4-7, left panel, see black line) shows a consistent slightly cooler water near the sea bed (by 0.1 to 0.2 °C) with short periods of larger differences (0.7 to 1 °C). These short periods of larger water temperature appear to correspond to the periods of upwelling wind conditions and lower DO levels.

The low passed signals for each variable show that the scales of variability between winds, sea surface level, water temperature and DO levels are of similar scale. On the other hand the variability at time scales of a day or less is not easily identified from the time series shown above. Therefore, spectral analysis was carried in this signal and the results are shown in Figure 4-8 below.

The spectral analysis clearly demonstrates that all signals with the exception of the sea level present the most energy at a frequency corresponding to once a day. Although a peak at semidiurnal frequency was also present, this was one to two orders of magnitude lower than that corresponding to the diurnal frequency. The only exception to this was the signal from the sea water level, where the semidiurnal frequency corresponding to the major tidal constituent in the area was the maximum. These results clearly indicate that there was not significant correlation between water quality and tidal forcing and that if any correlation exists this takes place at the diurnal frequency which coincides with the day-night cycle.

Various events of low oxygen conditions in the near bed have been identified by low-passed time-series and these were related to the wind and water temperature conditions (Figure 4-9). Overall, there was a correspondence between low oxygen conditions and upwelling favorable conditions (i.e., positive alongshore wind velocity) (Figure 4-9). Almost 90% of the low oxygen events correspond with upwelling conditions. Furthermore, it appears that the period of constant upwelling condition leads to more intense low oxygen conditions. As soon as the wind changes sign from upwelling to downwelling, then the low oxygen conditions cease to exist and the oxygen concentration in the water recovers almost instantly. Qualitatively it appears that winds with an upwelling favorable direction (i.e., toward the north/northeast) during the summer almost always coincide with reduced oxygen conditions, especially when their speed does not exceed the value of 7 m/s (i.e. 15.6 miles/hr, Figure 4-8, see straight blue line). It is believed that at speeds higher than that mixing was dominant and oxygen concentration increased as a result.

When we evaluate the water temperature during the periods of low oxygen events identified earlier we see that the water temperature near the bed was always a few fractions to a couple of degrees colder than the water temperature at the sea surface (Figure 4-9). It is important to note that the intensity of low oxygen event was much larger when the thermal stratification was larger. For example, during the second decrease of DO in 2007, the DO near the sea bed was approximately 4 mg/l. This is a short lived event corresponding to moderate upwelling winds of 4 m/s (Figure 4-9, left panel) but coincides with strong vertical thermal stratification. In comparison, the first three decreases in DO during the summer of 2010 exhibited more severe low oxygen conditions, but the thermal stratification was much smaller than that of 2007. However, in 2007 the upwelling wind conditions appeared to be much stronger than in 2010. These observations suggest that the low oxygen events are correlated to thermal stratification and upwelling favorable wind conditions. The correlation of these events with the intra-daily variability was examined by looking at the short-term variability of the DO concentrations (Figure 4-11, left panel) and the tidal variability as expressed through the sea surface variation (Figure 4-11, right panel).

Figure 4-10 shows that there was no correlation between tidal range (i.e., spring – neap tides) and times of occurrence of low DO events. The high frequency variability of the DO signal

showed that this variability was higher during the periods of the low oxygen events. The spectral analysis shown earlier in Figure 4-7 revealed that this occurs once a day. Closer examination of the time-series (not shown here) revealed that during the day time and when the sea temperature is higher in response to solar heating, the DO levels take the maximum value while during the night and when the sea temperature was lower the DO level takes its lowest value. This short term variability was superimposed on the longer term variability which correlates with the meteorological conditions and water stratification.

Conclusions

Although a number of data exist in the region of Long Bay, SC most of these data have severe limitations in terms of spatial and/or temporal resolution. Therefore, this analysis has focused on the analysis of meteorological and water quality data collected over a period of 5.5 years (2006 to 2011) once an hour. Climatological analysis revealed that lower DO conditions occur mainly during the summer, especially in the June to September time frame. During this period, the mean winds were toward the north-east (upwelling favorable).

Low oxygen events correlated with upwelling favorable winds. The intensity of the event appeared to depend on the period of prevalence of the upwelling conditions and their intensity. Too strong winds allowed for mixing of the nearshore and thus no low DO events developed. These prevailing winds led to lower DO levels in the near sea bed (up to 4 mg/l) but higher frequency oscillations in DO superimposed on these low levels can drive DO level to 2 mg/l or even to hypoxic conditions. However, these events were short lived and driven by daily oscillatory signals in addition to the varying DO background level. No significant tidal correlation was found in the signal.

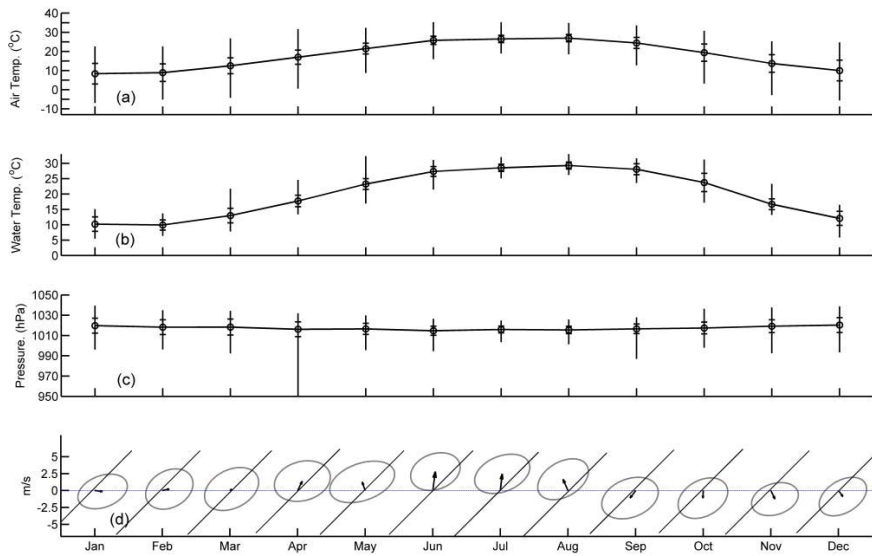


Figure 4-1. Climate of meteorological conditions as derived from the analysis of 5.5 years of hourly data (2006 to 2011) from the NOAA/NOS Meteorological station at Springmaid, SC. Monthly means of (a) air temperature; (b) sea temperature; and (c) atmospheric pressure. Monthly mean wind speed and directions are shown as a vector in (d). Standard deviations for (a) to (c) are denoted by crosses around the mean (+/- one standard deviation) while the length of the straight lines shown denote the monthly maximum and minimum values obtained over the period of data collection for each month. The ellipses in (d) represent the variability of the wind vector (based on its standard deviation) while the straight lines shown indicate the orientation of the coastline.

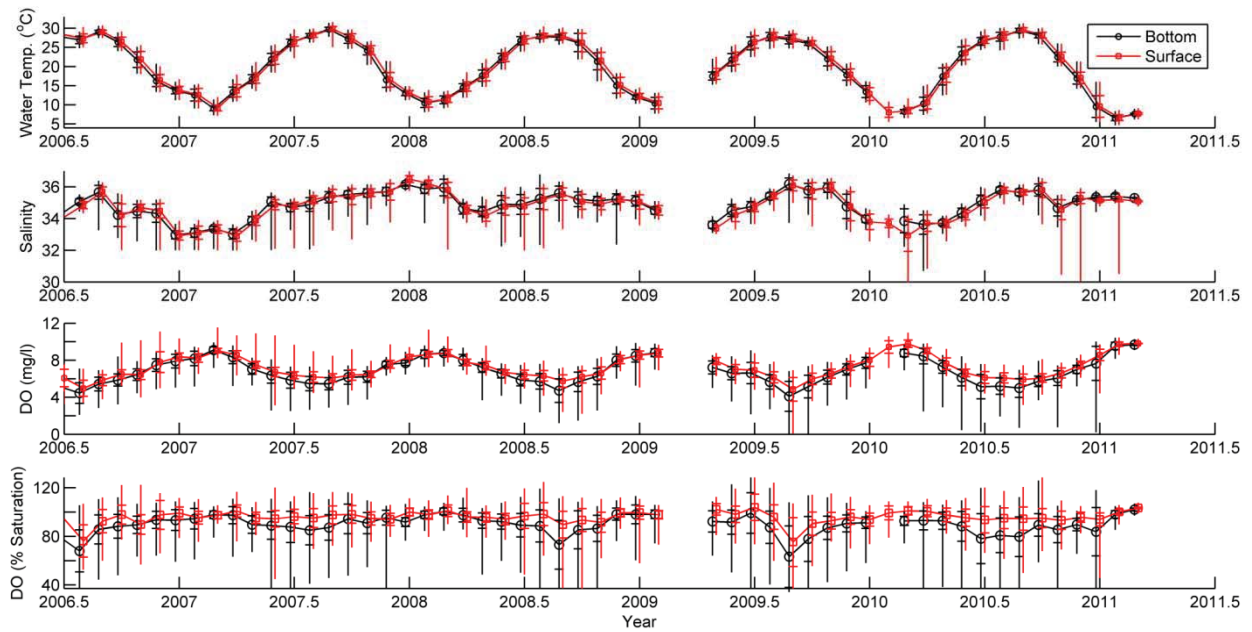


Figure 4-2. Time-series of monthly statistics (mean (o), standard deviation (+) and monthly minimum – maximum range (line) for the period June 2006 to February 2011 as collected by the station at Apache Pier. Values of water temperature, salinity, dissolved oxygen (in mg/l), and % saturation are shown for both the sensor located near the sea surface (red) and that located near the sea bed (black). Note the values of the two stations have been laterally shifted from each other for clarity.

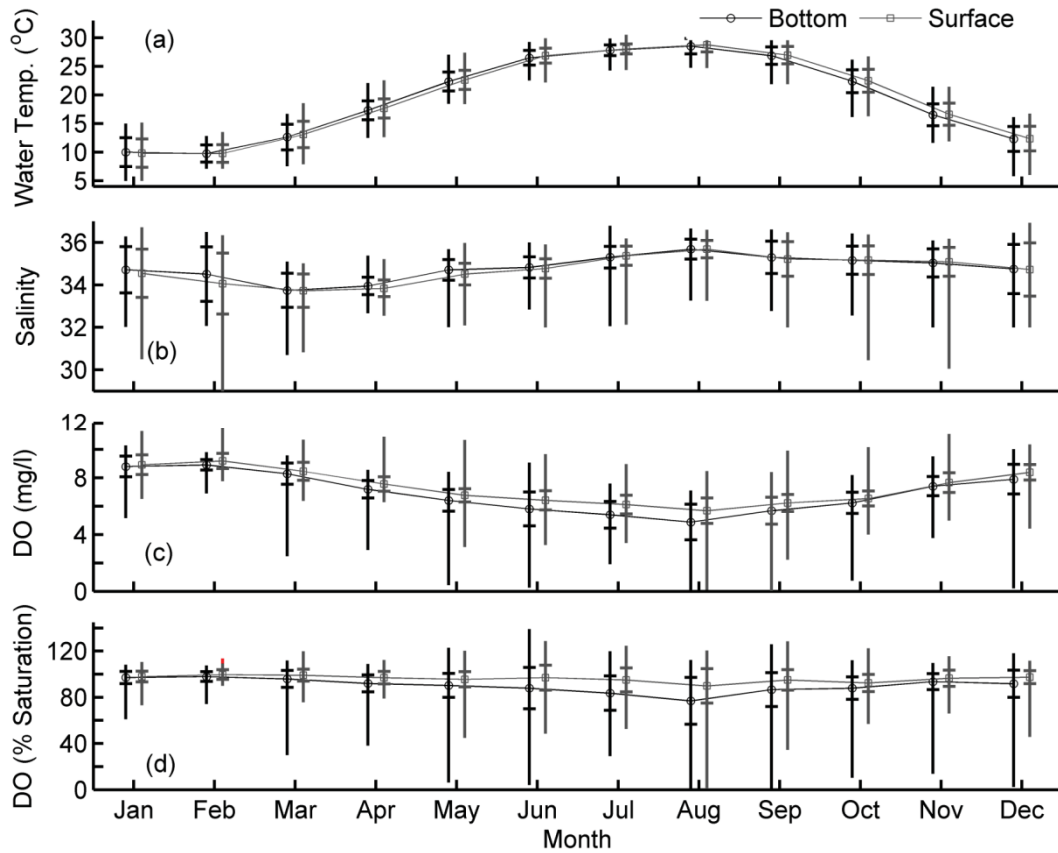


Figure 4-3. Monthly climatology of water quality data shown by year in Figure 4-2. Length of lines indicates range of minimum-maximum values while the distance between the (+) symbols corresponds to 2 standard deviations. The values from the near surface (grey) and near sea bed (black) are slightly offset in time for clarity.

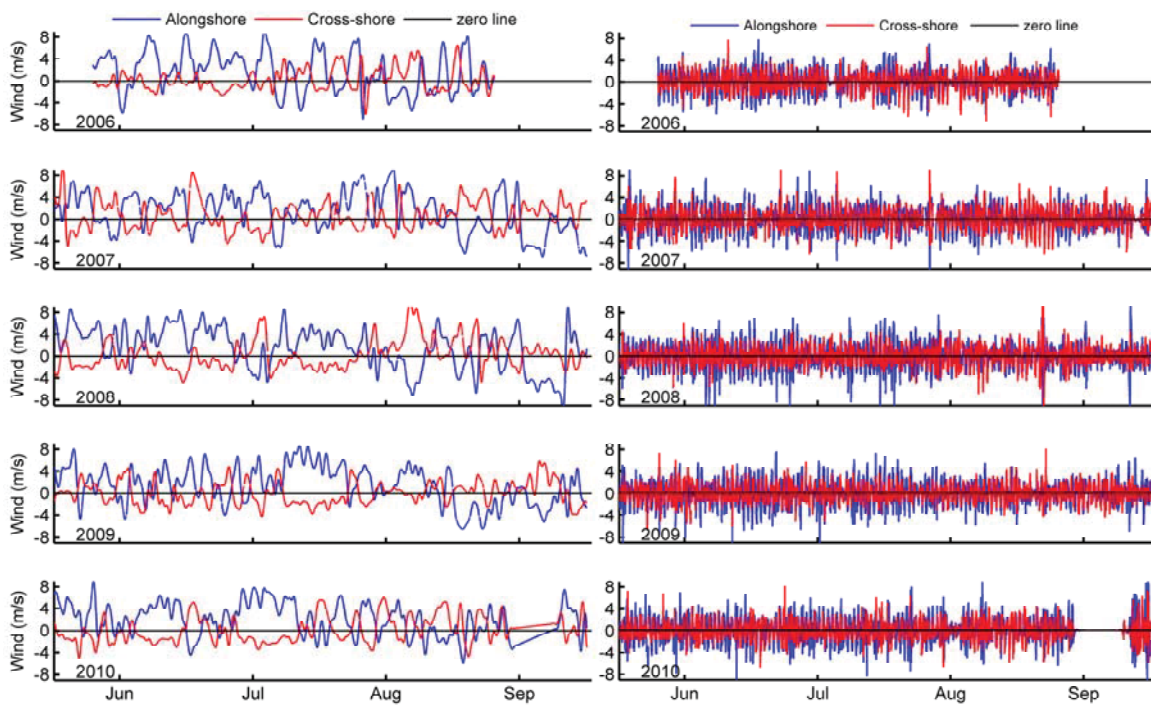


Figure 4-4. Alongshore (blue) and cross-shore (red) wind speed for the summer periods of 2006 to 2010 decomposed into a low passed (left) and intra-daily variable signal (right). Positive alongshore wind values correspond to upwelling favorable conditions.

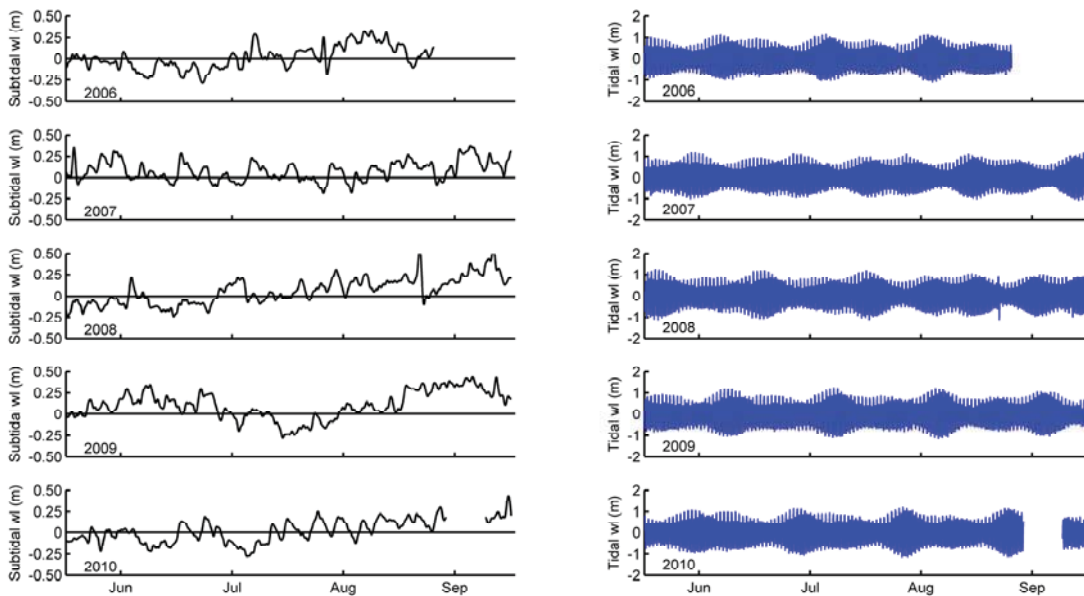


Figure 4-5. Similar time-series as in Figure 4-4 for sea level measured at Springmaid Pier. Intra-daily variable signal in this case corresponds to tidal variability. Note correlation between lower mean sea levels (left) with positive values of alongshore wind corresponding to upwelling conditions.

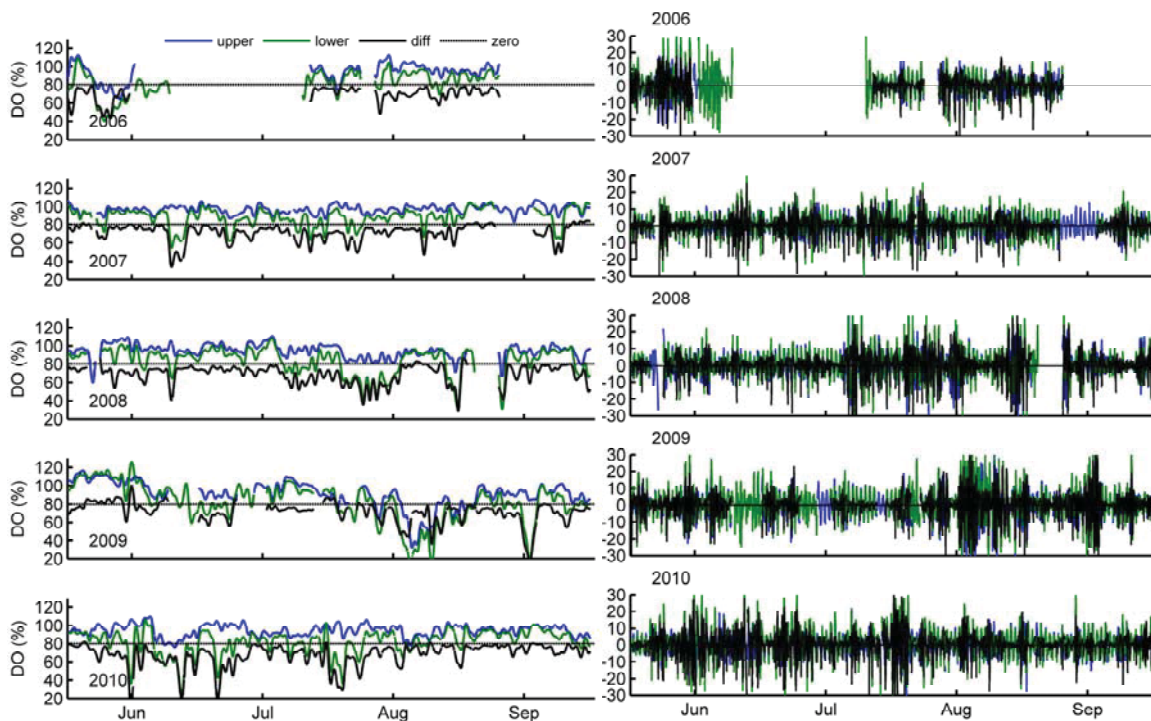


Figure 4-6. Dissolved oxygen (% saturation) for the near sea surface (blue) and near bed (green) elevations in the water column. The difference in values between the two levels is also shown (black line) with negative values indicating lower DO levels in the near bed. Left panel - low passed signal (>33hrs) and right panel - variability with oscillations faster than 33 hrs.

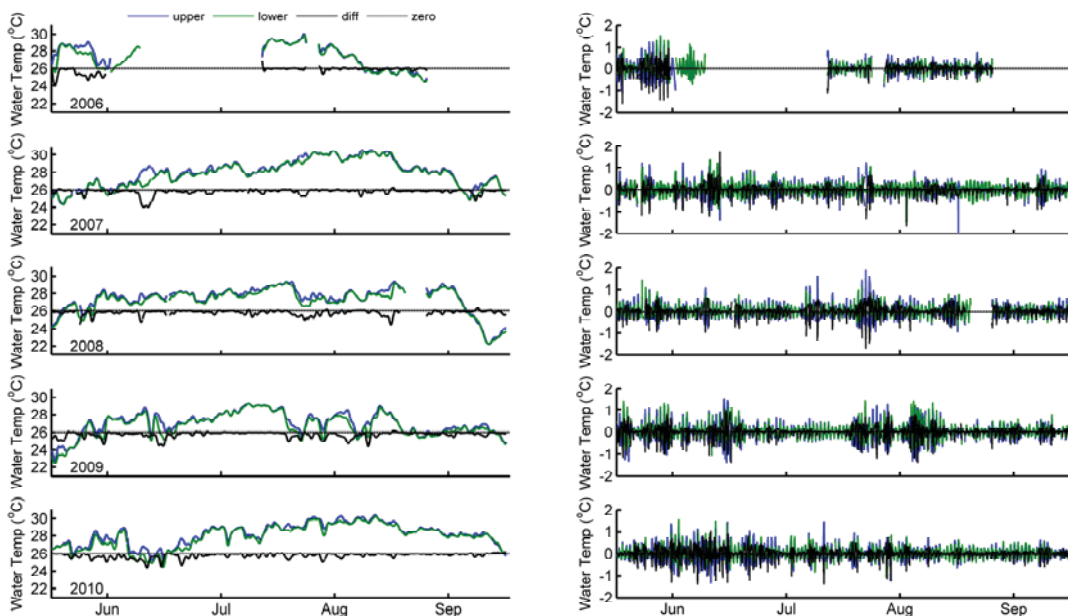


Figure 4-7. Sea water temperature values from the Apache Pier station for near the sea surface (blue) and near the bed (green) as well as their difference (near bed temperature minus sea surface temperature). Negative values of temperature difference indicate colder near bed water. Left panel - low passed signal (>33hrs) and right panel - variability with oscillations faster than 33 hrs.

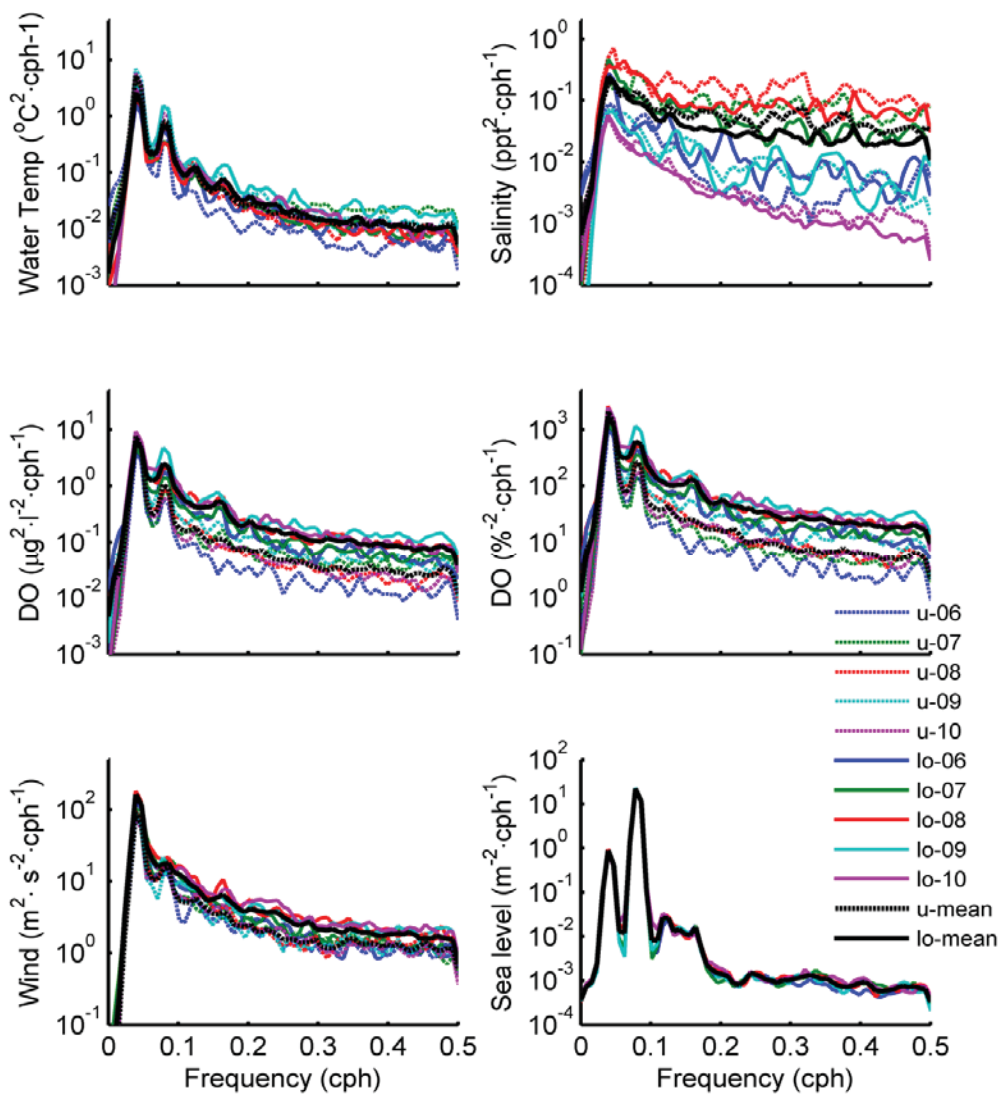


Figure 4-8. Spectral density plots of the time-series with a variability smaller than 33 hrs for the water quality parameters measured in Apache Pier and the meteorological conditions and sea level measured in Springmaid. Spectral density plots for each summer for the years 2006 to 2010 are shown as well as a mean spectral density for all summers (black line).

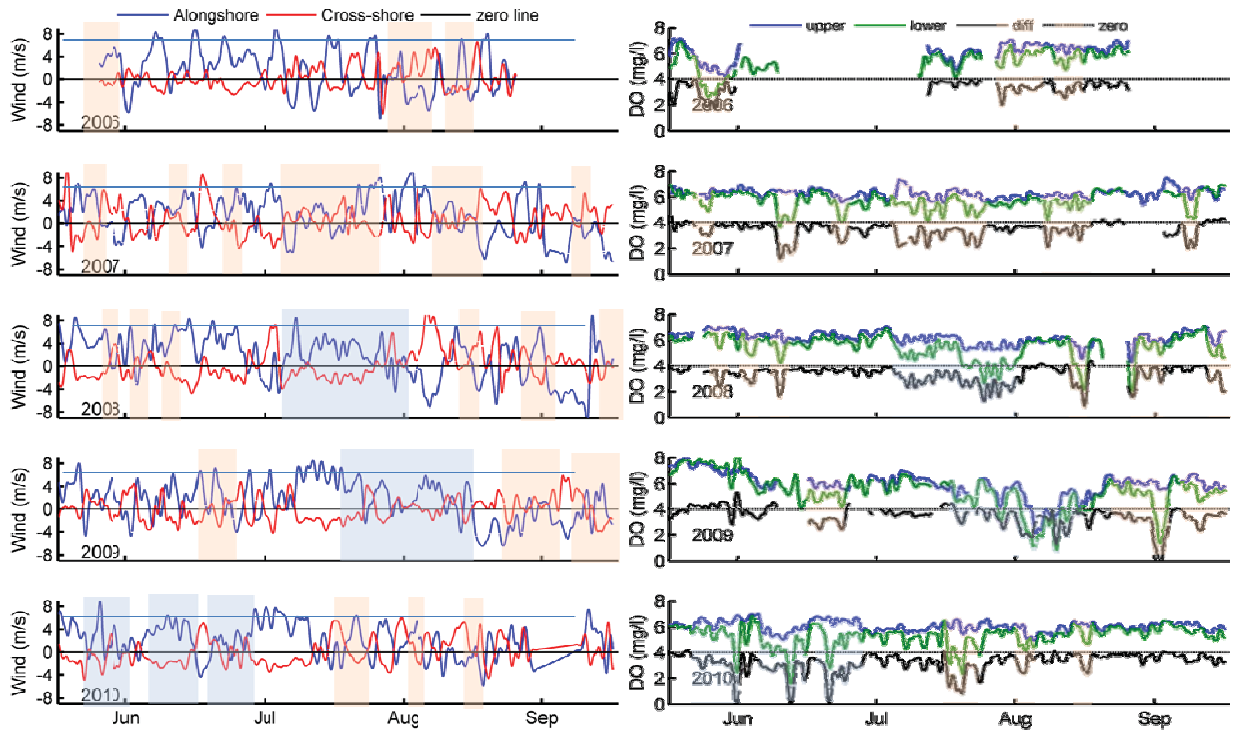


Figure 4-9. Low-passed time-series of wind velocity (left) and dissolved oxygen concentration (right) with events of low oxygen conditions being identified and marked as shaded areas. Blue shaded areas identify short lived low DO events, while blue shaded areas correspond to extended periods of low DO occurrence.

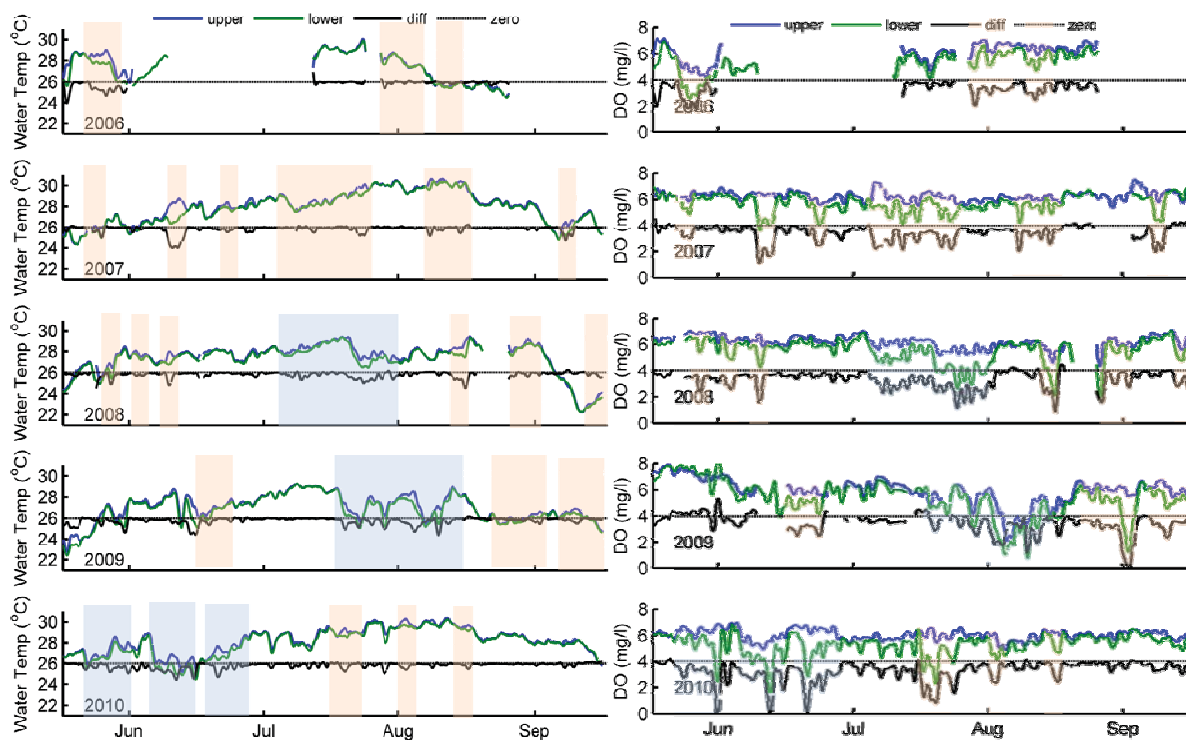


Figure 4-10. Low-passed time-series of sea temperature (left panel) and dissolved oxygen concentration (right panel) near the surface and near the bed as well as their difference. The same events of low oxygen conditions identified in Figure 4-8 are shown here.

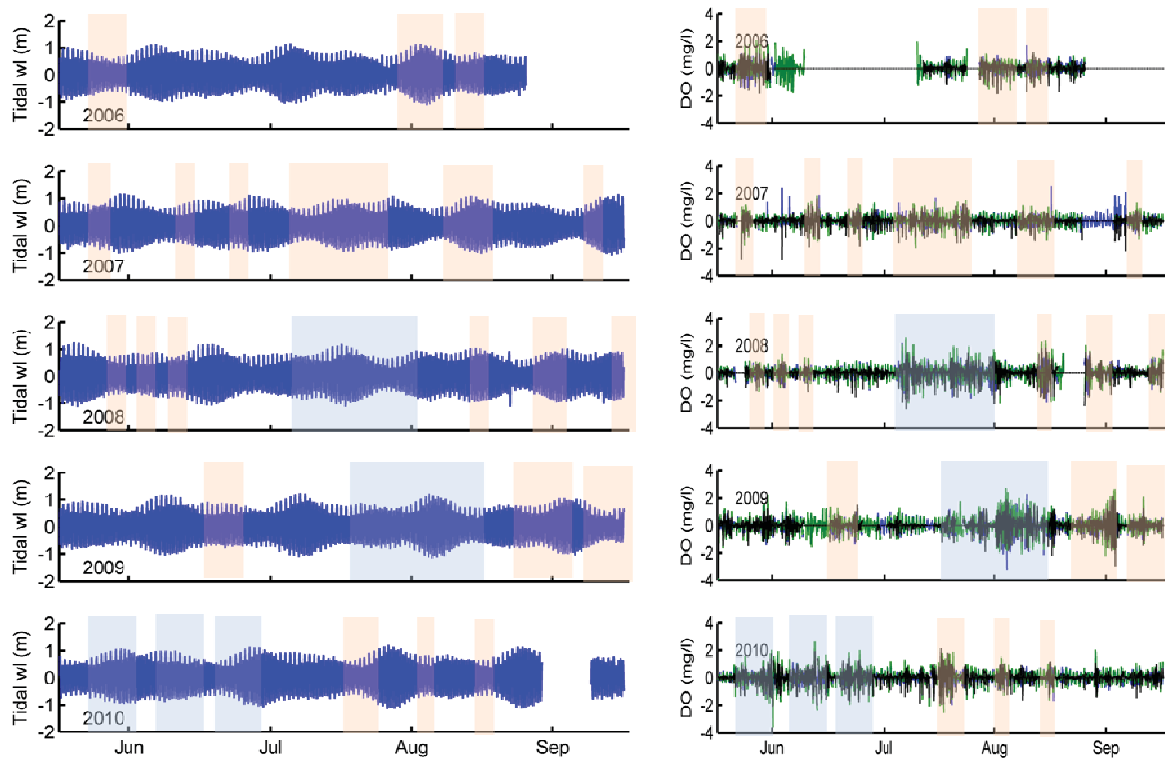


Figure 4-11. Left: Sea level tidal variability with the times of low DO events shown as shaded areas (left panel). High frequency (<33hrs) variability of the DO signal during the low DO events identified in Figure 4-8 (right panel).

Section V: Synthesis and Analysis of Available Information

The following manuscript was prepared and has been accepted for publication in Marine Ecology Progress Series. Not all of the data collected from this study are included in this manuscript; however, all of the conclusions arrived at are relevant and supported by this study.

Title: Constrained Enrichment Contributes to Hypoxia Formation in Long Bay, South Carolina (USA), an Open Water Urbanized Coastline

Authors

Denise M. Sanger¹, Erik M. Smith², George Voulgaris², Eric T. Koepfler³, Susan M. Libes³, George H.M. Riekerk⁴, Derk C. Bergquist⁴, Dianne I. Greenfield^{2,4}, P. Ansley Wren³, Clayton A. McCoy^{1,3}, Richard F. Viso³, Richard N. Peterson³, J. David Whitaker⁴

¹ South Carolina Sea Grant Consortium, Charleston, SC 29401

² University of South Carolina, Columbia, SC 29208

³ Coastal Carolina University, Conway, SC 29528

⁴ South Carolina Department of Natural Resources, Charleston, SC 29412

Abstract: Hypoxic conditions in the shallow nearshore waters of Long Bay, South Carolina, USA, an open coast embayment on the South Atlantic Bight, have been observed on a number of occasions during the summer months from 2004 to 2009, with the most pronounced episodes of hypoxia occurring in July of 2004, August and September of 2009. A synthesis of available data that included time-series oxygen measurements, synoptic surveys of water quality and oxygen consumption rates, and circulation numerical modeling aimed at explaining these hypoxic events is presented. Periods of hypoxia were found to coincide with coastal upwelling conditions (i.e., winds from the southwest and colder bottom waters). Field flow data and numerical simulations confirmed that these conditions create onshore directed bottom flows. The latter also showed that this onshore water intrusion can penetrate into very shallow waters (5-7 m depth) and is separated from the very shallow waters by a mixing front. Nutrient and organic matter concentrations, especially the particulate forms, were found to be higher in the nearshore (approximately 0.3 km from the coastline) compared to offshore (2-3 km from the coastline) waters, while dissolved oxygen concentrations tended to show increasing concentrations with distance from shore. Oxygen consumption rates via water column respiration were highly variable (5.6 – 73.6 $\mu\text{g O}_2 \text{ l}^{-1} \text{ h}^{-1}$), but showed significant correlations with spatial variability in particulate nutrient and organic matter concentrations. These observational and modeling results suggest that occurrences of low dissolved oxygen in Long Bay result from regional-scale oceanographic processes that constrain water masses to the nearshore and thus prevent the wider dispersion of local-scale terrestrial inputs. The resulting enhanced material concentrations stimulate heterotrophic oxygen demand, producing low dissolved oxygen conditions in the immediate nearshore waters.

INTRODUCTION

Coastal hypoxia, defined as the depletion of dissolved oxygen (DO) to concentrations less than 2 $\text{mg O}_2 \text{ l}^{-1}$, has been increasing in frequency, duration, and extent worldwide over the last 5 decades (Diaz and Rosenberg 1995, Wu 2002, Chan et al. 2006, Hawley et al. 2006, Diaz and

Rosenberg 2008). In addition, coastal marine ecosystems tend to exhibit thresholds whereby repeated occurrences of hypoxic events promote an increased susceptibility of further prolonged hypoxia and accelerated eutrophication (Conley et al. 2009). Hypoxic events can significantly impact biological communities in the coastal ocean (Boesch and Rabalais 1991) and the impact of low DO on sediment diagenesis and nutrient biogeochemistry can alter and further exacerbate nutrient conditions in coastal waters (Kemp et al. 2005). As such, negative economic impacts resulting from recurring hypoxia, especially with respect to recreational and commercial fisheries, can be substantial (Diaz and Solow 1999).

It is clear from previous studies of coastal hypoxia that occurrences of low DO are the result of an interaction between physical and biogeochemical processes. Increased prevalence of coastal hypoxia is most often the result of increased production of organic matter associated with excessive nutrient input (Rabalais et al. 2010). Depending on the physical processes operating within a particular system, such as stratification and mixing, this increased organic loading alters the balance between oxygen supply through physical forcing and oxygen consumption from organic matter decomposition. Thus, in the absence of stratification, or in the presence of intense mixing, hypoxia is not generally expected to occur, regardless of organic matter loading rates (Conley et al. 2009, although see Verity et al. 2006). As a result of this interplay between physical and biogeochemical processes, hypoxic events have been reported for a variety of coastal settings; ranging from regions with narrow continental shelves such as that of the west coast of the USA (e.g., Grantham et al. 2004, Chan et al. 2006, Connolly et al. 2010), shallow shelves influenced by river discharge such as the Gulf of Mexico (e.g., Wiseman et al. 1997, Turner et al. 2005, Bianchi et al. 2010), enclosed basins such as the Chesapeake Bay and Long Island Sound (e.g., Anderson and Taylor 2001, Hagy et al. 2004), or shallow continental shelves influenced by bottom bathymetry such as the New Jersey Shelf (e.g., Glenn et al. 1996, Glenn et al. 2004). Zhang et al. (2010) suggested a classification of coastal systems based on the location and mechanisms responsible for the generation of hypoxic conditions. These are: (1) “coastal upwelling systems” – driven by physical transport of deep bottom water high in nutrients and low in DO to inshore waters; (2) “off river mouths and in estuaries” – driven by nutrient input from land sources and water column stratification; and (3) “semi-enclosed seas and basins” – driven by land derived nutrient inputs and water column stratification in combination with restricted physical exchange that promotes long water residence times.

Few cases of hypoxia have been observed for shallow coastal ocean environments such as along the open ocean, shallow shelf, coastal region off of South Carolina (SC), USA, where hypoxia was first quantitatively observed in 2004 (Sanger et al. 2010). At this time, hypoxic conditions were found in the nearshore waters (5-7 m depth) off an open beach in the central portion of Long Bay. That hypoxia occurred just seaward of the surf zone (approximately 0.3 km from the beach-face) was somewhat surprising, given this is an area generally considered to experience high physical mixing. Analysis of limited water quality and meteorological data revealed that the first documented hypoxic event occurred during a period of sustained southwesterly upwelling-favorable winds that coincided with the occurrence of cold bottom water (Sanger et al. 2010). Although Long Bay is influenced by coastal upwelling, no evidence existed to suggest that the upwelled water is a direct source of high nutrients and/or low DO. In addition, the location is not adjacent a major river source and the adjacent estuaries of Winyah Bay in the south and Cape Fear in the north do not discharge large amounts of water during the summer (McCarney-Castle

et al. 2010), and no evidence of surface buoyant plumes have been reported. The region is, however, subject to significant inputs of non-point source pollution from the Greater Myrtle Beach area, a highly urbanized ocean-front resort community. Given the shape of the coastline, Long Bay cannot be considered a semi-enclosed sea or basin, nor is it close to the continental slope. As such, it cannot easily be classified as any of the system types presented by Zhang et al. (2010) for hypoxia formation. Instead, it seems that hypoxia formation in the central region of Long Bay, SC, USA, results from a unique combination of physical and biological mechanisms that are a mixture of the three types of systems identified by Zhang et al. (2010).

Following the initial observation of hypoxia in the summer of 2004, a multidisciplinary team of scientists and managers from a variety of academic, state, and federal institutions was assembled to investigate the potential cause of hypoxia in Long Bay (Sanger et al. 2010). Several alternative mechanisms/hypotheses for hypoxia generation were proposed at that time, based on experiences from well-known hypoxic events elsewhere (Sanger et al. 2010). This then led to a variety of research and monitoring activities conducted in these waters during 2006 – 2008, with the goal of further documenting and understanding the occurrence of hypoxia in this shallow open coast environment. The objective of this contribution is to synthesize available data from these efforts relating to the formation of hypoxic conditions in the nearshore waters of Long Bay and assess the contributions of oceanographic and biogeochemical processes in promoting hypoxia in this region.

MATERIALS AND METHODS

Study Area

Long Bay, an open ocean, shallow embayment is located on the South Atlantic Bight (SAB) of the USA, which extends for 145 km from the Cape Fear Estuary, North Carolina, in the north, to Winyah Bay, South Carolina, in the south, which are the two main riverine sources (Figure 5-1). The shoreline along the central portion of Long Bay includes the urbanized beach-front resort community of Greater Myrtle Beach, SC (approximately 57 km of shoreline). This area, with a resident population on the order of 300,000 (based on 2008 U.S. Census data), receives approximately 14 million visitors per year with 90 % visiting the beach (MBCC 2009). Tourism accounts for \$3.1 billion or 31.6 % of the state's total domestic travel expenditures (US Travel Association 2009). Stormwater runoff from Greater Myrtle Beach is discharged directly into nearshore waters via 14 anthropogenically modified tidal creeks that traverse the beach face and approximately 100 stormwater discharge outlets (ocean and beach-front outfall pipes). Together these outlets drain a highly urbanized landscape that includes a large network of stormwater detention ponds.

Data Availability

Following the initial observation of hypoxia in Long Bay, several individual research projects were initiated and carried out during the period 2006 – 2008. In addition, a program of continuous monitoring of DO in surface and bottom waters at a central location in the nearshore waters off Greater Myrtle Beach was established. Although periods of depressed DO ($< 4 \text{ mg O}_2 \text{ l}^{-1}$) were often observed during the summer months of this period, no sustained hypoxic periods similar to the 2004 event were observed. During the summer of 2009, however, a period of sustained hypoxia, this time with periods of anoxia, was observed (Libes and Kindelberger 2010, McCoy et al. 2011), suggesting that the 2004 event was not an isolated incident. In response to

this event, an ad-hoc effort was conducted to gather as much information about the event as possible despite limited resources available at the time. Data available from the planned research during 2006 – 2008 and from the rapid response to the 2009 event are described in the following sections and broadly categorized as continuous monitoring, targeted research, and response sampling to the 2009 events.

Continuous Dissolved Oxygen Monitoring

At the north end of Greater Myrtle Beach, SC, near the northern limit of the low DO observations made in July of 2004, a continuous monitoring station was established in June of 2006. The station consists of two sondes (Yellow Springs Instruments [YSI] 600R with Clark DO cells) installed at the seaward end of a fishing pier (Apache Pier, located at 33.7615 N, 78.7798 W) at a mean water depth of 7 m. The sensors were placed in perforated PVC standpipe painted with antifouling paint and provided measurements of DO, temperature and conductivity at 15-minute intervals at the surface (approximately 1 m below the instantaneous sea level) and at 1.5 m above the sea bed. The performance of the sensors and data quality was validated through pre- and post-deployment calibration checks and by comparison with *in situ* measurements made with other instruments. These procedures provided measurements with uncertainties of ± 0.4 psu, ± 0.4 mg O₂ l⁻¹, ± 5 %, and ± 0.1 °C, for salinity, DO concentration, % DO saturation, and water temperature, respectively.

Targeted Hypoxia Research Projects

Two targeted research projects were undertaken during the period 2006 to 2008: (1) field sampling of inner shelf waters (0.3 – 3.0 km from shore) for water column oxygen consumption rates and biogeochemical conditions associated with occurrences of low oxygen waters; and (2) numerical simulation modeling of physical scenarios under which Gulf Stream Water (GSW) can reach nearshore in Long Bay. The first project was aimed at quantifying the potential for local biogeochemical conditions to drive *in situ* depletion of oxygen through enhanced pelagic respiration (local forcing of low DO conditions), while the second project was aimed at examining the validity of the hypothesis that the hypoxia is the result of the advection of deep, cold GSW that may be rich in nutrients and low in oxygen concentration (remote forcing of low DO conditions).

Biogeochemical Conditions and Pelagic Respiration Rates: To understand the relationships between nearshore and offshore distributions of DO, chlorophyll, nutrients, organic matter, and DO consumption due to pelagic respiration, a series of sampling excursions were conducted during the summers of 2006 (7/10/06-7/11/06, 7/27/06-7/28/06, 8/7/06-8/8/06, 8/24/06-8/25/06), 2007 (7/24/07-7/25/07, 8/15/07), and 2008 (7/11/08, 7/25/08, 8/29/08). Sampling focused on dates with spring tidal conditions (± 3 days) and low slack tidal stages (± 2.5 hours). Two to three shore-perpendicular transects were sampled for each date running between 0.3 to 3.0 km from shore. The transects were located off sites suspected of being influenced by land-based stormwater contributions (i.e., tidal creeks), as well as sites away from such influences, with all transects confined in the region between Apache and Springmaid piers (Figure 5-1). Along each transect, DO and chlorophyll *a* (Chl *a*) were routinely sampled in surface and bottom waters using a YSI 85 DO sensor and WETLABS fluorometer, respectively. The fluorometer was calibrated using independently collected acetone-extracted Chl *a* samples that were quantified by bench-top fluorometry (Arar and Collins 1997). In addition, water samples were collected from

the surface and bottom waters, using a Van Dorn sampler, from the 0.3 km and 3.0 km sites of each transect, hereafter referred to as nearshore and offshore sites, respectively. Samples were stored on ice until returned to the laboratory for processing.

Water samples were analyzed for total nitrogen (TN) (whole [TNW] and filtered [TNF]), total phosphorus (TP) (whole [TPW] and filtered [TPF]), orthophosphate, nitrate + nitrite, ammonium, particulate organic matter (POM), dissolved organic carbon (DOC), Chl *a*, and pheophytin (Pheo). TN, TP, orthophosphate, nitrate + nitrite, and ammonium were measured using seawater methods for a Technicon nutrient autoanalyzer with working ranges suitable for coastal waters. The TN and TP method was based on a dual persulfate digestion (Glibert et al. 1977). The particulate component of the total nitrogen (TN_{part}) and total phosphorus (TP_{part}) were determined by subtraction of the whole minus the filtered components. Dissolved organic nitrogen (DON) and phosphorus (DOP) were calculated by difference. Total suspended sediment (TSS) concentrations were determined by standard gravimetric methods, with the organic fraction of TSS (here after referred to as POM) determined by loss on ignition at 450 °C. DOC concentrations were determined on filtered (GF/F), acidified water samples by high-temperature combustion using a Shimadzu TOC-VCPN following the procedures of Benner and Strom (1993). Phytoplankton pigments were analyzed via acetone extraction for Chl *a* and Pheo and quantified by fluorometry (Arar and Collins 1997).

A subset of water samples collected for the above analyses were also subjected to microplankton respiration rate measurements. These water samples were maintained at *in situ* temperatures during transport (< 4 h) back to the laboratory, where respiration incubations were conducted. Respiration rates were determined from standard dark-bottle oxygen consumption rates during 6 h incubations in 300-mL borosilicate glass biochemical oxygen demand (BOD) bottles (e.g., Smith and Kemp 2001). Oxygen concentrations were determined by automated Winkler titrations of whole bottle samples using a Metrohm 798 Titrino with potentiometric end-point detection (Carnigan et al. 1998). Temperatures during incubation were maintained at ± 1 °C of *in situ* temperatures, which ranged from 26 – 28 °C for all sampling events.

Numerical Simulation Model: Previous research in the SAB has shown that it is not uncommon for cold GSW to be present in the outer shelf bottom layer during the summer season (Atkinson and Blanton 1986, Lee and Pietrafesa 1987, Hamilton 1987). Once the GSW is present on the outer-shelf, upwelling-favorable southwesterly winds, a common climatological occurrence in the summer (Blanton et al. 2003), can transport it across the shelf (Hoffman et al. 1980, 1981) with the occurrence of GSW on the middle shelf not being unusual. Such events had been identified in Long Bay from the analysis of salinity – temperature data (T-S diagrams) from a data buoy located at 10 m water depth (Voulgaris and Sanay 2010). These observations led to the development of the hypothesis that GSW intrusions might be associated with the observed hypoxic events. In order to identify the physical scenarios under which GSW intrusions can reach the inner-shelf and the relative importance of each forcing mechanism, a series of process-oriented 3-D numerical simulations were carried out.

The numerical model used was the Regional Ocean Model System (ROMS), a primitive equation, free-surface, hydrostatic, sigma-coordinate model (Shchepetkin and McWilliams 2005). The model setup included all the terms of the primitive equations except horizontal

viscosity (Haidvogel et al. 2000, Umlauf and Burchard 2003). The model domain (Sanay et al. 2008, Voulgaris and Sanay 2010) was set up to simulate a concave-shaped bay (300 km long) bounded by a cape in the north (Cape Fear, NC) and one in the south (Cape Romain, SC). The characteristics of the central part of the domain resemble the morphological and bathymetric features of Long Bay from the coast (5 m depth) to about 150 km offshore (55 m depth). In both horizontal directions, the grid resolution varied from 1.5 to 3 km with the highest resolution near the coast.

Several numerical simulations were carried out to elucidate the physical conditions under which GSW can reach the inner-shelf. The direction, magnitude, and duration of the wind patterns used in the simulations were consistent with those observed in this section of the SAB during summer (Blanton et al. 2003). The initial conditions used included: (a) well mixed conditions, and (b) an initial vertical stratification consisting of a well-mixed surface layer (4 m thick, 22 °C) and a bottom layer (15 °C) with a linearly stratified thermocline density in between extending from 4 to 10 m below the surface, resembling typical summer stratification conditions in the SAB (Alexabareta et al. 2006). Each of the initial conditions presented above were forced with (a) constant wind stress linearly ramped up to a maximum value of 0.10 N m^{-2} within a period of 6 h which then remained constant, and (b) an oscillatory wind stress with a period of 3 d and minimum and maximum values 0.01 and 0.20 N m^{-2} , respectively. Each simulation case was carried out with and without solar radiation, resulting in 8 simulation scenarios that combined all conditions described above. The wind stress levels and periods of oscillations were selected to correspond to the most common atmospheric conditions observed during the hypoxic events of 2004 and in accordance with the published wind climatology. Additional simulations were carried out with freshwater discharge inputs of approximately $350 \text{ m}^3 \text{ s}^{-1}$ from the north and south boundaries representing buoyancy fluxes for the Cape Fear and Pee Dee rivers, respectively.

2009 Hypoxia Event Sampling

With the onset of significant hypoxia observed at the Apache Pier monitoring station in August of 2009, several *ad hoc* sampling programs were undertaken to resolve the cross-shore (nearshore to offshore) and alongshore extent of hypoxic waters and the physical-chemical conditions associated with these waters. Ship-based spatial surveys of surface (0.3 m below water surface) and bottom (0.5 m above sediment surface) water DO concentrations and water column physical properties were conducted on three separate dates during the hypoxic period (8/20/09, 8/24/09 and 8/27/09). Discrete samples were also collected from surface and bottom samples on 8/20/09 (n=28) and 8/27/09 (n=10) at a number of sites both within and outside the observed hypoxic area. These water samples were analyzed in the laboratory for nutrients, organic matter, Chl *a*, and Pheo, as described previously. Phytoplankton community composition was also determined from 250 ml of water preserved with Lugol's iodine solution diluted to 3 %. Phytoplankton identification to the lowest taxonomic level possible was carried out using light microscopy but this analysis was limited only to samples collected on 8/20/09.

Flow measurement data was available for the same period from two locations at approximately 0.85 km (7 m water depth) and 2.5 km (10 m water depth) off the shoreline of Second Avenue Pier (Figure 5-1, triangles). The nearshore site was instrumented with a high-resolution downward-looking 1200 KHz RDI/ Teledyne Acoustic Doppler Current Profiler (ADCP)

mounted at 1.5 m above the seabed and an upward-looking Nortek Acoustic Wave and Current (AWAC) profiler. The ADCP measurements were limited to the lowest 1 m of the water column with a 10 cm bin size, while the AWAC measured current velocities throughout the entire water column with a 1 m bin size from 2 m above the sea bed to the surface. The offshore site was instrumented with a Sontek Acoustic Doppler Velocimeter (ADV) which measured currents at 15 cm above the seabed and an upward looking 1200 kHz RDI/ Teledyne ADCP measuring directional wave spectra and mean current profiles of the water column in 1 m bins. The instruments that measured currents within the lower water column at each site collected data simultaneously in “burst mode” at 1 Hz for approximately 17 min every two hours. The AWAC and upward-looking ADCP measured mean current velocities throughout the upper water column every 10 min.

At the onset of hypoxia, the above two flow measurement sites off Second Avenue Pier were also equipped with YSI 6600 sondes to measure DO, temperature, pH, conductivity, turbidity and chlorophyll every 15 minutes from 8/20/09 to 9/4/09. Two additional water quality Hydrolab 5 Datasondes were also deployed in the bottom waters at approximately 0.25 km and 2.5 km off Springmaid Pier (Figure 5-1, triangles) from 8/20/09 to 9/4/09.

Statistical Analysis

Statistical analysis of the various water column metrics (e.g., nutrients, organic matter, respiration rates) included Spearman Correlation analysis, Principle Component Analysis (PCA), and regression analysis using the SAS (v9.1) and JMP (v8.0) statistical packages. Spearman Correlation and PCA were used to determine the role of substrate regulation in respiration rates. The correlation alpha levels were corrected for multiple comparisons using a Proc MULTTEST Stepdown Bonferroni.

RESULTS

Dissolved Oxygen Temporal Dynamics

Time-series DO data from Apache Pier showed both surface and bottom waters of the central portion of nearshore Long Bay waters to be generally under-saturated with respect to DO (Figure 5-2). During the summer months (June-September) of 2006, 2007 and 2008, occurrences of depressed DO levels ($< 4 \text{ mg O}_2 \text{ l}^{-1}$) were common in the bottom waters (Figure 5-3a). These depressed DO levels developed into hypoxic conditions ($< 2 \text{ mg O}_2 \text{ l}^{-1}$) for some of these periods but they were of short duration (a few hours). Close examination of the wind speed and direction measurements from the Springmaid Pier NOAA station indicated that all of these events coincided with periods of upwelling favorable winds (Figure 5-3c, positive alongshore wind velocity or winds from the southwest). This coincidence of hypoxic conditions along with upwelling favorable winds implied a strong dependence on physical forcing.

Biogeochemical Conditions and Pelagic Respiration Rates

In the summers of 2006 to 2008, nutrient, Chl *a* and particulate organic matter concentrations tended to significantly co-vary, both within surveys and across years. In contrast, concentrations of DOC showed little spatial or temporal variation and were not significantly correlated to other water chemistry parameters. Across all samples, approximately half the nitrogen and phosphorus pools were found in particulate form with organic fractions comprising a majority of the total dissolved nitrogen (80-90 %) and phosphorus (40-60 %). On average, nutrient, Chl *a* and organic

matter concentrations all decreased from nearshore to offshore sites (Table 5-1). Pair-wise comparisons revealed these nearshore – offshore differences to be significant ($p < 0.01$) for all variables except for DOC and the dissolved inorganic nutrients. Similarly, concentrations of particulate nutrients and Chl *a* were significantly greater in bottom waters than in surface waters, but surface – bottom differences were not significant for dissolved nutrient or DOC concentrations.

Rates of pelagic respiration measured during the summer months of 2006 to 2008 were highly variable, both within and across sampling events. For the entire data set ($n = 72$), respiration rates ranged from $5.6 - 73.6 \mu\text{g O}_2 \text{ l}^{-1} \text{ h}^{-1}$ and showed a log-normal distribution, with a mean of $21.2 \mu\text{g O}_2 \text{ l}^{-1} \text{ h}^{-1}$ and a median of $18.3 \mu\text{g O}_2 \text{ l}^{-1} \text{ h}^{-1}$. On average, respiration rates measured in nearshore bottom waters exceeded rates measured in offshore bottom waters (25.4 ± 12.2 [average ± 1 standard deviation] versus $19.5 \pm 9.2 \mu\text{g O}_2 \text{ l}^{-1} \text{ h}^{-1}$, respectively), and in 15 paired-station comparisons of nearshore and offshore bottom waters along the same longitudinal transects, nearshore respiration rates were significantly higher ($p < 0.01$) than corresponding offshore rates on 12 occasions. In contrast to this general nearshore-offshore gradient in respiration rate, differences between surface and bottom water respiration rates (quantified in 2006 only) tended to be smaller. Surface water respiration rates averaged $14.7 \pm 5.3 \mu\text{g O}_2 \text{ l}^{-1} \text{ h}^{-1}$, compared to $18.9 \pm 15.0 \mu\text{g O}_2 \text{ l}^{-1} \text{ h}^{-1}$ in bottom water, and bottom water respiration was significantly greater ($p < 0.01$) than surface water respiration in 10 of 16 paired comparisons.

The lack of substantial temperature variation ($< 2 \text{ }^\circ\text{C}$) across sampling events allowed us to use relationships between respiration rate and *in situ* nutrient and organic matter concentrations to explore the role of substrate regulation in controlling the magnitude and variability in respiration in its absence. Across all sampling events, rates of respiration were significantly correlated ($p < 0.0025$) to concentrations of POM, Chl *a*, Pheo, DOC, TNW, and TPW (Table 5-2). Concentrations of these substrates showed significant co-variation, with the exception of DOC which was found to not be significantly related to either Chl *a* or Pheo. The role of substrates in regulating respiration rates was also explored using PCA (Figure 5-4). The first two axes explained 73 % of the variability in the dataset, with 50 % and 23 % attributed to PC 1 and PC 2, respectively. PC 1 had high positive loadings for all particulate substrate concentrations (POM, Chl *a*, and Pheo, TN_{part} , TP_{part}) and respiration rate, whereas PC 2 had high positive loadings for all of the dissolved substrate constituents (DOC, TNF, TPF) (Figure 5-4). The tight grouping of mean factor loadings for respiration, POM, Chl *a*, Pheo, TN_{part} , and TP_{part} suggests the importance of living and detrital particulates in determining variability in respiration rates, which is consistent with the fact that POM and Chl *a* were found to have the highest individual correlation coefficients with respiration rate (0.66 and 0.70, respectively) of the entire dataset.

Numerical Simulation Model

The results from the numerical modeling work clearly demonstrated the development of a cross-shore circulation (Figure 5-5, onshore flow near the bed and offshore directed flow near the surface in right column) in the outer and inner-shelf under oscillatory, southwesterly (i.e., upwelling favorable) wind conditions (Figure 5-5, top panel) and under the influence of solar radiation. A few hours after maximum wind stress, the water column near the shoreline (distances $< 4 \text{ km}$) was homogeneous (Figure 5-5, time = 8.0 days). Further offshore, the water column remained stratified and Ekman transport (i.e., offshore directed flows near the surface)

was present. When the magnitude of the wind stress decreased, the inner-shelf water column began to thermally stratify again due to solar radiation, and Ekman transport was re-established in the nearshore (Figure 5-5, time = 8.3 days, distances < 4 km). This Ekman transport carries cold water toward the coast at the bottom layer and further enhances stratification. As the wind stress increased again, the Ekman transport intensifies as well as the vertical stratification (Figure 5-5, time = 10.0 days), until the wind-stress became strong enough to break the stratification very close to the shoreline and mix the water column thereby allowing re-oxygenation of the bottom water (Figure 5-5, time = 10.3 days). The model simulations indicated that during this process, a mixing front developed in the very shoreward end of the domain that defined the area of stratified waters with onshore directed bottom flow from a nearshore zone of well mixed water column that clearly separated these two domains. Model runs under constant upwelling directed winds of similar strength as the oscillating winds showed no development of Ekman transport due to enhanced mixing. The same results were obtained for oscillating winds but with no solar radiation included.

The general pattern of flow and temperature conditions provided by the model simulations described above are in close agreement with that observed in Long Bay (water quality at Apache Pier and current/wind conditions at Springmaid Pier) in the summers of 2006 and 2007 (Figure 5-3). In 2006, low-oxygen (< 3 mg O₂ l⁻¹,) events in the coastal bottom layer occurred only during the summer season (with high solar radiation and low river discharge) and under long periods (more than 15 days) of upwelling favorable wind conditions. In contrast, during the summer of 2007, no periods of low DO were observed near the coast and the water column remained thermally homogeneous most of the time, providing no evidence of thermal stratification (Figure 5-3a and b).

2009 Hypoxic Event Sampling

In 2009, a severe hypoxic event occurred during the period 8/17/09 to 8/25/09, followed by a second event during the period 9/15/09 to 9/17/09 (Figure 5-6c). The instantaneously measured DO concentrations varied within each day following a predominantly diurnal cycle mixed with a secondary semidiurnal frequency which lead to absolute hypoxic conditions for a significant part of each day (Figure 5-6c). Diurnal variability in the instantaneous temperature record was observed, which is explained by solar radiation (Figure 5-6b). Examination of the low frequency variation of the DO concentration shows that this intra-diurnal variability was accompanied by a reduction of the diurnal average over time. This occurred for both surface and bottom signals, with the latter always being lower (Figure 5-6d). A similar vertical difference in daily mean water temperatures between surface and bottom waters indicated that thermal stratification had occurred and coincided with the decreases in DO concentration (Figure 5-6d).

Sampling showed that this hypoxic event was spatially limited to nearshore waters (0.25 – 2 km offshore) off Greater Myrtle Beach in a fairly cohesive water mass (Figs. 4-1 and 4-7). As with previous events, the 2009 events again coincided with periods of stratification (Figure 5-6b and d, vertical differences in water temperature or thermal stratification) and upwelling-favorable wind conditions (Figure 5-6a, north, north-eastern directed wind vectors). It is worth noting that the oscillating character of the wind prior to and at the initial stages of each event showed short times of wind reversal followed by consistent upwelling wind vectors, similar to those used in the numerical modeling (Figure 5-6a). Furthermore, DO concentrations were also found to

increase from nearshore (0.25 - 0.85 km) to offshore (2.5 km) (Figure 5-7a and b). It should be noted that the August event occurred during a period of unusually high astronomic spring tides (Figure 5-6e) (Sweet et al. 2009) and this was partially reflected in the bottom DO signal at Apache Pier (Figure 5-6c), but was not observed in the signal from the nearshore and offshore stations where the oscillatory signal recorded was mainly diurnal (Figure 5-7a and b). Low passed bottom temperature (Figure 5-6d) and cross-shore current velocity data (Figure 5-6g) showed a coincidence of lower bottom water temperatures with onshore directed bottom flows (Figure 5-6g, identified by x symbol), which indicated that after persistent upwelling favorable winds, colder bottom water was advected onto the inner-shelf at the two Second Avenue Pier locations (0.85 km and 2.5 km). These results follow the flow patterns demonstrated by the numerical model results presented earlier, indicating that a 10-15 day period of upwelling winds could advect GSW to the inner-shelf and the nearshore during the summer months when stratification of the water column occurs.

In comparison to the 2006 – 2008 summer data, the August of 2009 event was characterized by high concentrations of nutrients, organic matter, and Chl *a*. The highest concentrations coincided with the lowest DO levels. Average total nitrogen and total phosphorus (whole and filtered) values in August of 2009 were at least double those observed during the 2006 – 2008 sampling (Figure 5-8), although the proportion of total nutrients represented by the particulate fraction were generally similar. Furthermore, station averaged concentrations of POM and Chl *a* were also more than twice the averages observed during 2006 – 2008 (Figure 5-8). Concentrations of DOC measured in 2009 were only slightly higher than concentrations measured during 2006 – 2008 (Figure 5-8). Phytoplankton community composition was assessed on 8/20/09 and was found to be largely composed of *Proboscia alata*, a large, surface mat forming diatom. Concentrations ($\sim 5 \times 10^5$ to 1×10^6 cells l^{-1}) were higher in bottom water suggesting the senescence of *P. alata* cells.

DISCUSSION

Low DO directly off the beach of an open coastline, away from immediate riverine discharge, would not be expected from the traditional conceptual models of hypoxia development (Zhang et al. 2010, Rabalais et al. 2010). The various observations and the results presented in this paper lead us to conclude that low DO events in Long Bay are instead caused by a rather unique combination of regional- and local-scale drivers. The regional-scale drivers are mainly physical oceanographic processes and are associated with upwelling and solar radiation. These physical processes act to concentrate local-scale (terrestrial) inputs of nutrient and organic matter in the immediate nearshore waters, which greatly enhances localized heterotrophic metabolism and consequent oxygen demand, resulting in formation of low DO conditions in these waters.

The numerical simulations conducted as part of this study indicate that southwesterly wind conditions can transport offshore water masses all the way to the inner shelf (Figure 5-5), which is in agreement with previous studies that have shown these winds can force coastal upwelling along the continental shelf of the southeastern USA (Atkinson 1985, Gutierrez et al. 2006). The magnitude of the intrusion depends on the characteristics (i.e., intensity and duration) of the southwesterly wind events. The cross-shore advective scales of the cold-water on the inner-shelf (e.g., distance from the shore) depend on prevailing stratification (Aretxabareta et al. 2006) as this inhibits water column mixing. During the summer months, the thermal stratification is

promoted by intense solar radiation which is continuously maintained since the moderate intensity of the prevailing wind stress inhibits intense water column mixing (i.e., moderate wind speed and oscillating strength, Figure 5-6a). This is intensified by the development of upwelling circulation from the southwesterly wind forcing which promotes an alongshore front or barrier to lateral mixing of the very nearshore water with the offshore water (Figure 5-5). It is worth noting that this mechanism does not operate on a tidal frequency, the only exception was the August of 2009 event where some tidal signal was observed which was likely due to coincidence of this event with the astronomically high tides observed during this period. However, this tidal signal appears to be of secondary importance as the subtidal levels dominate the signal (Figure 5-6c) and it might be associated more with a lateral movement of the front as a function of the highly variable water depth, as has been suggested by McCoy et al. (2011), or with changes in vertical mixing induced by large changes in water depth, or a combination of both.

The association of wind-driven upwelling and bottom water DO conditions predicted by the numerical simulations could best be seen in the 2009 data. In the September of 2009 event, hypoxic conditions persisted while the wind was predominately from the southwest with small oscillatory periods (Figure 5-6a and c, September 12-16). The DO concentrations increased when the wind direction changed, relaxing the upwelling conditions which led to a remixing of the water column both surface to bottom and nearshore to offshore (Figure 5-6a and c, September 16-18). During the August of 2009 event, the wind direction did not change but instead a slight increase in wind speed and seizing of the initial oscillatory nature of the wind similar to that in the model resulted in the mixing of the water column (Figure 5-6a and c). Under persistent wind directions, the ocean continuously gains energy and mixing increases over time as it allows for this energy to penetrate in larger depths keeping bottom waters oxygenated.

Although this combination of moderate, oscillatory upwelling favorable wind conditions and solar radiation creates the physical pre-conditions necessary for hypoxia development, the lack of evidence of low DO conditions at the offshore sites (Figure 5-7) indicate that upwelling does not advect a water mass with low DO or high nutrient concentrations from offshore sources, as in typical coastal upwelling systems (Grantham et al. 2004, Zhang et al. 2010). Rather, it appears that the nearshore front of the upwelling system, as identified in the model and 2009 data (Figs. 4-5 and 4-6), provides a barrier or front that limits dispersion and increases the residence time of materials entering the nearshore coastal waters from terrestrial sources (e.g., tidal creeks, stormwater discharge pipes, submarine groundwater discharge). As the model indicates, this front can extend to very shallow waters (up to 5 m, the limit of the model) suggesting a very limited offshore extent of the front. This is further supported by the limited spatial extent of hypoxic water both alongshore (~50 km along the length of the coast) and offshore (approximately 2 km). McCoy et al. (2011) observed greatly elevated radon-222 activities in the nearshore of Long Bay during the August of 2009 hypoxia period, which can be explained by the restricted dispersion and trapping of this groundwater tracer in nearshore waters. This observation directly supports the notion that materials were not being mixed out of the nearshore, but instead were confined, both surface to bottom by stratification and nearshore to offshore by the upwelling front, in a water mass immediately adjacent to the shoreline.

The importance of terrestrial inputs of nutrient and organic matter substrates is suggested by consistent decreasing material concentrations from nearshore to offshore waters, especially for

particulate matter concentrations (Table 5-1). During the August of 2009 hypoxia event, nutrient and organic matter concentrations were substantially elevated relative to mean concentrations measured during previous summers (2006 – 2008) when no significant hypoxia events were observed (Figure 5-8). These increases were not uniform, however. The increase in mean POM concentration (123 %) was much greater than that of DOC (42 %) but, interestingly, the relative ratio of Chl:POM for the 2009 data was essentially identical to that for the 2006 – 2008 data. Examination of precipitation records from the study area revealed no evidence of significant rainfall immediately prior to this event and no differences in precipitation values between years (except 2007 was a drought year) was found that would result in a significant change in the input of materials into the Bay during the August or September of 2009 time periods (SC State Climatology Office, unpublished data). This indicates a lack of dispersion of terrestrial materials consistently entering the Bay (e.g., via flow from irrigation of urban landscapes, tidal flushing from tidal creeks, groundwater) instead of an episodic influx of new materials. In addition, most of the particulate forms of organic matter and nutrients measured tended to show a high degree of covariation (Table 5-2) suggesting that upwelling processes simply act to constrain and concentrate all particulate materials equally in the nearshore bottom waters.

Pelagic respiration rates in Long Bay were both substantial and highly variable. The general pattern of higher rates in nearshore waters compared to offshore waters (Table 5-1) is consistent with previous observations of respiration in the South Atlantic Bight (Jiang et al. 2010). Respiration rates measured in this study were much more variable, however, than those reported by Jiang et al. (2010) for inner continental shelf waters off Georgia in summers of 2003 – 2006 ($20.5 - 28.3 \mu\text{g O}_2 \text{ L}^{-1} \text{ h}^{-1}$) and substantially greater than respiration rates reported for the region of the Gulf of Mexico susceptible to hypoxia formation ($5.5 - 14.4 \mu\text{g O}_2 \text{ L}^{-1} \text{ h}^{-1}$; Murrell and Lehrter 2011). The significant correlations between respiration rates and POM, Chl *a*, TNW, TPW, and DOC concentrations (Table 5-2) indicate a strong dependence of heterotrophic metabolism on substrate availability. The fact that these substrates, with the exception of DOC, were themselves significantly correlated makes the use of simple correlation analysis problematic in determining which individual resource most strongly regulated the magnitude of *in situ* respiration rates in these waters. However, the fact that respiration rate tightly clustered with particulate matter concentrations (Figure 5-8) certainly implicates particulate, rather than dissolved, resources in driving enhanced respiration rates under upwelling conditions.

In the majority of hypoxic areas, the organic matter fueling hypoxia is driven by high anthropogenic nutrient inputs stimulating algal blooms that fuel oxygen demand as the bloom collapses and decays (e.g., Pinckney et al. 2001, Conley et al. 2002, Nixon et al. 2008). Although no direct data on primary production rates in this area exist, several lines of evidence suggest that the formation of hypoxia in Long Bay, SC may not fit this conventional model. The general lack of oxygen supersaturation of the water column during normal conditions but also immediately preceding the 2009 hypoxia events (Figure 5-2) would imply that net heterotrophy predominates in these waters (Verity et al. 2006). While relatively high Chl *a* concentrations have been observed during hypoxic periods, Chl *a* concentrations were always highest in the bottom waters (Table 5-1) and always strongly correlated with POM concentrations (Table 5-2) such that Chl *a*:POM ratios remained relatively constant regardless of whether physical conditions promoted upwelling, or not. In addition, a strong inverse relationship has been observed in Long Bay, SC between DO and Chl *a* during both normoxic and hypoxic periods (Koepfler 2010). These

findings can only be explained if heterotrophic metabolism of particulate organic material, and its associated oxygen demand, exceeds *in situ* organic production due to phytoplankton photosynthesis, and its associated production of oxygen. Thus, it would appear that microbial respiration leading to hypoxia depends on a source of organic matter other than *in situ* phytoplankton production. However, the exact source or sources of this organic material remains unclear at present and further data are clearly necessary to obtain a full understanding of the input and processing of organic material that is driving this ecosystem, especially considering the following two observations: 1) the fraction of POM estimated to be represented by phytoplankton (averaged 20.2 ± 11.1 % assuming Chl *a* represents 1.15 % of the AFDW of organic phytoplankton biomass [Reynolds 2006]) is similar to the fraction typically observed in Chesapeake Bay, a eutrophic system driven by phytoplankton production (Canuel and Zimmerman 1999); and 2) the observation, at least on one date, of a large mat-forming diatom (*Proboscia alata*) occurring in high concentrations during the first hypoxic event of 2009.

In summary, hypoxia in Long Bay, SC appears to occur as the result of regional-scale oceanographic processes limiting cross shelf dispersion of local-scale terrestrial inputs, which then elevate local organic substrate concentrations that fuel enhanced heterotrophic metabolism and consequent oxygen demand, resulting in the formation of hypoxic conditions in nearshore waters. Such conditions persist until wind conditions change to relax upwelling, which both remixes the water column and allows for wider dispersion of terrestrial inputs, thereby restoring oxygen concentrations and reducing heterotrophic activity due to lowered substrate availability. This interaction between regional-scale physical processes and local-scale ecological processes appears to be a rather unique mechanism of hypoxia formation such that Long Bay does not fall into any of the categories of coastal systems experiencing hypoxia described in Zhang et al. (2010). If worldwide trends are true such that once an area experiences hypoxia, these low DO events tend to become more frequent and intense over time (Conley et al. 2009); we may, therefore, expect hypoxic conditions in Long Bay to increase, particularly as human population levels are projected to increase, which will likely enhance terrestrial runoff of nutrients and organic matter. We hypothesize that increasing terrestrial loadings associated with continued urban development along the Greater Myrtle Beach area, will decrease the physical threshold necessary for the development of hypoxia in Long Bay, and as such hypoxic events might affect tourism and consequently the economy of the region. Future research on the relative contributions of loadings from each terrestrial source (e.g., stormwater outfall pipes, tidal creeks, groundwater) is critical before developing potential management actions. In addition, ascertaining the specific threshold levels for hypoxia development in Long Bay will require a better mechanistic understanding of the relative roles played by physical conditions, terrestrial loading, and *in situ* DO processes in influencing nearshore water quality and DO dynamics.

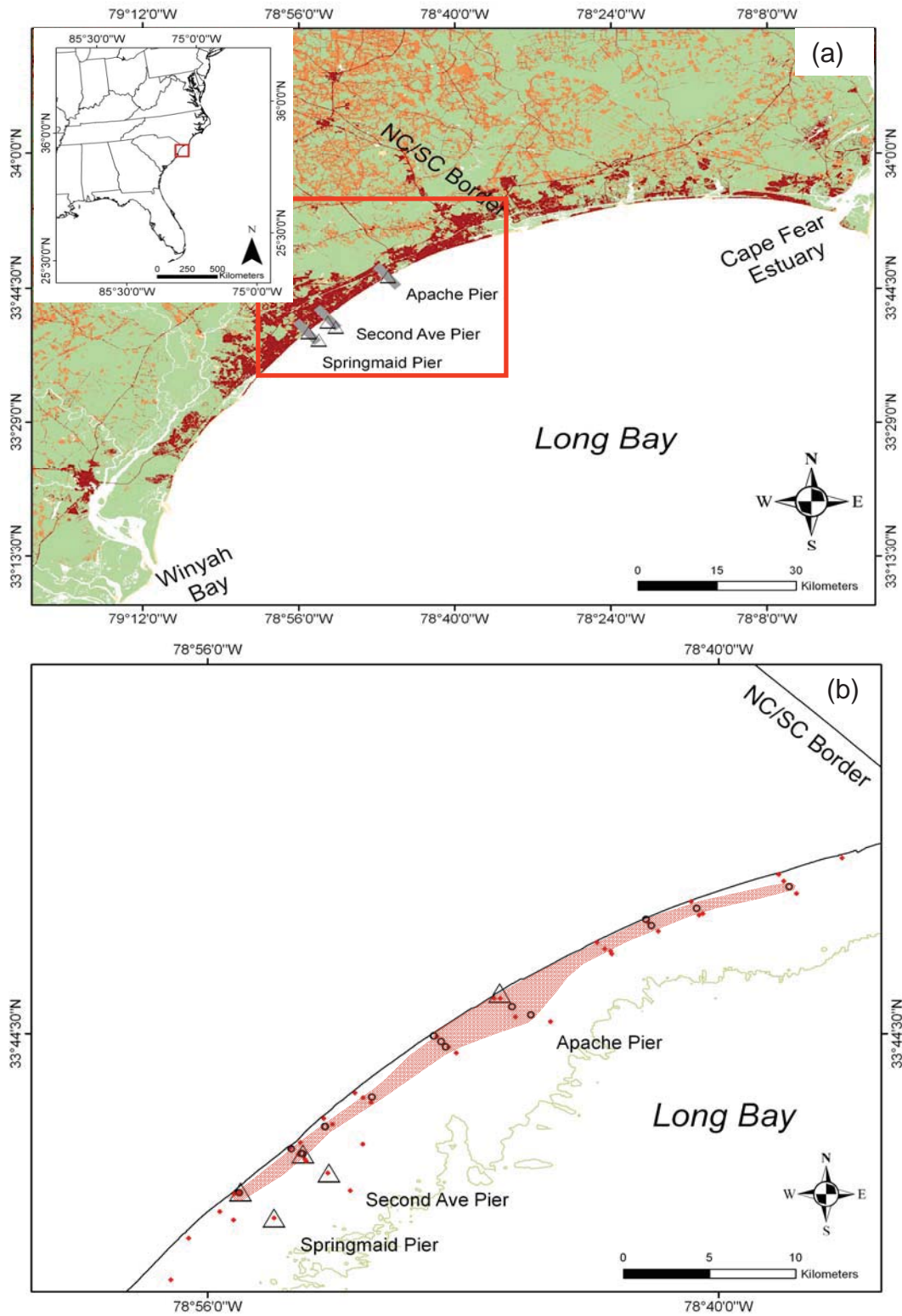


Figure 5-1. Map of the Long Bay region USA (a), with the general area over which hypoxia was observed at some point during August of 2009 in gray (b). Basic water quality semi-continuous monitoring sites near Apache, Second Avenue, and Springmaid piers are identified with triangles. The points and open circles are sites where measured bottom DO concentrations were $> 2 \text{ mg O}_2 \text{ l}^{-1}$ and $< 2 \text{ mg O}_2 \text{ l}^{-1}$, respectively, during the August of 2009 event (note- 5 sites to the south are not shown but were $> 2 \text{ mg O}_2 \text{ l}^{-1}$). Long Bay land use data (a) – dark gray = developed land, light gray = forested and wetlands, medium gray = agriculture (NOAA Coastal Change Analysis Program 2005). Bathymetric data (b) with the 10 m isobath shown is from NOAA Geophysical Data Center.

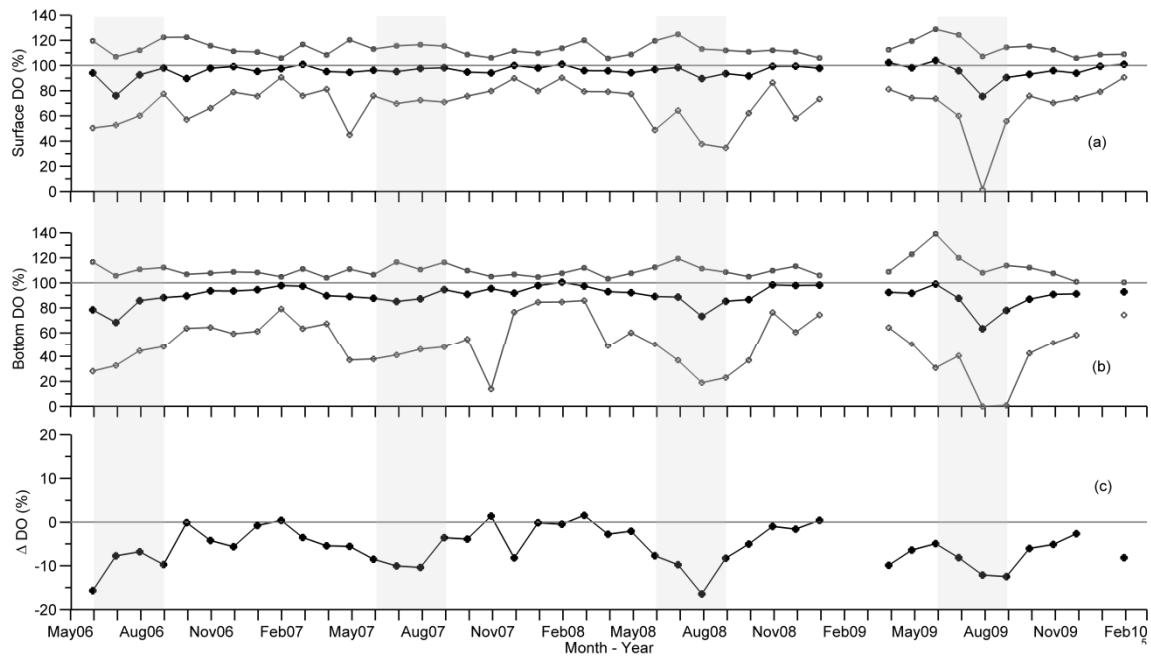


Figure 5-2. Time series of monthly mean, maximum and minimum values of dissolved oxygen saturation levels near the water surface (a) and near the sea bed (b). The difference of the monthly means from the surface to the bed is shown in (c). Data from the station located on Apache Pier.

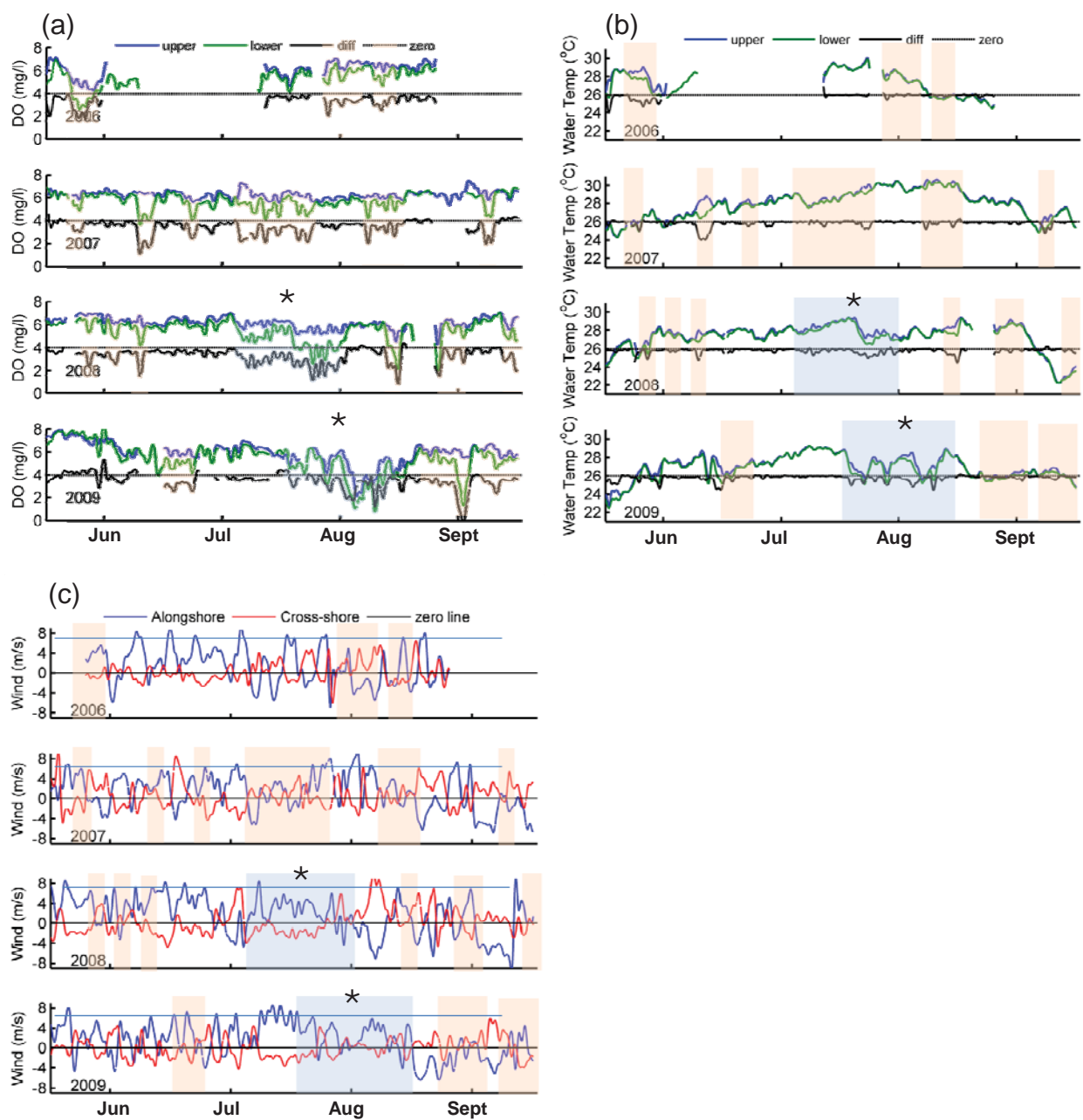


Figure 5-3. Low-passed time-series of dissolved oxygen concentration (a), water temperature (b), and wind velocity (c) in the surface (upper) and bottom (lower) water column as well as the difference between them. The events of low oxygen conditions are identified as shaded areas with an asterisk indicating the extended periods of low DO occurrence.

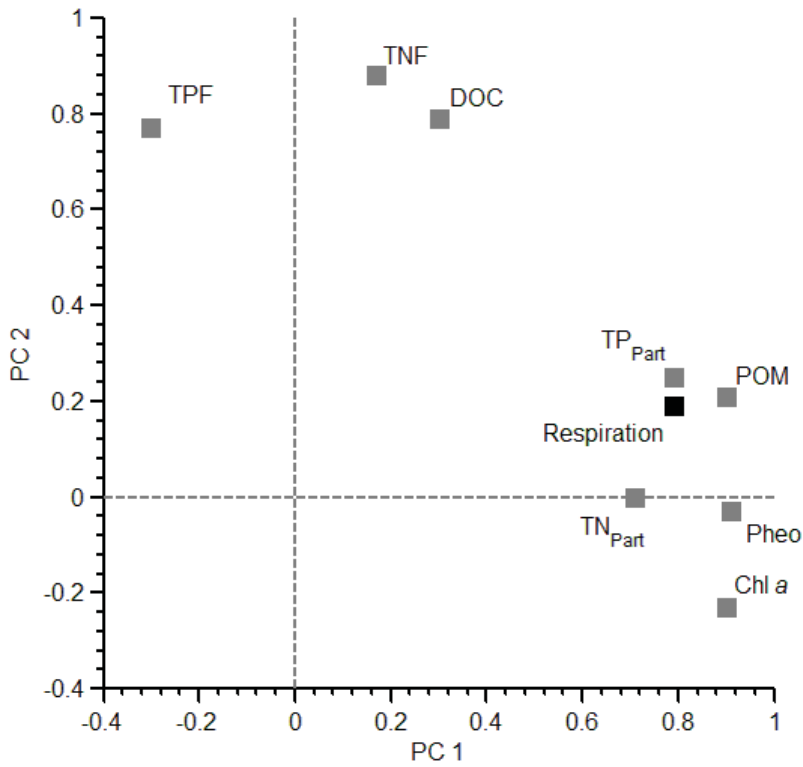


Figure 5-4. PCA biplot of mean factor loadings on PC 1 and PC 2. Rotated eigenvectors for each parameter are indicated by squares. The PC 1 and PC 2 eigenvalues were 4.5 and 2.1, respectively. The PC 1 and PC 2 percent variability explained by each was 50 % and 23.3 %, respectively.

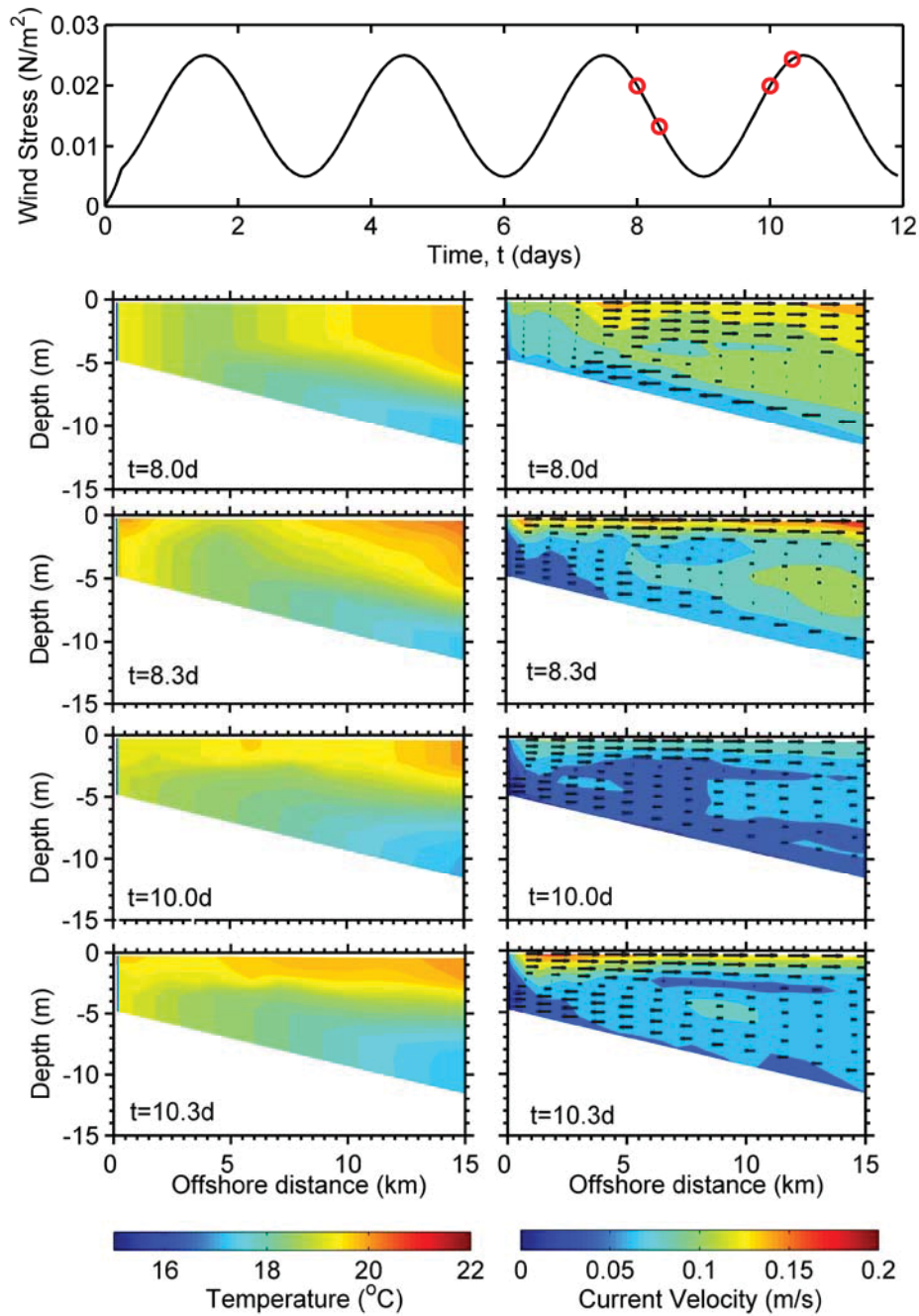


Figure 5-5. Sections (views toward the north) of temperature (left) and velocity (right) fields of the inner-shelf response to wind-driven upwelling at the middle of the bay after 8.0, 8.3, 10.0, and 10.3 days of simulation. The colors in the velocity field represent the alongshore velocity component, while the vectors represent the cross-shore velocity component. Wind forcing is shown in the upper panel.

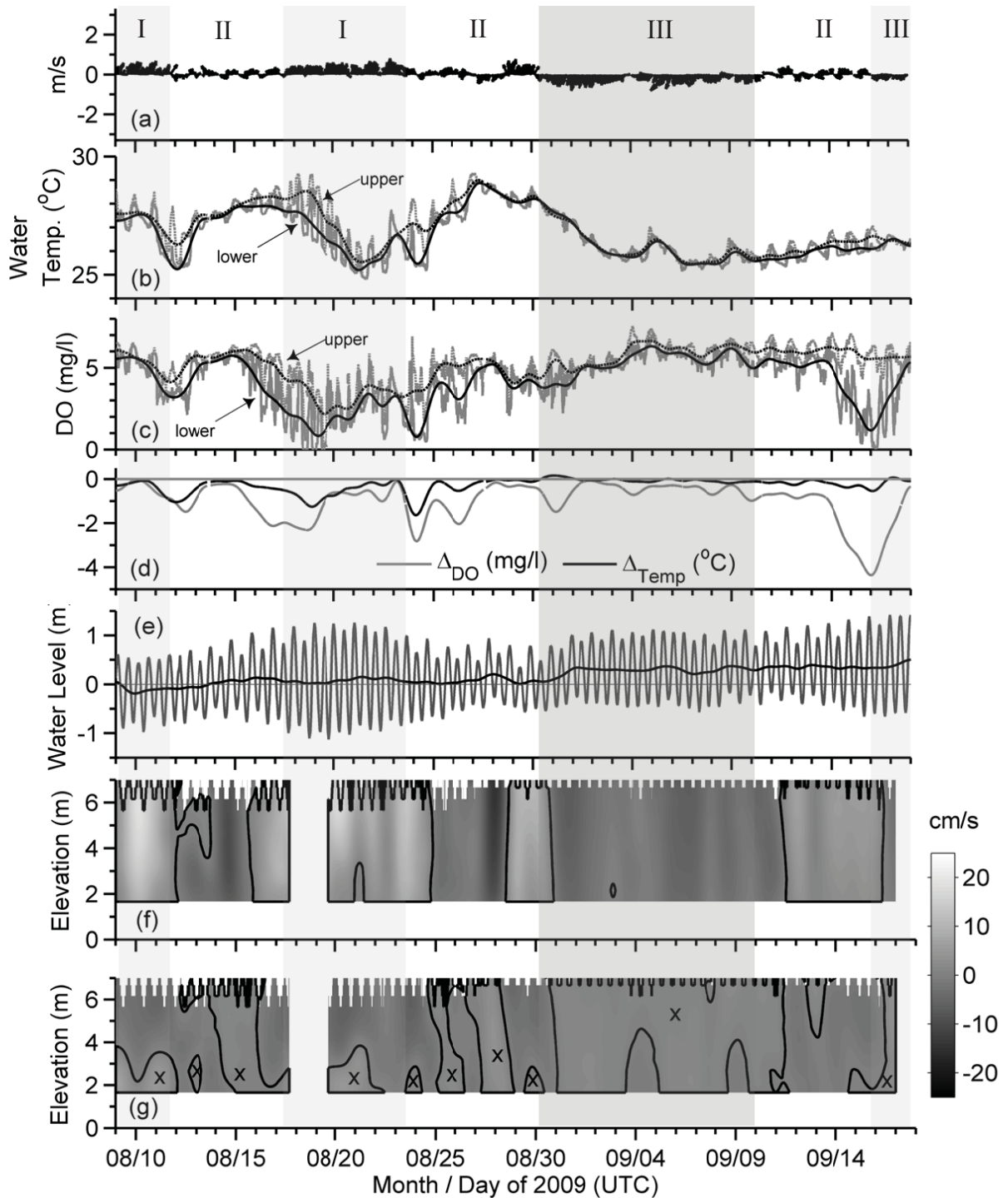


Figure 5-6. Meteorological and water quality time series in Long Bay for the period August 8 to September 19, 2009 showing the correlation of low DO events with upwelling conditions including: (a) vector diagram of wind velocity (oceanographic convention); (b) instantaneous (grey lines) and low-passed (33 hrs cut-off, black lines) water temperature at the upper (surface) and lower (bottom) water levels; (c) instantaneous (grey lines) and low-passed (black lines) dissolved oxygen concentration at the upper and lower levels in the water column; (d) difference

of low-passed dissolved oxygen concentration (grey line) and temperature (black line) between upper and lower levels (negative values indicate lower values in sensor closer to the sea bed); (e) tidal and mean water level variability; (f) low passed alongshore vertical structure of water flow measured at the offshore station (positive values shown in light grey colors indicate flow toward the northeast); and (g) low-passed cross-shore flow at the same offshore station (positive values indicate onshore flow, denoted by crosses). The contour lines in (f) and (g) represent zero velocity. Vertical shaded areas identified as I, II and III represent periods of (i) consistent upwelling favorable winds (light grey), (ii) oscillating upwelling winds most likely due to light upwelling conditions modulated by the local sea breeze; and (iii) downwelling favorable winds, respectively. Meteorological and tidal elevation data were collected at Springmaid Pier (NOAA NDBC and NOS stations MROS1 and 8661070). Water quality data were collected at Apache Pier. Coastline orientation is approximately 43 degrees from true North.

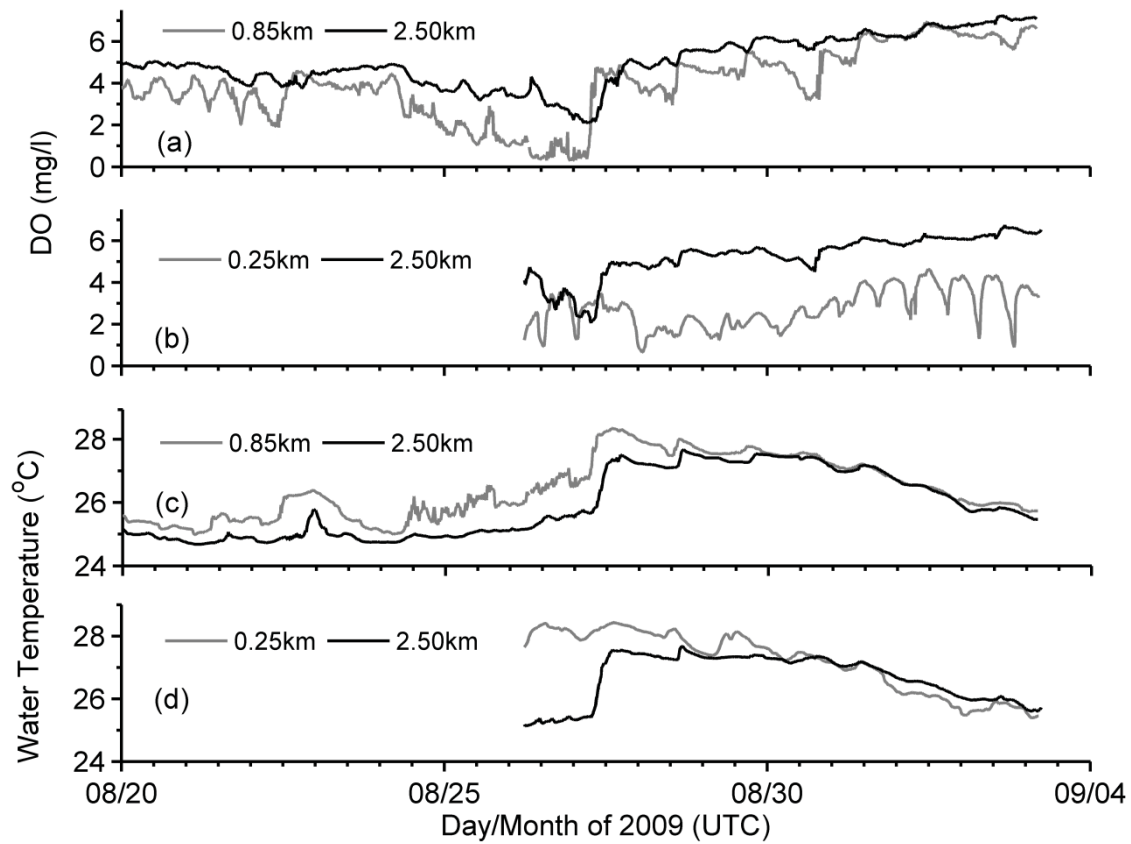


Figure 5-7. Water quality time series in Long Bay for the period 8/20/09 to 9/4/09 showing the DO and temperature concentrations off Second Avenue (a and c) and Springmaid piers (b and d). Two sites were sampled off Second Avenue Pier at 0.85 km and 2.5 km and two sites were sample off Springmaid Pier at 0.25 km and 2.5 km.

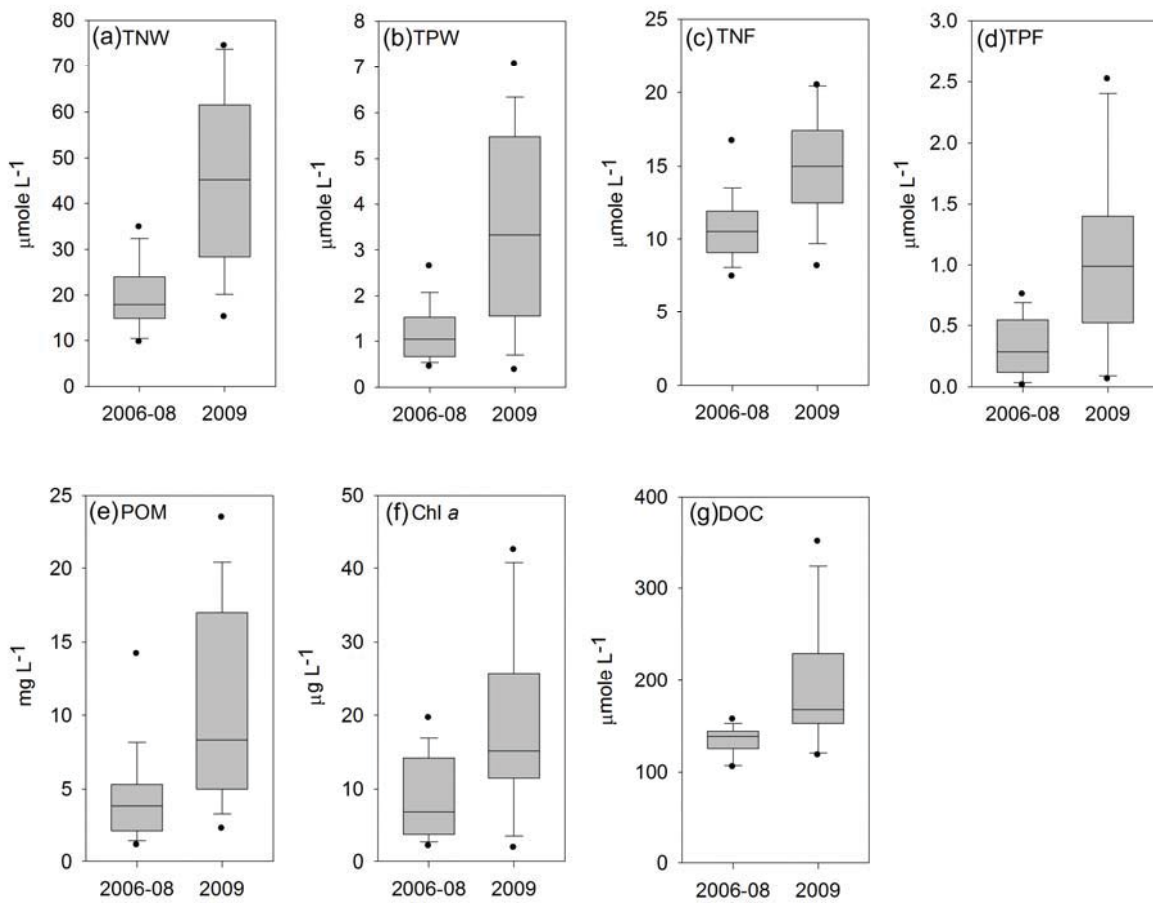


Figure 5-8. Comparisons of bottom water concentrations of (a) total nitrogen unfiltered (TNW), (b) total phosphorus unfiltered (TNP), (c) total nitrogen filtered (TNF), (d) total phosphorus filtered (TPF), (e) particulate organic matter (POM) as estimated on loss of ignition, (f) chlorophyll *a* (Chl *a*), (g) dissolved organic carbon (DOC) for summer nearshore 2006 – 2008 sampling events and August 2009 sampling event. The box and whisker plot shows the median (line), 25% and 75% (box), 10% and 90% (error bars), and the maximum and minimum (points).

Table 5-1. Means (standard deviation, n) for respiration rate ($\mu\text{g O}_2 \text{ L}^{-1} \text{ h}^{-1}$), chlorophyll *a* (Chl *a*, $\mu\text{g L}^{-1}$), unfiltered total nitrogen (TNW, $\mu\text{mole L}^{-1}$), filtered total nitrogen (TNF, $\mu\text{mole L}^{-1}$), unfiltered total phosphorus (TPW, $\mu\text{mole L}^{-1}$), unfiltered total phosphorus (TPF, $\mu\text{mole L}^{-1}$), and chlorophyll *a* (Chl *a*, $\mu\text{g L}^{-1}$) measured during summers of 2006 to 2008. Note that respiration rate in surface waters was only measured during 2006.

Location	Respiration rate	Chl <i>a</i>	TNW	TNF	TPW	TPF	DOC
Nearshore Surface	19.7 (3.8, 9)	4.80 (2.91, 49)	17.3 (5.4, 51)	12.4 (3.3, 51)	0.97 (0.43, 51)	0.59 (0.14, 51)	2.50 (0.86, 49)
Nearshore Bottom	25.4 (12.2, 27)	8.13 (5.03, 48)	19.8 (7.5, 50)	12.4 (3.1, 50)	1.42 (0.86, 50)	0.65 (0.26, 50)	2.67 (1.50, 48)
Offshore Surface	13.2 (8.8, 9)	2.49 (1.60, 30)	14.6 (5.0, 30)	11.6 (3.3, 30)	0.70 (0.22, 30)	0.54 (0.14, 30)	2.50 (0.88, 27)
Offshore Bottom	19.5 (9.2, 27)	6.77 (5.97, 31)	16.3 (4.9, 31)	11.6 (2.2, 31)	0.98 (0.42, 31)	0.61 (0.14, 31)	2.43 (0.69, 28)

Table 5-2. Nonparametric correlation matrix (Spearman's rho value) for respiration rate, particulate organic matter (POM), chlorophyll *a* (Chl *a*), pheophytin (Pheo), dissolved organic carbon (DOC), total nitrogen (TNW), and total phosphorus (TPW) concentrations. Statistically significance ($p < 0.01$) correlation are designated with an *.

	POM	Chl <i>a</i>	Pheo	DOC	TNW	TPW
Resp	0.661*	0.698*	0.576*	0.558*	0.602*	0.555*
POM		0.724*	0.825*	0.405*	0.745*	0.706*
Chl <i>a</i>			0.875*	0.191	0.488*	0.398*
Pheo				0.215	0.600*	0.546*
DOC					0.556*	0.474*
TNW						0.841*

Section VI: REFERENCES

- Alexabareta A, Nelson JR, Blanton JO, Seim HE, Werner FE, Bane JM, Weisberg R (2006) Cold event in the South Atlantic Bight during summer of 2003: Anomalous hydrographic and atmospheric conditions. *J Geophys Res*, 111, C06007, doi:10.1029/2005JC003105
- Anderson TH, Taylor GT (2001) Nutrient pulses, plankton blooms, and seasonal hypoxia in western Long Island Sound. *Estuaries* 24:228-243
- Arar EJ, Collins GB (1997) Method 445.0: *In vitro* determination of chlorophyll *a* and Pheophytin *a* in marine and freshwater algae by fluorescence. National Exposure Research Laboratory, Office of Research and Development, US Environmental Protection Agency. Cincinnati, OH
- Atkinson LP (1985) Hydrography and nutrients of the southeastern US continental shelf. In: Atkinson LP, Menzel DW, Bush KA (eds) *Oceanography of the southeastern U.S. continental shelf*. AGU Coastal and Estuarine Sciences 2:77-92
- Atkinson LP, Blanton JO (1986) Processes that affect stratification in shelf waters. In *Baroclinic processes in Continental Shelves*, Mooers CNK (Ed). AGU Coastal and Estuarine Series 3:117-130
- Benner R, Strom M (1993) A critical evaluation of the analytical blank associated with DOC measurements by high-temperature catalytic oxidation. *Mar Chem* 41:153-160
- Bianchi TS, DiMarco SF, Cowan JH, Jr, Hetland RD, Chapman P, Day JW, Allison MA (2010) The science of hypoxia in the Northern Gulf of Mexico: A review. *Sci Total Environ* 408:1471-1484
- Blanton JO, Aretxabaleta AL, Werner FE, Seim H (2003) Monthly climatology of the continental shelf waters of the South Atlantic Bight. *J Geophys Res*, doi:10.1029/2002JC001609
- Boesch DF, Rabalais NN (1991) Effects of hypoxia on continental shelf benthos: Comparisons between the New York Bight and the northern Gulf of Mexico. In Tyson RV, Pearson TH (ed) *Modern and ancient continental shelf anoxia*. Geological Society Special Publications No. 58. The Geological Society, London
- Burnett WC, Kim G, Lane-Smith D (2001) A continuous monitor for assessment of ²²²Rn in the coastal ocean. *J Radioanal Nucl Chem* 249:167-172.
- Canuel EA, Zimmerman AR (1999) Composition of particulate organic matter in the lower Chesapeake Bay: sources and reactivity. *Estuaries* 4:980-994
- Carnigan R, Blais AM, Vis C (1998) Measurement of primary production and community respiration in oligotrophic lakes using the Winkler method. *Can J Fish Aquat Sci* 55:1078-1084
- Chan F, Kirincich A, Barth J, Lubchenco J, Menge BA (2006) Upwelling-driven hypoxia off the central Oregon coast. *Eos Trans AGU* 87, Ocean Sci Meet Suppl, Abstract OS53J-06
- Conley DJ, Humborg C, Rahm L, Savchuk OP, Wulff F (2002) Hypoxia in the Baltic Sea and basin-scale changes in phosphorus biogeochemistry. *Environ Sci Technol* 36(24):5315-20
- Conley DJ, Carstensen J, Vaquer-Sunyer R, Duarte CM (2009) Ecosystem thresholds with hypoxia. *Hydrobiologia* 629:21-29
- Connolly TP, Hickey BM, Geier SL, Cochlan WP (2010) Processes influencing seasonal hypoxia in the northern California Current System. *J Geophys Res C* 115

- Diaz RJ, Rosenberg R (1995) Marine benthic hypoxia: A review of its ecological effects and the behavioral responses of benthic macrofauna. *Oceanogr Mar Biol Annu Rev* 33:245-303
- Diaz RJ, Rosenberg R (2008) Spreading dead zones and consequences for marine ecosystems. *Science* 321:926-929
- Diaz RJ, Solow A (1999) Ecological and Economic Consequences of Hypoxia: Topic 2 Report for the Integrated Assessment on Hypoxia in the Gulf of Mexico. NOAA Coastal Ocean Program Decision Analysis Series No. 16. NOAA Coastal Ocean Program, Silver Spring, MD
- Glenn SM, Crowley MF, Haidvogel DB, Song YT (1996) Underwater observatory captures coastal upwelling events off New Jersey. *EOS Trans AGU* 77:233-236
- Glenn S, Arnone R, Bergmann T, Bissett WP, Crowley M, Cullen J, Gryzmski J, Haidvogel D, Kohut J, Moline M, Oliver M, Orrico C, Sherrell R, Song T, Weidemann A, Chant R, Schofield O (2004) Biogeochemical impact of summertime coastal upwelling on the New Jersey Shelf. *J Geophys Res C* 109
- Glibert PM, Mlodzinska Z, D'Elia CF (1977) A semi-automated persulfate oxidation technique for simultaneous total nitrogen and total phosphorus determination in natural water samples. Woods Hole Oceanographic Institution Contribution Number 3954. Ocean Industry Program of the Woods Hole Oceanographic Institution, Woods Hole, MA 02543
- Grantham BA, Chan F, Nielsen KJ, Fox DS, Barth JA, Huyer A, Lubchenco J, Menge BA (2004) Upwelling-driven nearshore hypoxia signals ecosystem and oceanographic changes in the northeast Pacific. *Nature* 429:749-754
- Gutierrez BT, Voulgaris G, Work PA (2006) Cross-shore variation of wind-driven flows on the inner shelf in Long Bay, South Carolina, USA. *J Geophys Res* 111, doi:10.1029/2005JC003121
- Hagy JD, Boynton WR, Keefe CW, Wood KV (2004) Hypoxia in Chesapeake Bay, 1950-2001: Long-term change in relation to nutrient loading and river flow. *Estuaries* 27:634-658
- Haidvogel DB, Arango HG, Hedstrom K, Beckmann A, Malanotte-Rizzoli P, Shchepetkin AF (2000) Model evaluation experiments in the North Atlantic Basin: simulations in nonlinear terrain-following coordinates. *Dynam Atmos Oceans* 32:239-281
- Hamilton P (1987) Summer upwelling on the southeastern continental shelf of the USA during 1981: The structure of the shelf and Gulf Stream motions in the Georgia Bight. *Prog Oceanogr* 19: 329-351
- Hawley N, Johengen TH, Rao R, Ruberg SA, Beletsky D, Ludsin SA, Eadie BJ, Schwab DJ, Croley TE, Brandt SB (2006) Lake Erie hypoxia prompts Canada-US study. *EOS Trans AGU* 87(32):317
- Hoffman EE, Pietrafesa LJ, Klinck JM, Atkinson LP (1980) A time-dependent model of nutrient distribution in continental shelf waters. *Ecol Model* 10:193-214
- Hoffman EE, Pietrafesa LJ, Atkinson LP (1981) A bottom water intrusion in Onslow Bay, North Carolina. *Deep-Sea Res* 28:329-345
- Jiang L-Q, Cai W-J, Wang Y, Diaz J, Yager PL, Hu X (2010) Pelagic community respiration on the continental shelf off Georgia, USA. *Biogeochemistry* 98:101-113
- Kemp WM, Boynton WR, Adolf JE, Boesch DF, Boicourt WC, Brush G, Cornwell JC, Fisher TR, Glibert PM, Hagy JD, Harding LW, Houde ED, Kimmel DG, Miller WD, Newell RIE, Roman MR, Smith EM, Stevenson JC (2005) Eutrophication of Chesapeake Bay: historical trends and ecological interactions. *Mar Ecol Prog Ser* 303:1-29

- Koepfler ET (2010) Surface water and depth profile spatial patterns of hypoxia development along the Grand Strand, South Carolina. Proceedings of the 2010 South Carolina Water Resources Conference, October 13 -14, 2010, Columbia, SC. (Available at: http://media.clemson.edu/public/restoration/scwrc/2010/manuscripts/t2/koepfler_10scwrcpaper.pdf)
- Lee TN, Pietrafesa LJ (1987) Summer upwelling on the southeastern continental shelf of the USA during 1981: Circulation. *Prog Oceanogr* 19:267-312
- Libes S, Kindelberger S (2010) Hypoxia in the nearshore coastal waters of South Carolina along the Grand Strand. Proceedings of the 2010 South Carolina Water Resources Conference, October 13 -14, 2010, Columbia, SC. (Available at: http://media.clemson.edu/public/restoration/scwrc/2010/manuscripts/t2/libes_kindelberger_10scwrcpaper.pdf)
- MBCC (2009) The Myrtle Beach statistical abstract, 19th Ed. Myrtle Beach Chamber of Commerce, SC
- McCarney-Castle K, Voulgaris G, Kettner AJ (2010) Analysis of fluvial suspended sediment load contribution through Anthropocene history to the South Atlantic Bight coastal zone, U.S.A. *J Geol* 118(4):339-416
- McCoy CA, Viso RF, Peterson RN, Libes SM, Lewis BL, Ledoux JG, Voulgaris G, Smith E, Sanger D (2011) Radon as an indicator of limited cross-shelf mixing and submarine groundwater discharge in a coastal embayment along the South Atlantic Bight. *Contin Shelf Res* 31:1306-1317
- Murrell MC, Lehrter JC (2011) Sediment and lower water column oxygen consumption in the seasonally hypoxic region of the Louisiana Continental Shelf. *Estuaries and Coasts* 34:912-924
- Nixon SW, Buckley BA, Granger SL, Harris LA, Oczkowski, AJ, Fulweiler RW, Cole LW (2008) Nitrogen and phosphorus inputs to Narragansett Bay: past, present, and future. In: *Science for ecosystem-based management*, Springer, NY
- NOAA Coastal Change Analysis Program (2005) Digital Coasts. Accessed 9 Aug 2010. <http://www.csc.noaa.gov/digitalcoast/data/ccapregional/>
- Pinckney J, Paerl H, Tester P, Richardson T (2001) The role of nutrient loading and eutrophication in estuarine ecology. *Environ Health Perspect* 109:699-706
- Rabalais NN, Diaz RJ, Levin LA, Turner RE, Gilbert D, Zhang J (2010) Dynamics and distribution of natural and human-caused hypoxia. *Biogeosciences* 7:585-619
- Reynolds CS (2006) *Ecology of phytoplankton*. Cambridge University Press, Cambridge.
- Sanay R, Yankovsky A, Voulgaris G (2008) Inner shelf circulation patterns and nearshore flow reversal under downwelling and stratified conditions off a curved coastline. *J Geophys Res* 113, C08050, doi:10.1029/2007JC004487
- Sanger D, Hernandez D, Libes S, Voulgaris G, Davis B, Smith E, Shuford R, Porter D, Koepfler E, Bennett J (2010) A case history of the science and management collaboration in understanding hypoxia events in Long Bay, South Carolina, USA. *Environ Manage* 46:340-350
- Shchepetkin AF, McWilliams JC (2005) The Regional Oceanic Modeling System: A split-explicit, free-surface, topography-following coordinate oceanic model. *Ocean Model* 347-404 doi:10.1016/j.ocemod.2004.08.002
- Smith EM, Kemp WM (2001) Size structure and the production/respiration balance in a coastal plankton community. *Limnol Oceanogr* 46:473-485

- Sweet W, Zervas C, Gill S (2009) Elevated east coast sea levels anomaly: July – June 2009. NOAA Technical Report NOS CO-OPS 051. Silver Springs, MD
- Turner RE, Rabalais NN, Justic D (2005) Predicting summer hypoxia in the northern Gulf of Mexico: Riverine N, P, and Si loading. *Mar Pollut Bull* 52:139-148
- Umlauf L, Burchard H (2003) A generic length-scale equation for geophysical turbulence models. *J Mar Res* 61:235-265
- US Travel Association (2009) The economic impact of travel on South Carolina counties, 2008. U.S. Travel Association, Washington, DC
- Verity PG, Alber M, Bricker SB (2006) Development of hypoxia in well-mixed subtropical estuaries in the southeastern USA. *Estuaries and Coasts* 29:665-673
- Voulgaris G, Sanay R (2010) Physical oceanographic constraints contributing to the development of low oxygen events in Long Bay, SC. Proceedings of the 2010 South Carolina Water Resources Conference, October 13 -14, 2010, Columbia, SC. (Available at: http://media.clemson.edu/public/restoration/scwrc/2010/manuscripts/t2/voulgarisg2_sanay_10scwrcpaper.pdf)
- Wiseman WJ Jr, Rabalais NN, Turner RE, Dinnel SP, MacNaughton A (1997) Seasonal and interannual variability within the Louisiana Coastal Current: stratification and hypoxia. *J Mar Systems* 12:237-248
- Wu RSS (2002) Hypoxia: from molecular responses to ecological responses. *Mar Pollut Bull* 45:35-45
- Zhang J, Gilbert D, Gooday AJ, Levin L, Naqvi SWA, Middelburg JJ, Scranton M, Ekau W, Pena A, Dewitte B, Oguz T, Monteiro PMS, Urban E, Rabalais NN, Ittekkot V, Kemp WM, Ulloa O, Elmgren R, Escobar-Briones E, Van der Plas AK (2010) Natural and human-induced hypoxia and consequences for coastal areas: synthesis and future development. *Biogeosciences* 7:1443-1467